Reinhold Pommer, BSc

Investigation and Optimization of Formulations and Processing Parameters on Latex Materials for Disposable Rubber Gloves

DIPLOMA THESIS

To achieve the university degree of

Diplom-Ingenieur

Master's degree programme: Technical Chemistry

submitted to

Graz University of Technology

Supervisor

Assoc.Prof. Dipl.Ing. Dr.techn. Gregor Trimmel

Institute for Chemistry and Technology of Materials

Graz, January 2019

AFFIDAVIT

I declare that I have authored this thesis independently, that I have not used other than the declared sources/resources, and that I have explicitly indicated all material which has been quoted either literally or by content from the sources used. The text document uploaded to TUGRAZonline is identical to the present diploma thesis.

Date	Signature

ABSTRACT

As a protective device in various fields of applications, rubber gloves are not only essential against physical and chemical impact, but also against viral and bacterial infection. The utilization of disposable gloves made from natural rubber (NR) in medical applications dates back to the 19th century. Due to its superior performance regarding durability, barrier protection, tear resistance and comfort, NR still one of the most commonly used raw materials. However, products made from natural rubber are found to be among the most frequent causes for occupational allergies and dermatitis, especially in the healthcare sector. In that respect, the desire for higher safety and protection of the personnel has led to increasing substitution of NR by synthetic rubbers, such as chloroprene rubber (CR), isoprene rubber (IR) and acrylonitrile-butadiene rubber (NBR).

Within the glove manufacturing process, the most established method is the coagulant dipping process, in which ceramic formers of a desired shape are immersed into an aqueous latex mixture, containing vulcanization agents, accelerators and various additives. A final vulcanization step following the coagulation is crucial for optimization of the product properties and processability.

The objective of this thesis was the investigation and optimization of vulcanization formulations for latex films made from chloroprene, isoprene and acrylonitrile-butadiene rubber along with blends thereof, produced by the before mentioned coagulant dipping process. Properties of the films were examined and the influence of different production parameters, e.g. composition, curing temperature and time, gel leaching or pre-vulcanization was studied. Therefore, CR, IR and NBR latexes were cross-linked using different quantities and combinations of vulcanization agents, accelerating chemicals and fillers at various curing conditions. Further, blended rubber latex materials were prepared by combining IR and CR as well as commercially available NBR latexes. Characterization of the films comprised primarily the testing of mechanical properties, such as tensile strength and ultimate elongation. Additionally, electron microscopy (SEM-EDX) was applied to study morphology and phase behavior of blended materials. Differential scanning calorimetry (DSC) and dynamic light scattering (DLS) were used to investigate the thermal properties and the latex particle size respectively.

KURZFASSUNG

Als Schutzmittel vor physikalischen und chemischen Einwirkungen, als auch vor viralen und bakteriellen Infektionen, ist in vielen Bereichen die Verwendung von Latexhandschuhen, welche aus natürlichen oder synthetischen Kautschuken hergestellt werden, unumgänglich. Der Einsatz von Naturkautschuk (NR) in medizinischen Anwendungen datiert bereits zurück bis auf das 19. Jahrhundert und aufgrund seiner überlegenen Eigenschaften in Hinblick auf Strapazierfähigkeit, Schutzeigenschaften, Zugfestigkeit sowie Komfort, halten Produkte aus Naturkautschuk noch heute einen signifikanten Marktanteil. Indes gehören NR-Produkte zu den mitunter häufigsten Ursachen für berufsbedingte Allergien und Dermatitis, speziell für Beschäftigte im Gesundheitswesen. Aus diesem Grund werden gegenwärtig vermehrt synthetische Materialien, wie Chloropren-Kautschuk (CR), Isopren-Kautschuk (IR) oder Acrylnitril-Butadien-Kautschuk (NBR) als Alternativen für Naturkautschuk eingesetzt.

Die konventionelle Methode für die Herstellung von Latexhandschuhen ist das sogenannte Koagulationstauchverfahren. Hierbei werden Keramikformer in eine Latexmischung getaucht, welcher Vernetzungschemikalien, Beschleuniger und gegebenenfalls weitere Additive zugesetzt sind. Die anschließende Vulkanisation der getauchten Filme ist entscheidend für die Produkteigenschaften und Verarbeitbarkeit.

Ziel der vorliegenden Arbeit war die Untersuchung von Vernetzungsrezepturen für Filme aus Chloropren-, Isopren-, Acrylnitril-Butadien-Kautschuk und diversen Mischungen davon, welche nach oben genanntem Tauchverfahren hergestellt wurden. Dabei sollte der Einfluss von diversen Prozessparametern wie z.B. Trocknungsbedingungen, Gel-Leaching oder Vorvulkanisation evaluiert werden. Latexfilme wurden hierzu unter Verwendung verschiedener Vernetzungschemikalien, Beschleunigern und entsprechenden Additiven hergestellt. Die Charakterisierung der Materialien erfolgte in erster Linie in Form von mechanischen Tests (Zugfestigkeit, Bruchdehnung), als auch mittels Elektronenmikroskopie (SEM-EDX) zur Untersuchung der Morphologie und des Phasenverhaltens von Latex-Blends. Dynamische Differenzkalorimetrie (DSC) sowie dynamische Lichtstreuung (DLS) wurden zur Bestimmung der Glasübergangstemperaturen bzw. zur Partikelgrößenbestimmung herangezogen.

ACKNOWLEDGEMENTS

First and foremost, I would like to express my gratitude to my supervisor Prof. Gregor Trimmel, for the opportunity to work on the project as part of the working group and the guidance throughout the project.

To my dear colleagues at the institute, especially Bianca Prem, for mental support and practical assistance, the pleasant working atmosphere, constructive discussions and activities.

Thanks also to the Institute for Chemistry and Technology of Materials (ICTM) and the cooperation partners, the Polymer Competence Center Leoben (PCCL) and Semperit Technische Produkte GmbH, for providing the necessary equipment and financial support.

To the staff of the PCCL, the Austrian Centre for Electron Microscopy (FELMI-ZFE) and Graz University of Technology for all kind of assistance.

Finally, I must express my appreciation to my family and friends for providing continuous encouragement and unfailing support, not only throughout my years of study.

TABLE OF CONTENTS

1 INTRODUCTION

Latexes are defined as thermodynamically stable dispersions of polymer particles in an essentially aqueous medium. Distinguished by their origin, latexes are classified as either natural rubber latex, arising as a metabolic product of a variety of plants, or as synthetic rubber latexes, implying the industrial production of the polymeric material from the corresponding monomers.[1; 2] Natural rubber latex, as the basic raw material used in various manufacturing processes, is obtained from the bark of *Hevea brasiliensis*, most commonly known as Pará rubber tree, which is native to Brazil as well as parts of the Guianas.[3]

The white, opaque liquid can be described as a colloidal and lyophilic system of mostly spherical rubber particles – approximately 97% high molecular weight *cis*-1,4-poly(isoprene) - dispersed in an aqueous fluid. Those particles are surrounded by layers of proteins and phospholipids, which contribute to the stability of the colloidal system and give the natural rubber highly specific properties. Further, a variety of inorganic and organic constituents are present in the system. Generally, the composition of the natural rubber latex is not uniform and depends mainly on the type of plant, the origin, nutrition and climate.[3; 4]

Cultivation of the Pará rubber tree dates from the pre-Columbian era in large parts of Central and South America. Ancient cultures, e.g. Mayans or Aztecs, processed the rubbery material for clothing, toys and various other applications. The material experienced increasing worldwide attention just in the 18th century, when Macquer and Hérissant produced the first molded rubber articles (1765). Less than 80 years later, Charles Goodyear discovered the process of vulcanization (1841), and therewith laid the foundation of the modern rubber industry. In the 1870s, the Pará tree was imported to Africa and Southeast Asia, especially Malaysia, Singapore and Sri Lanka. Large scale production of synthetic rubbers was initiated in Germany during World War One, when the access to natural rubber supplies was blocked.[5; 6]

Nowadays, the world's largest suppliers of natural rubber are plants located in Malaysia, Indonesia, Thailand and Vietnam. The overall global consumption of rubber - natural as well as synthetic - increases steadily, as it is utilized in uncountable applications.[7] Figure 1 illustrates the rubber market share by application in the year of 2015, as well as the consumption of rubber by type as of 2014:

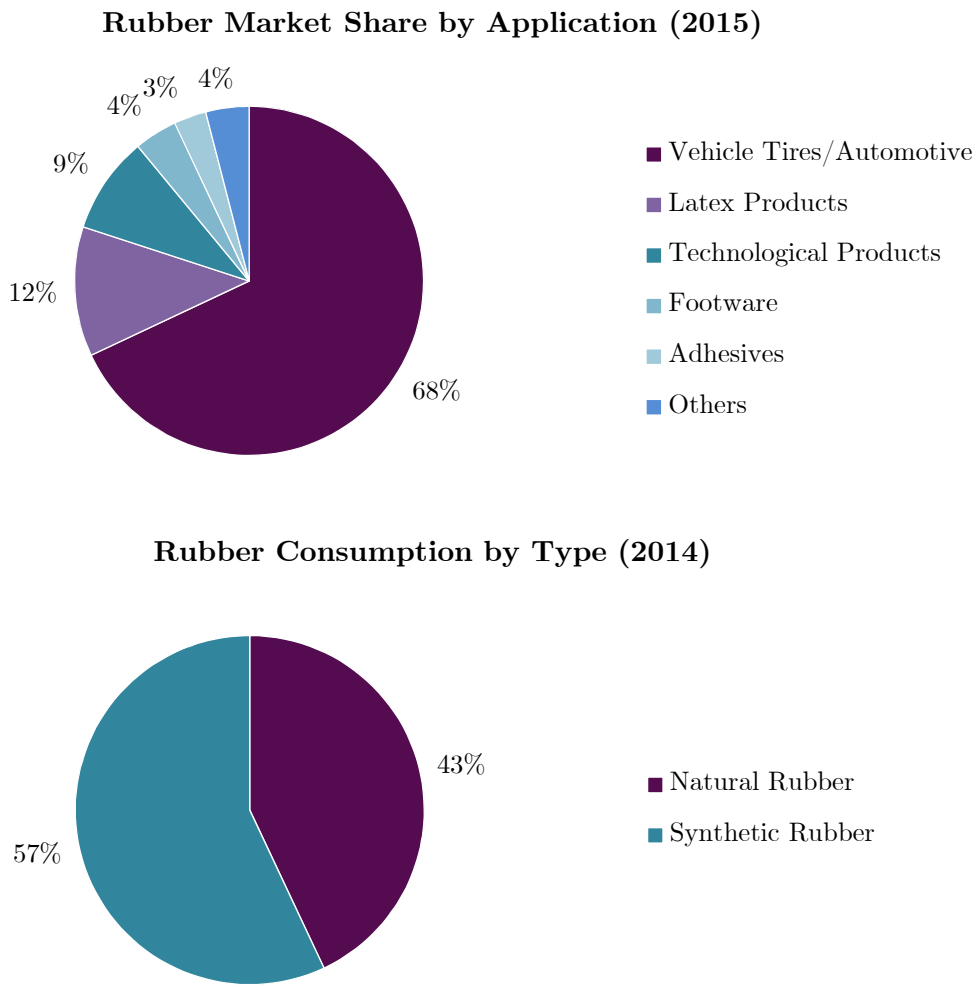

Figure 1. Declared rubber market share and consumption by type. (based on [7; 8])

Major players in terms of rubber consumption are obviously the tire and automotive industry, technical products in the engineering and construction sector, along with producers of consumer and latex health care products. Generally, the amount of processed solid rubber is much greater than the amount of directly processed latex. In terms of rubber type, natural rubber holds a share of up to 43% of the total consumption.[7; 9]

In the health care and consumer goods sector, rubber gloves are used as protectives against physical and chemical impact, but primarily against viral and bacterial infection. The utilization of natural rubber (NR) gloves in medical applications dates back to the 19th century and due to its superior performance regarding durability, barrier protection, tear resistance and comfort it is still one of the most commonly used material on the market.[8; 10] However, materials made from natural rubber are found to be among the most common causes for occupational allergies and dermatitis, especially in the sector of health care.[11] In that respect, the desire for higher safety and protection of the personnel has led to an increasing substitution of NR by synthetic rubbers, such as chloroprene rubber (CR), isoprene rubber (IR) and acrylonitrile-butadiene rubber (NBR).[12]

The established method for glove manufacturing is the coagulant dipping process, in which ceramic formers of a desired shape are immersed into an aqueous compounded latex mixture, containing vulcanization agents, accelerators and various additives. A final vulcanization step following the coagulation is crucial for optimization of the product properties and processability.[4; 13] Improvement of product properties is not only sought by optimization of formulations and processing parameters for the vulcanization process, but likewise, attempts of blending different rubber materials or adding reinforcing fillers have shown to improve material qualities. Latex blends have been of interest for many years in industry and research due to novel material properties.[7; 14; 15]

The first part of the present thesis deals with the basic theoretical information regarding different rubber materials, their chemical composition, properties and fields of application. Further, an insight into different vulcanization processes and the respective chemical compounds, such as accelerators and activators, which are utilized in rubber cross-linking is provided. In a second part, the methodological work along with the characterization methods are described. This compromises the screening of different curing formulations and conditions for single latex materials (CR, IR and NBR) and latex blends. Different characterization methods, in particular mechanical testing and electron microscopy were used to investigate the produced materials. Conclusively, the thesis is completed by discussion and interpretation of the obtained results and the methodological developments.

2 BASIC INFORMATION

Within this chapter, the basic theoretical background of latex materials, principles of vulcanization and compounding, as well as latex glove preparation are briefly discussed.

2.1 Latex Materials

2.1.1 Natural Rubber Latex (NR)

Natural rubber latex is a general term for a colloidal polymer dispersion of natural origin. Roughly 2000 plant species are known to produce the milky sap, of which only about a dozen is used for commercial purposes. A large percentage of natural rubber latex is obtained by tree tapping from the bark of *Hevea brasiliensis*, most commonly known as Pará rubber tree, which is native to Brazil and parts of the Guianas. However, most production sites are nowadays located in Southeast Asia.[3; 5]

The white, opaque liquid can be defined as a colloidal and lyophilic system of spherical rubber particles in the broad size range of 50 to 2000 nm, which are dispersed in an aqueous fluid.[16; 17] Approximately 97% of the total rubber amount is composed of high molecular weight *cis*-1,4-poly(isoprene), forming the core of the rubber particles. This rubber phase is concentrically surrounded by layers of phospholipids and proteins. Electric charges at the surface region and the resulting repelling forces contribute to the stability of the particles. Additionally, a layer of water molecules surrounding the protein layer prevents coalescence of the particles.[3] Further, a variety of inorganic and organic constituents, such as salts, sugars or resins are present in the system.[18] The composition of natural rubber latex is not uniform and depends mainly on the type of plant, its origin, nutrition and climate. A typical composition of freshly tapped natural rubber latex is shown in Table 1:

Table 1. Typical composition of fresh natural rubber latex.[3]

Component	wt%
Total solid content (tsc)	**35**
Dry rubber content (drc)	**30**
Proteins	**1–2**
Fatty acids	**1**
Resins	**2**
Carbohydrates	**< 1**
Inorganic salts	**< 1**

Production

Crude natural rubber latex is obtained from the respective plants by special tree tapping techniques, involving the sequential removal of thin bark layers. The extracted latex is then collected and dosed with ammonia or other stabilizing agents up to 0.2% in order to prevent coagulation. For further processing, the stabilized latex is usually filtered and concentrated mainly by centrifugation (about 90% of the latex), evaporation or latex creaming. Desired concentrations of up to 60 wt% are advantageous for transportation and distribution purposes.[1; 6] Processing methods of the crude natural rubber latex to latex products are described in section 2.4.

Properties and Applications

Due to its unique raw composition, natural rubber products exhibit superior properties, such as a great structural stability, rather high elasticity and consequentially, favorable tensile strength and elongation. Additionally, the good dynamic properties and cold flexibility are features of natural rubber latex products, just as an excellent barrier protection. On the down side, natural rubber latex is prone to ozone and oil degradation, as well as aging. Considering the physical properties, which mostly outperform those of

synthetic rubber latexes, natural rubber latex can be found in a wide range of applications. Those include, but are not limited to household and examination gloves, surgical gloves, molded goods, balloons or contraceptives.[10; 12; 18]

2.1.2 Allergy Controversy

Natural rubber latex is currently the most commonly used crude material for disposable rubber gloves and various medicinal products. This is despite the fact, that several studies within the last two decades have led to the result, that it is directly linked to different occupational allergies at an increased frequency.[19] Already in the late 80s, latex rubber allergy was a considerable healthcare problem. Allergen sources in that respect could be attributed to the proteins of the natural rubber latex, as well as to additives, which were, and are still used in the production process.[20] *Irritant contact dermatitis*, the most frequent reaction to latex products, is caused by chemicals in the rubber formulation, which directly affect the skin. However, this type of response is not considered a true allergy and symptoms decline within several hours after the exposure. In contrast to that, *allergic contact dermatitis* may occur as a delayed response to the stimulus, in which the symptoms arise 24 to 48 hours after exposure. The major concern relating to natural rubber gloves is *latex allergy*, an immediate response of hypersensitivity, caused by proteins.[21; 22] Findings of different studies, mainly carried out on health care and rubber industry workers, show that 17.0% to 24.4% of the test subjects reported some type of glove induced symptoms.[23] The majority of complaints could be attributed to skin irritation, rather than latex allergy. However, published data suggests, that the prevalence of natural rubber latex allergy amounts to 9.7% among healthcare workers and 4.3% among the general population.[24]

Reduction of the allergen concentration, potentially done either by chemical or enzymatic deproteinization, chlorination or polymer coating, has been investigated, but not established. For that reason, natural rubber latex is gradually replaced by synthetic rubber latexes.[7; 20]

2.1.3 Synthetic Rubber Latex

2.1.3.1 Isoprene Rubber Latex (IR)

Isoprene rubber, poly(*cis*-1,4-isoprene,) is the synthetic counterpart to natural rubber and used in various fields of applications.[18] With the discovery by Fritz Hoffmann dating back to 1909, isoprene rubber marks the first applicable synthetic rubber. Commercial synthesis was initially conducted by Goodrich-Gulf Inc. (US) in 1954, via a Ziegler-Natta polymerization of isoprene (2-methyl-1,3-butadiene). Just the following year, Firestone Tire Company (US) produced isoprene rubber via anionic polymerization.[4] Isoprene rubber can replace natural rubber in most applications with only minor adaptions of compounding formulations needed.[3; 25] However, due to the rather high price of the raw isoprene, significant industrial production had not started before the 1970s. The annual capacity of produced synthetic isoprene rubber is yet clearly lower than for natural rubber latex.[26] Poly(isoprene) is obtained as a mixture of isomeric structures (as shown in Figure 2), the ratio of which can be tuned by variation of polymerization conditions and catalysts.

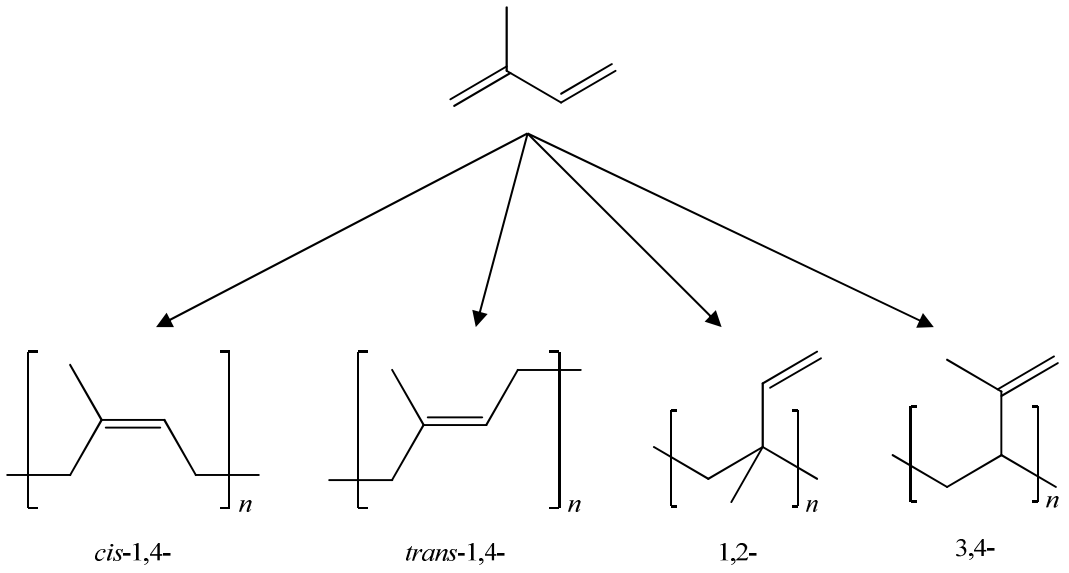

Figure 2. Isomeric structures of the isoprene units.[3]

Typically, the portion of poly(*cis*-1,4-isoprene) in the synthetic isoprene rubber amounts up to 98%, while the other isomeric units, poly(*trans*-1,4-isoprene), poly(1,2-isoprene) and poly(3,4-isoprene) are present in respectively smaller amounts.[25]

Production

As mentioned above, poly(isoprene) is mainly produced by two polymerization techniques: anionic polymerization and Ziegler-Natta coordination polymerization of isoprene.[25] The former is realized by utilizing Li-alkyl initiators, typically *n*-butyl-Li or *s*-Bu-Li in aliphatic and low boiling solvents. Anionic polymerization ultimately yields up to 92% poly(*cis*-1,4-isoprene).[27] A significantly higher *cis*-content (96 - 98%), as well as a regular tacticity can be obtained using stereospecific Ziegler-Natta type catalysts, such as titanium tetrachloride ($TiCl_4$) in combination with alkyl aluminum (AlR_3). Coordination polymerization is carried out at low temperatures in aliphatic solvents.[3; 25] In both cases, the produced poly(isoprene) is dissolved in an organic solvent, from which the solid rubber is obtained by subsequent coagulation and drying. The conversion to concentrated isoprene rubber happens by post-emulsification into an aqueous soap solution and removal of the residual organic solvent.[3; 28] More recently, stereospecific polymerization using lanthanides has been developed resulting in poly(isoprene) with *cis*-1,4-content of up to 99.5%. However, large scale industrial application of this method has not been reported.[29]

Properties and Applications

Even though natural and synthetic poly(isoprene) rubber latexes are basically composed of the same polymer on a molecular level, the properties of the counterparts differ noticeably.[30; 31] The lack of natural constituents in the synthetic rubber latex, especially the absence of proteins, makes it less prone to hardening, but at the same time impairs the mechanical properties.[3; 32] Further, a higher amount of *cis*-1,4-units facilitates

crystallization, impacting the glass transition temperature and mechanical features.[25] However, synthetic poly(isoprene) has a good fatigue resistance as well as an excellent abrasion resistance, compression set and creep above the working temperature. Just as natural rubber latex, it exhibits a poor resistance to ozone and organic solvents.[3] In general terms, synthetic isoprene rubber latex is used as a substitute for natural rubber latex in all conceivable applications, such as tires and engineering applications. Blending of IR with other types of rubbers is a commonly used approach to improve the properties. Applications are for instance conveyer lines, tubes, footwear, sealing materials, etc.[7; 33]

2.1.3.2 Chloroprene Rubber Latex (CR)

Chloroprene rubber, poly(2-chloro-1,3-butadiene), was the result of intensive research in the field of synthetic rubbers and firstly introduced by the American company DuPont (1930s). Since 1935, it is industrially produced by radical emulsion polymerization and generally known under its tradename Neoprene. As of the 1970s, chloroprene rubber holds relatively high market shares, due to its favorable properties, such as oil-, temperature- and ozone resistance.[4; 34]

By analogy with isoprene rubber, there are four possible isomeric configurations of the monomeric chloroprene unit. In contrast to IR, *trans*-1,4-poly(chloroprene) is dominating.[3] The corresponding structures are shown in Figure 3:

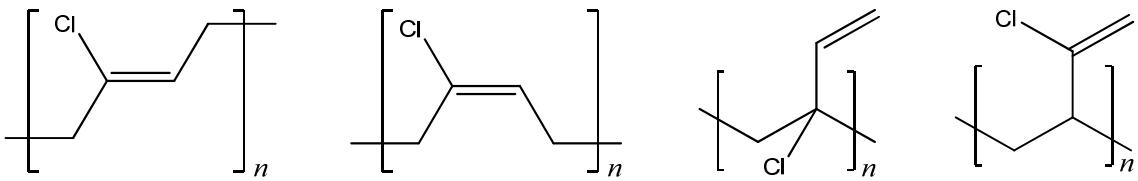

Figure 3. Isomeric structures of the chloroprene units[1]. (based on [3])

[1] By convention, *trans* and *cis* denotation for monomeric units is determined by the steric arrangement of the backbone C-atoms of the polymer, rather than by side chain atoms.[35]

Production

Chloroprene, the monomeric unit of chloroprene rubber, is produced by addition of chlorine to butadiene in the Distillers-Process, yielding a mixture of 1,2- and 1,4-dichlorobutadiene.[1; 36] Isomerization and cleavage of hydrochloric acid results in the desired 2-chloro-1,2-butadiene. Poly(chloroprene) is thereafter produced via radical polymerization in aqueous emulsion, at temperatures between 10 and 45 °C and pH between 9 and 13. Alkali salts of rosin acid are used as emulsifying agents along with sodium sulfonates. Depending on the reaction temperatures, the ratio of isomeric units can be modified. High *trans*-1,4-poly(chloroprene) is yielded at lower temperatures, while an increasing content of *cis*-1,4-, 1,2-, or 3,4-poly(chloroprene) is obtained at higher temperatures.[3] At a conversion of approximately 70%, the reaction is shortstopped and acidified to pH 5.5 to 7.0 (usually with acetic acid). Finally, the rubber is coagulated at -15 °C, washed up, dried and crushed.[3; 37; 38]

Properties and Application

Chloroprene rubber products generally tend to have a good resistance to weathering, ozone cracking, chemical degradation and heat aging. Its resistance to aliphatic hydrocarbons, mineral oils and greases is eminent; however, it exhibits poor resistance to acids, organic solvents and fuels. To mention is the excellent flame resistance of chloroprene rubber, as in fact it is a self-extinguishing material. Further, it provides good rubber-metal bonding features. Besides the outstanding properties of chloroprene rubber, its mechanical properties are typically inferior to those of natural or even synthetic poly(isoprene) rubber and the material tends to harden with time.[1; 39; 40]

In terms of vulcanization, chloroprene rubber exhibits fundamentally different chemical characteristics than other diene rubbers. The highly electronegative chlorine atoms deactivate the C-C double bonds in the backbone chain of the polymer, and therefore sulfur vulcanization occurs only to a limited or almost negligible extent. For this reason, chloroprene rubber is cross-linked by the addition of metal oxides, usually zinc oxide or

magnesium oxide. Chloroprene rubber latex is most commonly used for dipped goods, such as meteorological balloons or rubber gloves. It is also applied for impregnating, coating and lining woven tissues. In addition, molded foams for furniture and mattresses, as well as binding agents or elastic concretes are made from chloroprene rubber latex.[39; 41]

2.1.3.3 Acrylonitrile-Butadiene Rubber Latex (NBR)

Acrylonitrile-butadiene rubber, usually abbreviated to nitrile rubber, is the product of copolymerization of butadiene with 15 to 45% acrylonitrile. The poly(acrylonitrile-*co*-1,3-butadiene) was firstly synthesized in 1930 by I.G. Farben (Germany), via emulsion polymerization.[18; 42] The chemical structure of the copolymer is shown in Figure 4:

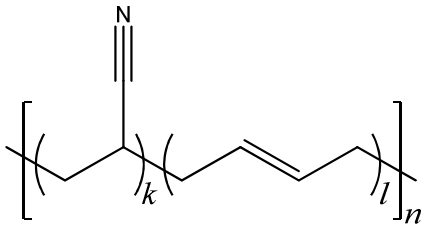

Figure 4. Chemical structure of the acrylonitrile-butadiene copolymer.[3]

Production

Nitrile rubber is produced via copolymerization in an aqueous emulsion, starting with acrylonitrile and butadiene at mild temperatures ranging from 0 to 30 °C and operating pressures between 2 and 7 bar. Among the most commonly used emulsifying agents are alkali salts of fatty acids and rosin acid. The polymerization is initiated by redox systems and co-catalyzed by metal salts. At a turnover of 70 to 80%, the reaction is usually terminated by a shortstopping agent, e.g. a reducing agent. Residual monomeric units are removed by distillation and the obtained product is stabilized by adding phenols or

diphenylamine. Finally, the rubber is coagulated by addition of electrolytes at elevated temperatures and subsequently dried and pressed.[3; 28; 42]

Considering the kinetics of the reaction, the rates of polymerization of acrylonitrile and butadiene vary distinctly. As a result, the ratio of monomeric units in the final product, which is a random copolymer, differs from the ratio in the reaction mixture. The nitrile content in commercially available acrylonitrile-butadiene rubber materials varies from approximately 15 wt% (low nitrile) up to $>$ 50 wt% (high nitrile).[3; 32; 42]

Properties and Applications

Main properties of the nitrile rubber can be tuned by simply adapting the acrylonitrile content of the copolymer. It exhibits rather good swelling resistance against oils, fats and fuels, which can be improved by increasing the acrylonitrile portion. However, the resistance to polar solvents decreases at the same time. A higher nitrile content leads also to an improved abrasion resistance and hardness. Rubbers with lower nitrile content on the other hand, exhibit a better cold temperature behavior. In any case, the acrylonitrile-butadiene rubbers are prone to ozone degradation.[4; 43]

In contrast to other synthetic rubbers, NBR may be vulcanized with different crosslinking systems and curing can be carried out at low (room temperature) and high temperatures likewise.[4; 44]

NBR products are used in applications, which demand high mechanical stability. Hence, it is the material of choice for seals, hoses, protective clothes, conveyers but also disposable nitrile rubber gloves.[3]

2.2 Polymer Blends

Blending of readily available substances is an important approach to develop novel polymer materials. By blending, the favorable features of two or more polymers can be combined, leading to a product with unique properties. The development and application of polymer latex blends in different industrial fields has been of great interest, mainly to avoid the cost intensive development of new polymers and also to meet newly defined requirements. Polymer blend materials are applicable for instance in automotive industry, packaging, electrical applications and many more.[18; 45]

2.2.1 Thermodynamics of Polymer Blends

Polymer mixtures or polymer blends can be divided into three major types, based on their mixing behavior: The first group comprises *miscible* or *completely miscible* polymer materials, resulting in a homogenous polymer blend. In that case, the blended material exhibits a single-phase structure and a single glass transition temperature. *Immiscible polymer blends*, in which the polymeric materials are thermodynamically incompatible, are more frequently observed. They can be identified by two (or more) distinct glass transition temperatures. However, the transition between these two types is not well-defined. Polymer blends can therefore also be present in a *partially miscible* system, having distinct glass transition temperatures, which are shifted from the corresponding values of the single materials. Additionally, the definition of *compatible polymer blends* must be mentioned, describing basically immiscible polymer materials, which exhibit uniform physical properties due to a high degree of internal interactions.[15; 33; 46]

Whether or not two polymers are miscible, is fundamentally depending on the Gibb's free energy of mixing, which is directly related to the enthalpy of mixing and the entropy of mixing[47] according to:

$$\Delta G_{mix} = \Delta H_{mix} - T\,\Delta S_{mix} \qquad \textbf{(Eq. 1)}$$

ΔG_{mix} ... free energy of mixing [J]
ΔH_{mix} ... enthalpy of mixing [J]
T ... temperature [K]
ΔS_{mix} ... entropy of mixing [J K^{-1}]

Only in case of a negative free energy of mixing of ($\Delta G < 0$), the polymers or constituents are completely miscible. However, even for negative values of Gibb's free energy, phase separation can occur.[47; 46] Consequently, a homogenous blend of two components A and B can only be produced if also the following equation holds true:

$$\left(\frac{\partial^2 \Delta G_{mix}}{\partial \varphi^2}\right)_{p,T} > 0 \qquad \textbf{(Eq. 2)}$$

φ ... volume fraction of component B [1]

The generalized possibilities for the dependency of the free energy of mixing ΔG_{mix} on the blending ratio φ of an idealized binary mixture (at constant temperature and pressure) are illustrated in Figure 5:

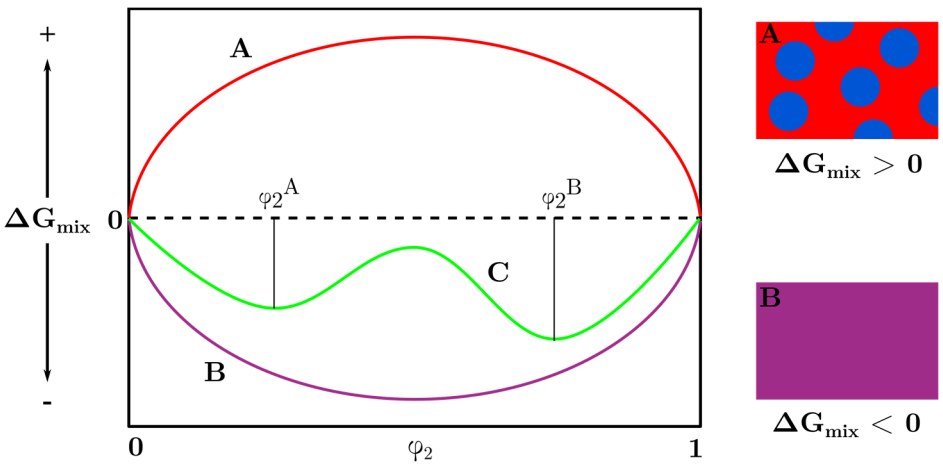

Figure 5. Idealized representation of the three possibilities for the dependence of ΔG_{mix} of a binary mixture on composition (φ_2 = volume fraction of polymer B). (based on [45])

In case of a positive ΔG_{mix} at all blending ratios, as illustrated by curve A, an immiscible and heterogeneous system is present, as per definition the mixing is thermodynamically hindered. Curve B, in contrast to that, represents a fully miscible and homogenous system down to a molecular level, for all mixing ratios. In that case, ΔG_{mix} takes negative values for the entire composition and the second derivative of ΔG_{mix} is positive throughout. The case of a partially miscible system is described by curve C. Here, two local minima at compositions φ_2^A and φ_2^B are shown, at which the second derivative of ΔG_{mix} changes signs. Any mixture with a blending ratio in between those two compositions will spontaneously exhibit phase separation.[45; 46; 48]

The entropy of mixing, ΔS_{mix}, is a direct function of all different possible combinations and configurations of the system. For molecules with a large molecular weight the segmental movement is strongly limited, which makes the mixing entropy negligibly small in case of polymer blends. Interaction forces, such as dispersion forces, dipole-dipole-interaction or hydrogen bonding between the components of the blend establish a certain interaction energy, which is expressed by the mixing enthalpy ΔH_{mix}. If $\Delta H_{mix} < 0$, the components of a polymer blend are either partially or completely miscible.[46; 47]

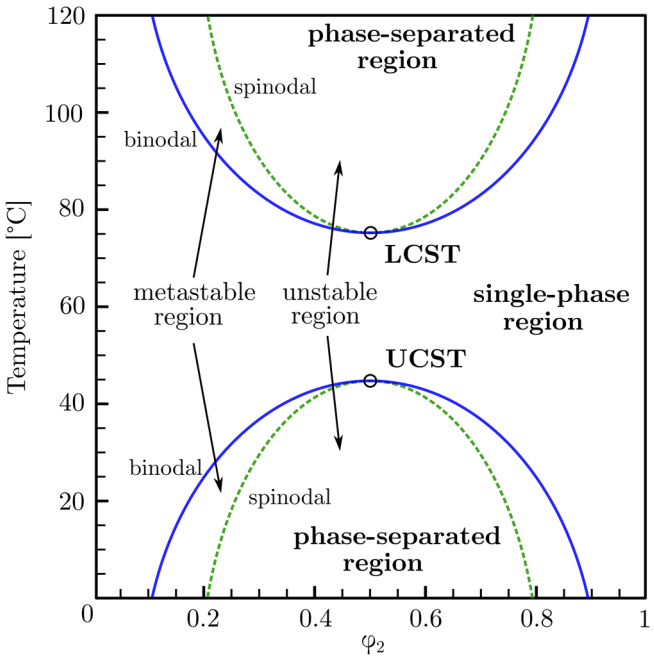

Figure 6. Phase diagram for a binary mixture showing UCST and LCST (φ_2 = volume fraction of polymer B). (based on [45])

Apart from molecular interactions, external physical values, especially temperature and pressure determine the miscibility of the polymer blend system. Figure 6 represents a general phase diagram for a binary system with dependency on temperature and blending ratio. Polymers that are immiscible at lower temperatures may become thermodynamically compatible and therefore miscible when increasing the temperature. The diagram shows three different regions of distinct miscibility properties: a miscible, single-phase region, metastable regions between binodal and spinodal curves and unstable, phase-separated regions, which are bounded by the spinodals. The upper critical solution temperature (UCST) describes the point, above which the blend is miscible. However, the UCST is obviously dependent on the composition of the mixture. When reaching even higher temperatures, exceeding the lower critical solution temperature (LCST), the previously single phased material will again become immiscible. It should be noted, that a phase diagram with two critical temperatures is generally valid for low molecular mass components. Polymer blends do not necessarily show lower or higher critical solution temperature points.[45; 46]

A total mutual solubility of two components is the ultimate condition, in which a single-phase system can be produced. Systems with a partial solubility exhibit finely dispersed, separated phases with a very low interfacial energy. Most polymer blends however, prevail principally an immiscible system resulting from a positive mixing enthalpy and very small mixing entropy.[45] To prevent demixing, the interaction energy in of the components can be increased by different measures, such as the application of compatabilizing agents.[3] Those lead to a decrease of interfacial tension, while the interfacial adhesion is increased at the same time. Further, the generation of very finely dispersed phases and stabilization thereof during the mixing process is possible. Compatabilizers are mostly AB-type block-copolymers, forming covalent linkages across the interface and ultimately lowering the interfacial tension.[3; 30]

2.3 Vulcanization Chemicals and Compounding Additives

2.3.1 Vulcanization

Vulcanization is the chemical process, in which the polymer matrix of an elastomer is converted into a cross-linked three-dimensional network. Briefly, a plastic and moldable substance is processed to an elastic and flexible material. The product properties are determined by the vulcanization process, which, in most cases, essentially requires the presence of a cross-linking agent and high temperatures. Colloidal sulfur, peroxides and metallic oxides in combination with activators and accelerators are the most commonly used vulcanization systems. In this work, only sulfur and metallic oxide curing systems were investigated and are therefore described in the following section.[3; 18; 49]

2.3.1.1 Sulfur Vulcanization

Colloidal sulfur is the most conventional vulcanization or cross-linking agent for poly(diene) rubbers, forming thioether bonds and polysulfide bridges between the distinct polymer molecules under elevated temperatures. In modern rubber processing, vulcanization activators (e.g. ZnO or MgO) and various accelerators are applied to control the curing rate and the degree of cross-linking, as well as other features of the vulcanizate.[1; 44; 50] An example of a typical sulfur curing system is shown in Table 2:

Table 2. Example of a typical sulfur curing system.[3]

Component	phr
Sulfur (sulfur donor)	**0.5–7**
Activator (e.g. ZnO, MgO)	**1–10**
Accelerator system	**0.25–10**

Sulfur forms a variety of different intermolecular and intramolecular crosslinks (as shown in Figure 7): monosulfide bridges (thioether bonds), di- and polysulfide bridges as well as intramolecular main-chain bonded sulfur bridges.

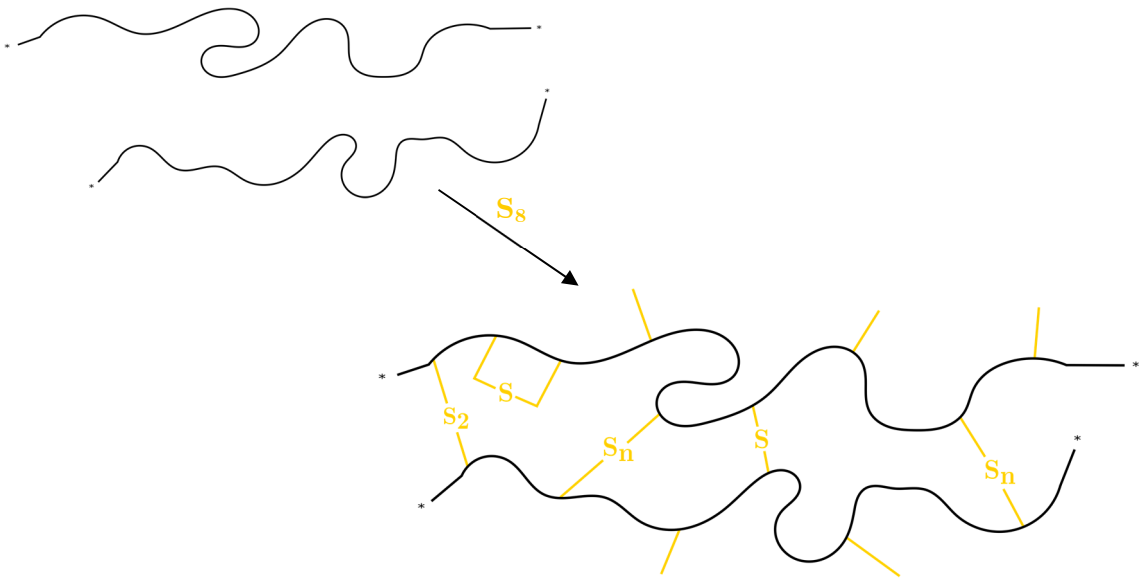

Figure 7. Schematic illustration of sulfur links between polymer chains. (based on [45])

2.3.1.2 Metal Oxide Vulcanization

Chloroprene rubber exhibits fundamentally different chemical characteristics in terms of vulcanization than other diene rubbers. The highly electronegative chlorine atoms deactivate the C-C double bonds in the backbone chain of the polymer, which makes sulfur vulcanization not applicable for CR. For this reason, metal oxide vulcanization is the method of choice, which is usually carried out by addition of zinc oxide or magnesium oxide. [39; 41; 50] Several possible reaction mechanisms for the cross-linking of CR using metal oxides have been proposed, e.g. by *Kovacic* (1955)[51], *Pariser* (1960)[52], *Vukov* (1984)[53] or more recently by *Berry et al.*(2015)[41].

2.3.2 Accelerating Agents

Due to the relatively slow cross-linking reaction between the rubber chains and sulfur, vulcanization without the addition of accelerating agents is time consuming and inefficient. The number of known accelerating chemicals is far beyond 100, of which about 50 are commonly used and established in rubber industry.[54] Accelerators are defined by their features: on the one hand they increase the rate of crosslink-formation, and on the other hand they lower the required vulcanization temperature and as well improve the overall efficiency of vulcanization.[55] In sulfur vulcanization, usually a combination of accelerators is used, which are denoted as primary and secondary accelerators. Whilst primary accelerators maintain a proper scorch delay and exhibit slow to fast curing, secondary accelerators contribute to very fast curing reactions.[56] Accelerators may be divided into several groups based on to their chemical structures. A classification according to the ASTM includes: *Thiazoles*, *sulfenamides*, *guanidines*, *dithiocarbamates*, *thiurams* and *thioureas*.[59] Of those, thiazoles and sulfenamides are considered primary accelerators, while guanidines, dithiocarbamates as well as thiurams are secondary ones. The thiourea type accelerator is a specialized compound for the crosslinking of chloroprene rubber. Other types of accelerators for rubber vulcanization are dithiophosphates, xanthogenates, benzothiazoles and benzothiazole sulfenamides.[56]

2.3.2.1 Thiazoles

Thiazole type accelerators are prepared from carbon disulfide, aniline and sulfur. The most prominent examples are 2-mercaptobenzothiazole disulfide (MBTS), 2-mercaptobenzothiazole (MBT) (shown in Figure 8) and the zinc salt of 2-mercaptobenzothiazole (ZMBT). While MBT and MBTS are commonly used in dry compound vulcanization, the zinc salt is rather used for processing of dipped goods, exhibiting a good scorch safety and aging characteristics. Because of the moderate curing rates, thiazoles are part of the primary accelerators.[1; 3; 56]

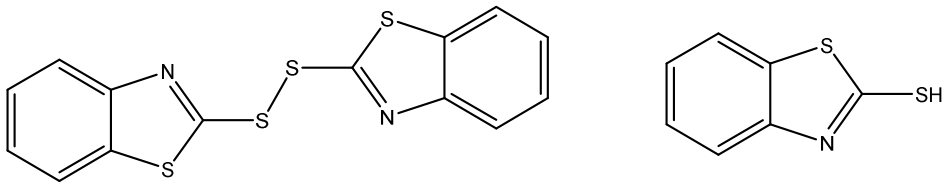

2-Mercaptobenzothiazole disulfide
(MBTS)

2-Mercaptobenzothiazole
(MBT)

Figure 8. Chemical structures of selected thiazole type accelerators.[3]

2.3.2.2 Sulfenamides

Primary accelerators of the sulfenamide type can either be prepared from an *N*-chloramine or derived from corresponding amine salts of 2-mercaptobenzothiazole. The characteristics, such as cure rate and scorch time are determined by the amine functional groups. Generally, sulfenamides with a high process safety are favored. Most popular accelerators within this group are *N*-cyclohexyl-2-benzothiazole sulfenamide (CBS or sometimes CBTS) and *N*-tert-butyl-2-benzothiazole sulfenamide (TBBS) (structures shown in Figure 9).[3; 56]

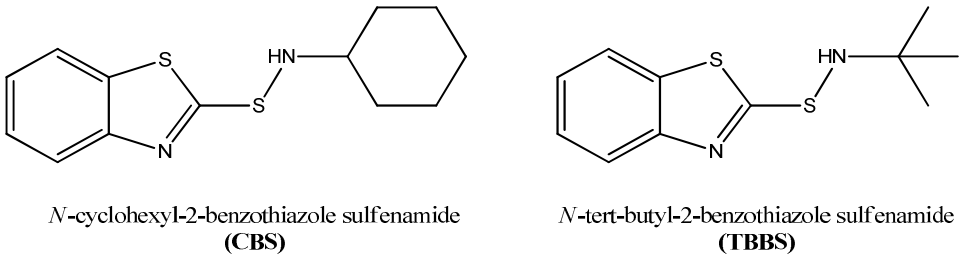

N-cyclohexyl-2-benzothiazole sulfenamide **(CBS)**

N-tert-butyl-2-benzothiazole sulfenamide **(TBBS)**

Figure 9. Chemical structures of selected sulfenamide type accelerators.

2.3.2.3 Guanidines

Guanidines are rather slow acting accelerators, and therefore rarely used as a single or main accelerator. However, they are important secondary accelerators for thiazole type components, especially in terms of diene rubber vulcanization. Activation of guanidine accelerators requires the presence of zinc oxide and sulfur, leading to formation of polysulfide cross-links and typically to vulcanizates of high tensile strength, satisfying elastic properties but also poor aging characteristics. Well known examples are diphenylguanidine (DPG) and di-*o*-tolylguanidine (DOTG) as shown in Figure 10.[1; 3; 56]

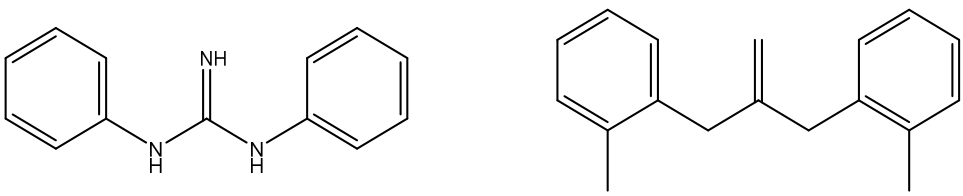

N,N'-diphenylguanidine **(DPG)**

N,N'-di-*o*-tolylguanidine **(DOTG)**

Figure 10. Chemical structures of selected guanidine type accelerators.[3]

2.3.2.4 Dithiocarbamates

Dithiocarbamates are very fast or "ultra-fast" curing accelerators, which are conventionally coupled with thiazole or sulfenamide type additives. Products obtained from curing with dithiocarbamates show good tensile strength and elasticity characteristics. They are usually applied as zinc salts or rarely as ammonia salts and especially suitable for pharmaceutical and medical products, including dipped goods. Zinc dimethyl- (ZDMC), zinc diethyl- (ZDEC) and zinc dibutyldithiocarbamate (ZDBC) (structures shown in Figure 11) rank among the most frequently used examples of this accelerator group.[1; 3; 56]

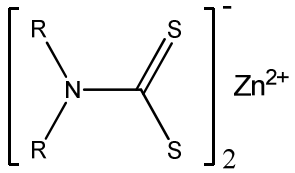

R=Methyl: Zinc dimethyldithiocarbamate **(ZDMC)**
R=Ethyl: Zinc diethyldithiocarbamate **(ZDEC)**
R=Butyl: Zinc dibutyldithiocarbamate **(ZDBC)**

Figure 11. Chemical structures of selected dithiocarbamate type accelerators.[3]

2.3.2.5 Thiurams

Thiuram type compounds are very fast to ultra-fast accelerators, which are derived from the dithiocarbamates and prepared from carbon disulfide and secondary amines. Besides accelerating the cross-linking, di- and trisulfide thiurams also serve as sulfur donors in systems with low elemental sulfur content. Thiurams are versatilely applicable as primary but also as secondary accelerators, resulting in products with high crosslinking densities, good tensile and elastic properties. Tetramethylthiuram disulfide (TMTD) along with tetramethylthiuram monosulfide (TMTM) are the most common examples (see Figure 12).[1; 3; 56]

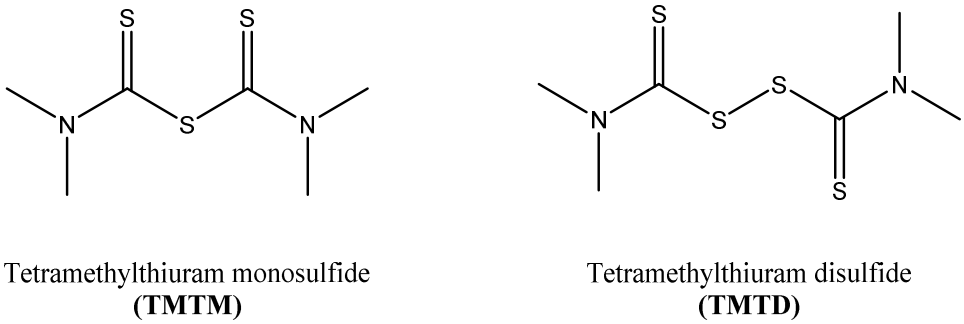

Tetramethylthiuram monosulfide **(TMTM)**

Tetramethylthiuram disulfide **(TMTD)**

Figure 12. Chemical structures of selected thiuram type accelerators.[3]

2.3.2.6 Thioureas

Thioureas are specialized compounds for cross-linking and accelerating vulcanization of chloroprene rubber and other polymers with labile allyl-chlorine atoms. Just as guanidines, they require zinc oxide for activation. The best-known example is ethylene thiourea (ETU) which, together with DPG, is the most effective accelerator system for chloroprene rubber. However, due to claimed carcinogenicity and reprotoxicity, substitute materials for ETU are demanded. Other examples of this class of accelerators are diethyl thiourea (DETU) and diphenyl thiourea (DPTU), shown in Figure 13.[1; 3; 56]

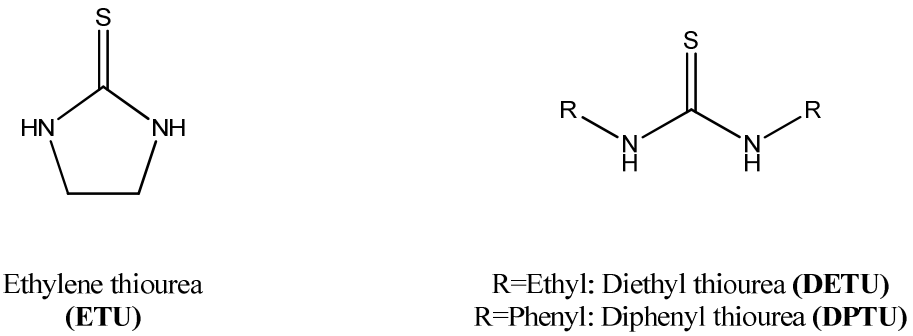

Ethylene thiourea **(ETU)**

R=Ethyl: Diethyl thiourea **(DETU)**
R=Phenyl: Diphenyl thiourea **(DPTU)**

Figure 13. Chemical structures of selected thiourea type accelerators.[3]

2.3.3 Fillers

Filling materials are used in plastics with the purpose of cheapening the product or improve the properties of the material. Most commonly, they are inexpensive inorganic materials, which simply extend the bulk mass or volume, and therefore lower the overall costs. Reinforcing fillers additionally improve certain properties, such as mechanical strength, moldability or stability, which results from a beneficial chemical interaction between the polymeric matrix and the filling material. Widely used fillers are calcium carbonate ($CaCO_3$), carbon black, silica (SiO_2), clay, mica, glass fibers and many others.[31; 55; 57; 58]

2.3.4 Functionalizing Additives

Functionalizing additives for rubber compounding include but are not limited to plasticizers, lubricants or flame retardants.

Plasticizers are generally used to enhance the flexibility as well as durability of plastics. By acting as spacers between the polymer chains, they facilitate rotational movement and make the material more flexible. Further, they can affect the Youngs modulus and the glass transition temperature. Most common plasticizers used in the rubber industry are based on mineral oils.[18; 30; 57; 59]

Lubricants improve the processability of the material by reducing friction to the processing equipment, but also by lowering the viscosity of the bulk. Typical examples are fatty acids, paraffins and metallic soaps.[18; 30; 57; 59]

Flame retardants are organic or inorganic chemicals, used to prevent combustion of the polymer by exposure to high temperatures. They either function by decomposition and generation of water, or they form a foamed protective layer against oxygen and heat. Examples are aluminum hydroxide, zinc borate, as well as chlorinated or brominated organic compounds.[18; 30; 57; 59]

2.3.5 Polymer Stabilizers

A big variety of stabilizers is applied in polymer processing, with the most important ones being antioxidant agents, light stabilizers and anti-aging agents. However, the border between those types of stabilizers is often not clearly defined. Stabilizing agents improve processability, durability and weatherability by preventing degradation of the polymers during the manufacturing process, as well as during shelf life and usage. Exposure to heat, oxygen, ozone, weathering or radiation are possible reasons for polymer degradation. Oxidative degradation is minimized by the application of antioxidants, which serve either as free-radical or peroxide scavengers (primary or secondary antioxidants). The most common primary antioxidants are sterically hindered phenols, while trivalent phosphorous compounds are used as secondary ones. Both types are usually applied in combination. Light stabilizers and UV-light absorbers are needed, to reduce the aging effects, which are induced by free radical or UV-light exposure.[18; 30; 57; 59]

2.3.6 Others

Further possible additives for polymer processing are organic and inorganic pigments, used for coloration. For different latex rubber products, also wetting and foaming agents, antifoams and surface-active agents can be used.[3] In case of polymer blends, compatibilizers are frequently used to support miscibility.[60]

2.4 Latex Product Manufacturing

As opposed to solid rubber processing, the manufacturing of products from latexes is much more convenient. It compromises compounding the latex with the respective vulcanization agents and additives of choice and subsequent coagulation by a variety of methods, including dipping, casting or foaming.[2; 48]

2.4.1 Latex Dipping

Fundamentally, the latex dipping process produces thin film polymer goods by immersing a specifically designed former, usually made from ceramic, glass or plastics, into a compounded latex mixture. By gently withdrawing the former, a homogenous latex layer is maintained. The vast majority of latex rubber products are made by these dipping processes. The thickness of produced films can be tuned by varying the dipping time or implementation of multiple dipping steps. Leaching, drying and finally curing and stripping off the product complete the manufacturing process.[1; 26]

Deposition of the latex rubber particles and subsequent film formation as part of the dipping process is performed using three different methods: straight dipping, heat-sensitive dipping and coagulation dipping, of which the latter is the most common one to be used in industry – termed coagulant latex dipping.[1] A schematic representation of the process is shown in Figure 14**:**

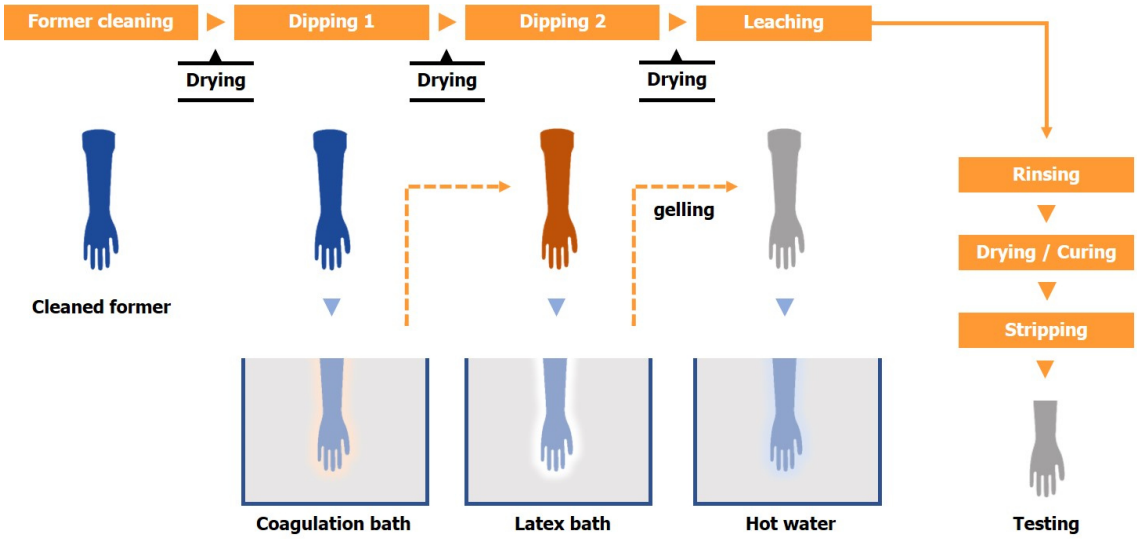

Figure 14. Schematic illustration of the coagulation dipping process. (based on [13])

Starting by thorough cleaning, drying and pre-heating of the porcelain former, they are thereafter immersed into a coagulant solution for a short dwell time of 20 to 40 seconds. The composition of the coagulation solution is crucially depending on the type of rubber particle stabilization. Typically, in case of ionically stabilized particles, it is prepared as an aqueous salt solution, containing a mixture of carbonates, chlorides and nitrates. After drying the coagulation salt layer on the former, it is dipped into the formerly compounded aqueous latex formulation for a defined dwell time. The latex bath is usually chilled to room temperature by a cooling system, to avoid unwanted premature vulcanization in the mixture. During this second dipping process, the actual latex film is formed on the surface of the former. By variation of the dwell time as well as the dry rubber content of the latex bath, the film thickness is determined.[13; 61]

The generally accepted mechanism of the film formation, as in the coagulant dipping process, is schematically illustrated in Figure 15:

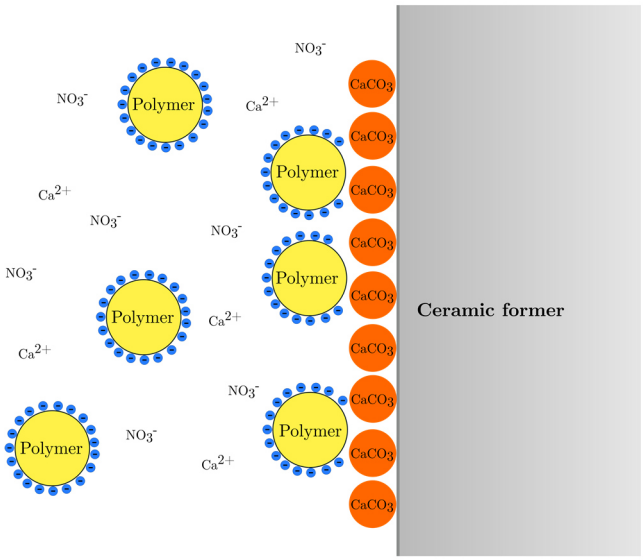

Figure 15. Schematic illustration of film formation (as in the coagulant dipping process). (based on [27])

Generally, polymer particles, which are in the illustrated case stabilized by negative charges, become destabilized in presence of other ionic species, such as nitrate or calcium ions. By immersing the former into the latex bath, which is held at ambient temperatures, parts of the previously applied salt re-dissolve immediately, leading to a high concentration of ions in the vicinity of the former. Destabilized latex particles then start to build up a continuous layer on the former. In the following, another short drying step is performed, in which the formation of a stable film is induced. A first leaching process, the so called wet-gel leaching is conducted, in which excess of water-soluble agents and residual coagulation salts are extracted. Leaching is conventionally done using hot deionized water (e.g. at 80 °C). Subsequently, the drying and vulcanization of the latex product, followed by an optional second leaching step (dry-gel leaching) is carried out. The final stripping off of the product concludes the coagulation dipping process. Post-treatment of the films is a further versatile process and is done according to the desired properties. Typical film thicknesses by this process range from 50 to 300 µm.[3; 13; 27; 62; 63] To obtain significantly thinner latex films (e.g. for membranes or contraceptives), the straight dipping process is the method of choice, which does not comprise the usage of

coagulation chemicals, but relies on former-wetting and latex viscosity. Contrary, heat-sensitized dipping is used for very thick latex products.[13]

2.4.2 Other Manufacturing Processes

Besides latex dipping, foaming and casting are two further important processing methods for latex rubber. Latex foaming is used to produce pillows, mattresses and similar products. In many applications however, latex is replaced by polyurethane foam products, due to its more convenient processability. Within the casting process, latex is gelled into a mold form or cavity to produce all sorts of latex toys, masks or tools.[1; 3]

3 Objectives of the Work

The goal of the thesis and the related practical work was the preparation and characterization of improved materials for disposable rubber gloves. Three major approaches towards the optimization of the latex materials were considered:

Firstly, the adaption of cross-linking formulations and variation of process parameters for the production of all kind of rubber films was implemented. This included the application of different types and quantities of vulcanization and cross-linking agents or accelerators as well as the adaption of processing steps and curing conditions. In a second approach, blending of different latex materials, especially isoprene rubber and chloroprene rubber, but also NBR/NBR blends at different ratios, was used to process latex films, in order to investigate the influence of the blending on the mechanical properties. Further, a series of tests using inexpensive filling materials for acrylonitrile-butadiene rubber films was carried out.

Conducted experiments should on the one hand serve as a general screening of the different approaches towards the improvement of rubber glove production. On the other hand, produced synthetic rubber latex products would ideally exhibit equal or even better mechanical properties than their natural rubber latex counterpart.

The produced latex films were primarily characterized by tensile tests, with the tensile strength, ultimate elongation and different moduli being of interest. Additionally, electron microscopy (SEM and ESEM) and energy dispersive X-ray spectroscopy (EDX) were used to investigate a number of selected materials, especially blended ones. Other utilized analytical methods include differential scanning calorimetry (DSC), dynamic light scattering (DLS) and swelling experiments, in order to obtain additional information about the produced materials.

4 EXPERIMENTAL PART

4.1 Materials and Methods

4.1.1 List of Chemicals

Table 3. List of used chemicals and respective suppliers and purity.

Chemical	**Supplier**	**Grade**
Acrylonitrile Butadiene Rubber KNL 834 (NBR "K")	Kumho *	Technical
Acrylonitrile Butadiene Rubber 6338 (NBR "S")	Synthomer *	Technical
Chloroprene Rubber LIPREN T (CR)	Synthomer *	Technical
$CaCO_3$ (dispersion)	In-house prep. *	Technical
Coagulation dispersion I ($Ca(NO_3)_2$)	In-house prep. *	Technical
Coagulation dispersion II ($Ca(NO_3)_2$, $CaCO_3$, $CaCl_2$)	In-house prep. *	Technical
Di-isopropyl xanthogen polysulfide (AS 100)	In-house prep. *	Technical
DPG (dispersion)	In-house prep. *	Technical
ETU (dispersion)	In-house prep. *	Technical
Isoprene Rubber Cariflex IR401 (IR)	Kraton *	Technical
Natural Rubber (NR)	In-house sample *	Technical
PM-IR 3 (dispersion)	In-house prep. *	Technical
Potassium hydroxide	Carl Roth	$\geq 85\%$
Sulfur (dispersion)	In-house prep. *	Technical
Sodium diisobutylnaphthalinsulfonat (Nekal BX)	Carl Roth	Technical
ZDBC (dispersion)	In-house prep. *	Technical
Zinc diisononyldithiocarbamate (Arbestab Z)	In-house prep. *	Technical
ZnO (dispersion)	In-house prep. *	Technical

* Prepared and/or provided by Semperit Technische Produkte GmbH, Wimpassing (Austria)

4.1.2 Mechanical Testing

4.1.2.1 Film Thickness

Film thickness of the produced materials was measured using a **Mitutoyo Digimatic Micrometer, Series 293** (Mitutoyo, Japan). Mean values were calculated from multiple measurements (minimum of five measuring points).

4.1.2.2 Preparation of Test Specimen

Due to highly varying elongation properties of the different materials, test specimen of two different geometries were used. On the one hand, dumbbell-shaped tensile test specimen with **a total length of 100 mm** (clamping length = 75 mm, width = 3 mm) were utilized for materials having a comparably low maximum elongation (less than 700%). This testing specimen (as seen in Figure 16) is in conformity with the testing norm for medicinal and examination gloves DIN EN 455-2:2015.[64] On the other hand, dumbbell-shaped test specimen with a **total length of 75 mm** (clamping length = 50 mm, width = 4 mm) were used. Specimen were stamped out using either a hydraulic press (Weber-Hydraulik, Germany) or a manual cutting press (Zwick Roell, Germany).

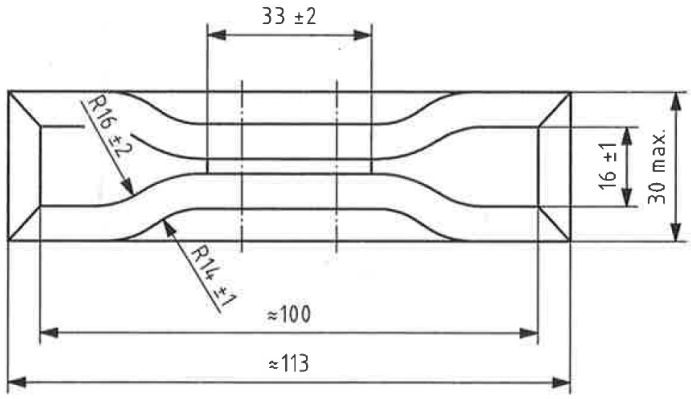

Figure 16. Specifications of a tensile test specimen according to DIN EN 455-2:2015.[64]

4.1.2.3 Tensile testing equipment

Mechanical characteristics, i.e. tensile strength, ultimate elongation and moduli of latex films were mainly carried out using an **Autograph AGS-X (5 kN)** universal tensile tester (Shimadzu, Japan). The applied tensile rate was set to 500 mm min^{-1} (according to DIN EN 455-2:2015) at a full force scale of 5 kN, measuring tensile testing specimen bars of different clamping lengths (50 mm or 75 mm).

Additionally, a **ProLine tensile tester Z005** (Zwick Roell, Germany), equipped with a pneumatic XForce P load cell system and a videoXtens camera system for optical measurement of extension (both Zwick Roell, Germany) was used to determine mechanical properties on tensile test specimen bars, again according to DIN EN 455-2:2015.

4.1.3 Electron Microscopy and EDX

Facilities and equipment for electron microscopy were provided by the Austrian Centre for Electron Microscopy (FELMI-ZFE, Graz, Austria).

4.1.3.1 ESEM-EDX

Electron microscopic imaging was performed utilizing a **FEI ESEM Quanta 600 FEG** Environmental Scanning Electron Microscope (Thermo Fisher Scientific, USA) coupled with energy dispersive X-ray spectroscopy (EDX) and equipped with a Thermal Field Emission Gun (FEG), a Large Field Detector (LFD) for secondary electron imaging and a Solid-State Backscattered Electron Detector (SSD). Analysis was conducted with an accelerating voltage (EHT or U_0) ranging from 2.0 to 4.0 kV and a relative spot size (Ss) between 2.0 and 3.0 at with a constant gas pressure of 70 Pa (H_2O). More precise measurement parameters are indicated in the caption of the corresponding images.

4.1.3.2 SEM-EDX

Further electron microscopy, specifically EDX-mapping, was done using a **Zeiss Sigma 300 VP** (Zeiss, Germany) coupled with energy dispersive X-ray spectroscopy (EDX). The device was equipped with a Thermal Field Emission Gun (FEG) and a C2D detector. For EDX-mapping, the accelerating voltage was set to 7.5 kV and the spot size value to 2.0. More precise measurement parameters are indicated in the caption of the images.

4.1.4 Differential Scanning Calorimetry (DSC)

DSC measurements were performed at Semperit Technische Produkte GmbH, utilizing a **DSC 214 Polyma** (NETZSCH Thermal Analysis, Germany). DSC curves were recorded at a range of -150 °C to 300 °C at a heating rate of 10 K min^{-1}, measured in N_2-atmosphere (40 and 60 mL min^{-1} respectively). Glass transition temperatures were defined by inflection point values.

4.1.5 Dynamic Light Scattering (DLS)

Dynamic Light Scattering analyses on the raw latex materials at a dilution of 1:50,000 were realized with an **Anton Paar Litesizer™ 500** equipped with a BM10 high end batch module (Anton Paar, Austria). Measurements were kindly performed by Dr. Chemelli (Institute of Inorganic Chemistry at Graz University of Technology, Austria).

4.1.6 Swelling and Crosslinking Density

Volumetric and mass swelling of the materials were determined by immersing latex film samples (50 to 60 mg) in vials filled with 20 mL toluene for 48 hours. The samples were weighed before and directly after swelling, as well as after drying to constant mass at 70 °C (fivefold evaluation). Crosslinking density and the degree of crosslinking were thereafter calculated according to the Flory-Rehner method, using the corresponding Flory-Huggins parameters for the different materials, as given in Table 4:

Table 4. Flory-Huggins interaction parameters χ, and densities of used materials.

Rubber	ρ **[g cm^{-3}]**	χ **[1]**
IR	**0.92** a)	**0.34** b)
CR	**1.23** a)	**0.386** a)
NBR	**0.97** a)	**0.435** c)

a) taken from [65]; b) taken from [66]; c) taken from [67]

After determining the degree of volumetric swelling, the Flory-Rehner equation for polymer-solvent-interaction[68] can be applied to determine the average molecular mass between two crosslinks, $\overline{M_C}$:

$$\overline{M_C} = V_l \rho_p \frac{\phi^{\frac{1}{3}} - \frac{\phi}{2}}{-[ln(1-\phi) + \phi + \chi\phi^2]} \qquad \textbf{(Eq. 3)}$$

$\overline{M_C}$ ... average molecular weight between crosslinks [g mol^{-1}]
V_l ... molar volume of the solvent [cm^3 mol^{-1}]
ρ_p ... density of the polymer [g cm^{-3}]
ϕ ... reciprocal volume swelling [1]
χ ... Flory-Huggins-parameter [1]

By convention, the crosslinking density, υ_e, is defined as the reciprocal value of $\overline{M_C}$.

4.2 Preparation Method of Latex Films

4.2.1 Preparation of Rubber Latex Compounds

Preparation of the latex rubber mixtures was realized using 500 mL beakers, starting with weighing out the crude latex material(s), deionized water and potassium hydroxide (10 wt% or 1 wt%) according to the corresponding formulations. The composition was moderately stirred at room temperature for about 5 min. Subsequently, the vulcanization agents (i.e. ZnO, S or PM-IR-3), as well as stabilizing agents were added and incorporated by continuous stirring. After 5 to 10 min of stirring, required activators, accelerators and (if applicable) fillers were added to the mixture and allowed another 10 min of stirring at room temperature to ensure a proper distribution of all ingredients. For the actual latex dipping step, the compounded latex mixture was transferred into a 100 mL graduated measuring cylinder, cooled with a water bath.

4.2.2 Coagulant Dipping Process

All dipped latex goods were produced by the coagulant dipping process, as depicted in Figure 14**.** Ceramic formers of a total length of about 20 cm, mimicking the shape of fingers, were thoroughly cleaned with a basic detergent to remove organic residues and consequently rinsed wish deionized water and acetone. Thereafter, the formers were pre-heated to the eventual drying temperature between 100 and 130 °C in a heating cabinet. In next instance, the formers were dipped into the coagulant solution at 65 °C for 30 sec. Within this work, two different coagulation mixtures were used: One the one hand, an aqueous dispersion of $Ca(NO_3)_2$ and on the other hand an aqueous dispersion of $CaCO_3$, $CaCl_2$ and $Ca(NO_3)_2$. The latter one may be referred to as "mixed coagulant" throughout this work. After applying the coagulant, formers were dried again for at least two minutes. Coagulant dipping was then performed for a dwell time of 20 sec, in most cases followed by wet-gel leaching (before curing) and dry-gel leaching (after curing) in deionized water

(60 sec and 30 sec respectively, at 80 °C). Certain materials were additionally treated with pre-vulcanization (3 h at 40 °C or 50 °C) under constant stirring.

4.2.3 Drying

Dipped latex films were crosslinked by drying, utilizing a **Heraeus T 6030** heating cabinet equipped with a kelvitron® microprocessor temperature controller (Heraeus, Germany). Drying temperatures and durations were varied and adapted to the respective materials.

4.3 Rubber Formulations and Processing Parameters

4.3.1 NR Latex Formulations

Natural rubber (drc = 60%) films were produced using an internal standard formulation (as used by Semperit Techn. Produkte GmbH) without further optimization of the curing system. For vulcanization, an aqueous dispersion (PM-IR-3, tsc = 50%) of vulcanization agents (containing 27.3 wt% S, 13.6 wt% ZnO and 9.1 wt% TiO_2) was applied. The accelerator system was a combination of di-isopropyl xanthogen polysulfide (AS 100) and zinc diisononyldithiocarbamate (Arbestab Z), provided as aqueous dispersions (60 wt% and 35 wt% respectively). Sodium diisobutylnaphthalinsulfonate (Nekal, 10 wt%) was used as stabilizing agent. KOH (10 wt%) and deionized water were used to adjust the pH value and the total solid content of the mixture (50%). The formulations and processing parameters are shown in Table 5:

Table 5. Formulations and processing parameters for NR latex (50% tsc).

	A	**B**
Component	phr	phr
Natural rubber	100	100
PM-IR-3	2.75	5
Nekal	1.25	1.25
AS100	1	1
Arbestab Z	1	1
KOH	2 wt%	2 wt%
Coagulant	$Ca(NO_3)_2$, $CaCl_2$, $CaCO_3$	
Pre-vulcanization	without with (3 h, 50 °C)	
Curing conditions	20 min, 120 °C 30 min, 120 °C	

4.3.2 IR Latex Formulations

Isoprene rubber materials were cured according to an internal standard formulation (as used by Semperit Techn. Produkte GmbH), which was slightly adapted and used at different curing conditions. IR Kraton 401 (drc = 0.62%) was used as starting material and the vulcanization chemical used was PM-IR-3, together with AS100 and Arbestab Z as accelerators. Films with and without pre-vulcanization were tested. The formulation and processing parameters are summarized in Table 6:

Table 6. Formulations and processing parameters for IR latex (50% tsc).

	A	**B**
Component	phr	phr
IR Kraton 401	100	100
PM-IR-3	2.75	5
Nekal	1.25	1.25
AS100	1	1
Arbestab Z	1	1
KOH	2 wt%	2 wt%
Coagulant	$Ca(NO_3)_2$, $CaCl_2$, $CaCO_3$	
Pre-vulcanization	without with (3 h, 50 °C)	
Curing conditions	20 min, 120 °C 30 min, 120 °C 40 min, 120 °C 20 min, 130 °C 30 min, 130 °C	
Leaching	Wet-gel + Dry-gel	

4.3.3 CR Latex Formulations

CR Lipren T (drc = 60%) was cross-linked using different amounts of zink oxide as cross-linking agent, and zinc(II) dibutyl dithiocarbamate (ZDBC) as accelerator at a fixed amount of sulfur. ZnO, ZDBC and S were provided as aqueous dispersions (tsc = 38% each). All films were produced with and without pre-vulcanization. The curing formulations **A**–**F** and processing parameters were applied according to Table 7:

Table 7. Formulations and processing parameters for CR latex with ZnO, S and ZDBC (50% tsc).

	A	**B**	**C**	**D**	**E**	**F**
Component	phr	phr	phr	phr	phr	phr
CR Lipren T	100	100	100	100	100	100
ZnO	3	3	3	5	5	5
S	2	2	2	2	2	2
ZDBC	0	0.5	1.5	0	0.5	1.5
KOH	2 wt%	2 wt%	2 wt%	2 wt%	2 wt%	2 wt%
Coagulant	$Ca(NO_3)_2$, $CaCl_2$, $CaCO_3$					
Pre-vulcanization	without with (3 h, 40 °C)					
Curing conditions	20 min, 120 °C					
Leaching	Wet-gel + Dry-gel					

Further, combinations of diphenyl guanidine (DPG) and ethylene thiourea (ETU), each provided as aqueous dispersion with tsc = 13.3%, were applied as accelerating agents for

CR latex films. In that case, the content of ZnO, as well as the contents of DPG and ETU were varied according to formulations **A**–**D in** Table 8:

Table 8. Formulations and processing parameters for CR latex using DPG and ETU (50% tsc).

	A	**B**	**C**	**D**
Component	phr	phr	phr	phr
CR Lipren T	100	100	100	100
ZnO	3.5	3.5	5	5
S	2	2	2	2
DPG	0	1	1	1
ETU	0	0.5	0.5	1
KOH	2 wt%	2 wt%	2 wt%	2 wt%
Coagulant	$Ca(NO_3)_2$, $CaCl_2$, $CaCO_3$			
Pre-vulcanization	without with (3 h, 50 °C)			
Curing conditions	20 min, 120 °C 30 min, 120 °C			
Leaching	Wet-gel + Dry-gel			

4.3.4 IR/CR Latex Blend Formulations

Blends of IR Kraton 401 and CR Lipren T, at a blending ratio of 50/50 (wt/wt, based on dry rubber content), were cured using the formulations **A**–**C** and conditions shown in Table 9. These formulations were derived from the standard IR curing formulations:

Table 9. Formulations and processing parameters for IR/CR latex blends (50% tsc).

	A	**B**	**C**
Component	phr	phr	phr
IR Kraton 401	50	50	50
CR Lipren T	50	50	50
PM-IR-3	2.75	5	2.75 [a)]
ZnO	0	0	5 [b)]
Nekal	1.25	1.25	1.25
AS100	1	1	1
Arbestab Z	1	1	1
KOH	2 wt%	2 wt%	2 wt%
Coagulant	$Ca(NO_3)_2$		
	$Ca(NO_3)_2$, $CaCl_2$, $CaCO_3$		
Pre-vulcanization	without		
	with (3 h, 50 °C)		
Curing conditions	20 min, 120 °C		
	30 min, 120 °C		
Leaching	Wet-gel + Dry-gel		

[a)] amount calculated in respect to IR content; [b)] amount calculated in respect to CR content

4.3.5 NBR Latex Formulations

4.3.5.1 Different Curing Systems

NBR latex Kumho KNL (drc = 40%) was cross-linked using a variety of formulations and different processing parameters. Basically, the curing of NBR was carried out using only ZnO at different temperatures and curing times. Additionally, systems using ZnO, sulfur and zinc(II) dibutyl dithiocarbamate (ZDBC) were tested. All films were produced with and without pre-vulcanization. Further, the effect of leaching and different coagulation-dispersions was tested. Formulations and processing parameters are shown in Table 10:

Table 10. Formulations and processing parameters for NBR latex (19% tsc).

	A	**B**	**C**
Component	phr	phr	phr
NBR KNL (Kumho)	100	100	100
ZnO	3.5	3.5	5
S	-	2	2
ZDBC	-	0.5	0.5
KOH	pH 10	pH 10	pH 10
Coagulant	$Ca(NO_3)_2$		
	$Ca(NO_3)_2$, $CaCl_2$, $CaCO_3$		
Pre-vulcanization	without		
	with (3 h, 50 °C)		
Curing conditions	20 min, 120 °C		
	30 min, 120 °C		
	20 min, 130 °C		
	30 min, 130 °C		
Leaching	Wet-gel + Dry-gel		

4.3.5.2 Filled NBR Latex

In another experiment, Kumho NBR latex was filled with calcium carbonate ($CaCO_3$, aqueous dispersion, tsc = 66%) up to 20 phr and cured according to the formulations **A**–**E** and conditions in Table 11:

Table 11. Formulations and parameters for filled NBR latex (19% tsc).

	A	**B**	**C**	**D**	**E**
Component	phr	phr	phr	phr	phr
NBR KNL (Kumho)	100	100	100	100	100
ZnO	3.5	3.5	3.5	3.5	3.5
$CaCO_3$	0	5	10	15	20
KOH	pH 10	pH 10	pH 10	pH 10	pH 10
Coagulant	$Ca(NO_3)_2$, $CaCl_2$, $CaCO_3$				
Pre-vulcanization	without with (3 h, 50 °C)				
Curing conditions	20 min, 120 °C 30 min, 120 °C 20 min, 130 °C 30 min, 130 °C				
Leaching	Wet-gel + Dry-gel				

4.3.5.3 NBR/NBR Latex Blends

Blends of different NBR latexes, Synthomer 6338 (drc = 45%) and Kumho KNL (drc = 40%), were blended in the ratios 100/0, 70/30, 50/50, 30/70 and 0/100 (wt/wt, based on drc) and cured according to the formulations **A**–**E** and conditions in Table 12:

Table 12. Formulations and parameters for NBR/NBR latex blends (19% tsc).

	A	**B**	**C**	**D**	**E**
Component	phr	phr	phr	phr	phr
NBR KNL (Kumho)	0	30	50	70	100
NBR 6338 (Synthomer)	100	70	50	30	0
ZnO	3.5	3.5	3.5	3.5	3.5
KOH	pH 10	pH 10	pH 10	pH 10	pH 10
Coagulant	$Ca(NO_3)_2$, $CaCl_2$, $CaCO_3$				
Pre-vulcanization	without with (3 h, 50 °C)				
Curing conditions	20 min, 120 °C 30 min, 120 °C 20 min, 130 °C 30 min, 130 °C				
Leaching	Wet-gel + Dry-gel				

4.3.6 Latex Blends for Electron Microscopy

For investigation of the morphology and phase behaviour of latex blends using ESEM-EDX and SEM-EDX, different series of blends including NR/CR, IR/CR and NBR/CR were produced and processed to latex films. In order to avoid disturbing elements or unnecessary particles in the measurements, the films were dipped using the $Ca(NO_3)_2$-coagulant dispersion and all mixtures were prepared without the addition of additives, such as vulcanization agents, accelerators or stabilizers. Simply, potassium hydroxide and deionized water were used for stabilization and adjusting the total solid content. All films were made without pre-vulcanization and cured for 20 min at 120 °C. The produced samples and blending ratios are shown in Table 13:

Table 13. Latex blend samples for electron microscopy (50% tsc).

NR/CR (wt/wt)	**IR/CR** (wt/wt)	**NBR (Kumho)/CR** (wt/wt)
100/0	100/0	100/0
75/25	75/25	75/25
50/50	50/50	50/50
25/75	25/75	25/75
0/100	0/100	0/100

5 Results and Discussion

5.1 Preparation of Latex Films

Latex films for mechanical testing were exclusively prepared by the described coagulant dipping method. Primarily, the used coagulation agent was an aqueous dispersion of $CaCO_3$, $CaCl_2$ and $Ca(NO_3)_2$. In this composition, the main function of calcium carbonate is to act as releasing agent and to facilitate the removal of the film from the former surface. Consequently, the application of this coagulation mixture ensures a better workability in comparison to the usage of only $Ca(NO_3)_2$ as a coagulation chemical. The $Ca(NO_3)_2$-dispersion was applied for comparative purposes as well as for materials, which were to be investigated by electron microscopy. The reason for that was to avoid unnecessary atomic species in the final product (especially Cl^-). Parameters of applying the coagulant, e.g. time and temperature, were not varied otherwise and therefore not investigated.

Pre-vulcanization was carried out on selected mixtures for 3 hours at 50 °C and generally showed no negative consequences on the following processing steps. However, certain curing systems, especially those containing ZDBC, exhibited a seemingly higher viscosity after pre-vulcanization, which complicated the latex-dipping step. Therefore, the pre-vulcanization temperature for these formulations was lowered to 40 °C.

With few exceptions, all prepared films show a continuous and smooth surface. The occasional formation of flow marks and grains can on the one hand be attributed to an imprecise or too fast immersion during coagulation dipping, and on the other hand to solidified rubber agglomerations in the mixture. By leaching and vulcanization those defects can be almost eradicated.

5.2 Mechanical Properties

5.2.1 NR Latex Films

For the processing of natural rubber latex, the internal standard formulation for IR latexes (according to Table 5) was used. Investigating NR latex films served the purpose of comparison and therefore, neither the formulations nor the processing parameters were optimized thoroughly. NR latex films were prepared with and without pre-vulcanization and curing at 120 °C for 20 and 30 min respectively. Experimentally determined tensile strength and ultimate elongations for the materials are summarized in Table 14:

Table 14. Mechanical properties of NR latex films.

Formulation	no pre-vulcan., 20 min, 120 °C	no pre-vulcan., 30 min, 120 °C	pre-vulcan., 20 min, 120 °C	pre-vulcan., 30 min, 120 °C
	Film thickness [µm]			
A	274 ± 12	285 ± 9	269 ± 11	284 ± 12
B	266 ± 14	280 ± 15	281 ± 16	272 ± 10
	Tensile strength [N mm^{-2}]			
A	17.6 ± 2.3	17.0 ± 0.8	19.3 ± 1.5	21.2 ± 2.7
B	18.2 ± 1.4	18.5 ± 1.8	20.0 ± 0.9	20.9 ± 2.1
	Elongation at break [%]			
A	828 ± 46	801 ± 40	834 ± 35	818 ± 19
B	821 ± 36	788 ± 21	809 ± 25	822 ± 32

A: using 2.75 phr PM-IR-3; **B:** using 5 phr PM-IR-3

The obtained results show a quite constant film thickness of the produced films, ranging from 266 to 285 µm, which are in accordance with findings from previously conducted

research.[69] Regarding the tensile strength values, longer vulcanization times generally tend to have improving effects. Besides that, pre-vulcanization also exhibits a clearly enhancing effect on the mechanical properties for both formulations. However, no significant differences can be found between formulations A and B. Tensile strength values range from 17.0 N mm^{-2} to 21.2 N mm^{-2} at ultimate elongations between 788% and 834%.

Comparable experiments reported in literature exhibit clearly better mechanical properties: similar curing formulations for NR consistently yield tensile strengths of above 25 N mm^{-2} and maximum values of almost 30 N mm^{-2} and therefore outvalue the obtained results.[70; 71] Optimization of the curing formulation and processing parameters could potentially lead to further improvement of the mechanical properties. However, the detailed investigation of NR latex films is not within the scope of the thesis.

5.2.2 IR Latex Films

Compounding of isoprene rubber latex (Kraton 401) was carried out according to formulations A and B shown in Table 6. Several different curing conditions were investigated to find the most suitable curing time and temperature. Firstly, an internal standard formulation (A) (as used by Semperit Techn. Produkte GmbH) was applied to produce films with and without pre-vulcanization. Curing times of 20, 30 and 40 min at temperatures of 120 to 130 °C were used.

Measured film thicknesses of the obtained latex films are given in Table 15. The IR latex films show comparably high thicknesses of 279 to 309 µm, which makes them the thickest samples prepared within this work. It is also noticeable, that the deviation is rather high for most investigated films:

Table 15. Film thickness of IR latex films at different curing conditions.

Formulation	20 min, 120 °C	20 min, 130 °C	30 min, 120 °C	30 min, 130 °C	40 min, 120 °C
	Film thickness [µm]				
A	279 ± 11	282 ± 8	301 ± 14	309 ± 14	302 ± 8
B	285 ± 8	294 ± 13	n.a.	291 ± 9	n.a.

A: using 2.75 phr PM-IR-3; **B:** using 5 phr PM-IR-3

Generally, the films show a smooth surface and little number of defects. At longer curing times of 30 and 40 min, the films exhibit blistering, which however does not damage the surface of the film ultimately. Mechanical tests were performed using 75 mm tensile test specimen; the results for the test series using formulation A are illustrated in Figure 17. The collected results for all pre-vulcanized tested specimen are gathered in Table 27.

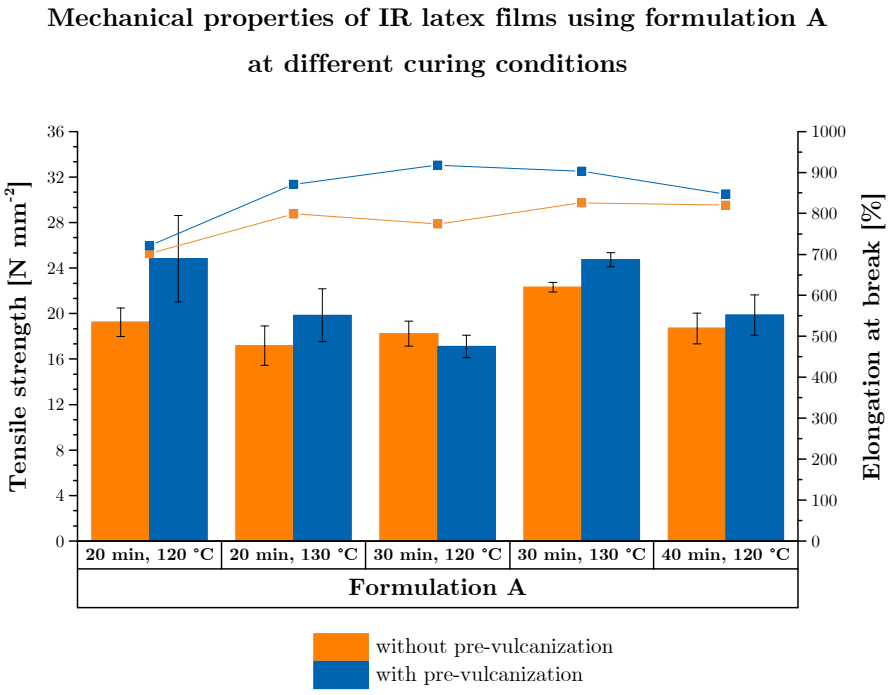

*(**bar charts** refer to left y-axis/tensile strength, **line charts** refer to right y-axis/elongation)*

Figure 17. Mechanical properties of IR latex films using standard formulation A at different curing conditions.

Vulcanization of IR latex compositions using the standard formulation A at different curing conditions shows, that for samples without pre-vulcanization, the highest tensile strength is yielded by curing at 130 °C for 30 min (22.3 N mm^{-2}). Second best condition for the used curing system is vulcanization at 120 °C for 20 min. Contrary to the expectations, curing at 120 °C for 30 and 40 min shows significantly lower tensile strength values than the optimal curing condition, not exceeding 19 N mm^{-2}. This might be related to the previously observed blistering during the curing process. Ultimate elongations range from 700% to 820% with the exact opposed tendency to the tensile strength. Regarding pre-vulcanized samples, curing for 20 min at 120 °C and 30 min at 130 °C yields the best tensile strength values of 24.8 and 24.7 N mm^{-2} respectively. Generally, pre-vulcanization leads to improved tensile strength (expect for curing at 120 °C for 30 min) as well as improved ultimate elongation for all samples. Internal reference values for IR Kraton 401, using an identical formulation and curing at 120 °C for 20 min, show a comparably lower tensile strength (19.2 N mm^{-2}) but a higher ultimate elongation (above 1000%).[1]

As mentioned, formulation B was additionally used for the vulcanization of IR latex mixtures. However, this test series did not show improved properties compared to formulation A. The results are shown in the appendix (Figure 39).

5.2.3 CR Latex Films

Formulations using different types of accelerators were investigated for the vulcanization of chloroprene rubber. ZnO and S were on the one side applied together with ZDBC, and on the other side with combinations of DPG and ETU. All samples were produced with and without pre-vulcanization, at varied curing conditions, resulting in film thicknesses between 180 µm and 195 µm. Figure 18 illustrates the mechanical properties of CR latex films produced with formulations using ZnO, S and ZDBC (formulations according to Table 7):

[1] Internal results provided by Semperit Techn. Produkte GmbH.

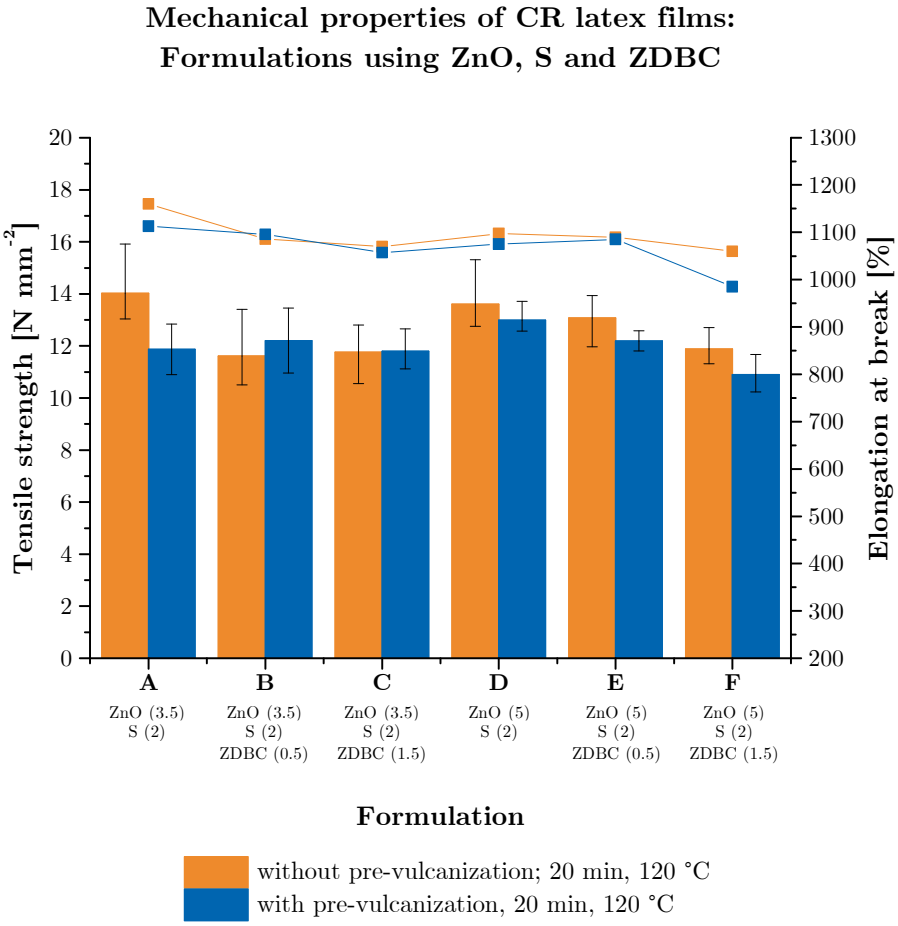

Figure 18. Mechanical properties of CR latex films using vulcanization formulations with ZnO, S and ZDBC.

The tested materials using different curing systems exhibit quite similar mechanical properties. Varying the amount of ZnO hardly effects the products tensile strength, which can be seen by little differences between formulations A–C (using 3.5 phr ZnO) and formulations D–E (5 phr ZnO). ZDBC-free formulations (A and D) reach the highest values for tensile strength and ultimate elongation (14.0 N mm^{-2} and 1000% respectively). By increasing the amount of ZDBC to 0.5 phr (B and E) and 1 phr (C and F), tensile strength decreases to values below 12 N mm^{-2} and the ultimate elongation ranges from 970 to 1050%. Conclusively, using ZDBC as a dithiocarbamate for curing chloroprene rubber latex leads to worsened properties.

In another test series, CR latex was cross-linked using DPG/ETU accelerator systems, together with ZnO and S (see formulations in Table 8). Determined film thicknesses of the produced and aged materials are very homogenous and range from 181 µm to 196 µm. A graphical comparison of the results from tensile testing is shown in Figure 19:

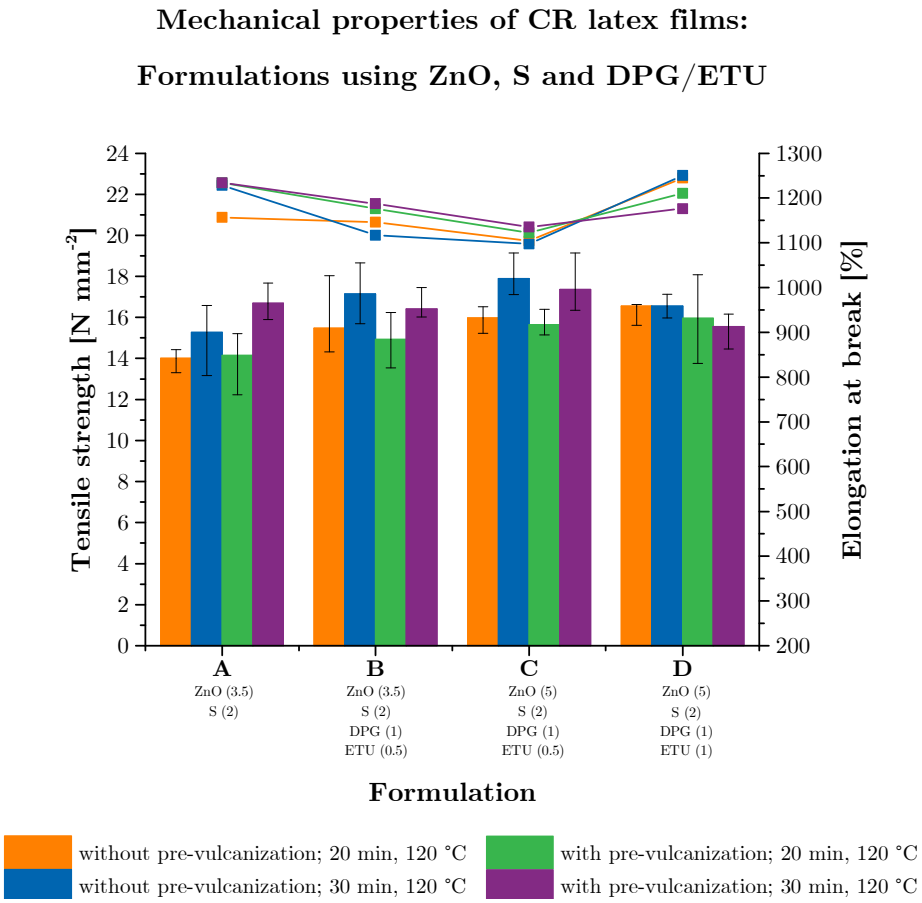

Figure 19. Mechanical properties of CR latex films using vulcanization formulations with ZnO, S and DPG/ETU at different curing conditions.

Here, formulation A corresponds to the system using only ZnO (3.5 phr) and S (2 phr), while formulations B–D use increasing amounts of ZnO, DPG and ETU. Despite health risk concerns, vulcanization formulations using DPG/ETU are still commonly used and

reportedly among the most efficient accelerator systems for chloroprene rubber latex, supposedly yielding the best mechanical properties.[72; 73] However, the use of DPG and ETU in the present systems together with ZnO and sulfur does not show significantly improved tensile strength or ultimate elongations. Formulation C yields the best single tensile strength values of 17.9 and 17.3 N mm^{-2} (at 30 min curing, without and with pre-vulcanization respectively). By the addition of higher quantities of DPG and ETU, only a small improvement (less than 10%) in terms of tensile strength can be seen for the samples with a curing time of 20 min. Generally, the variation of curing time and temperature shows little to no effect on the final product properties.

Optimization of CR latex vulcanization has been topic of internal investigation only to some extent, which is why no reliable reference values are available. In previous research work on the topic of latex blends by *Raunicher J.*, chloroprene rubber latex films were reported to reach tensile strengths of 14.5 N mm^{-2} and ultimate elongations of 1200%.[69] These values can be slightly improved with the present systems.

5.2.4 IR/CR Latex Blends

Blending of isoprene and chloroprene rubber latex was performed using different formulations and curing conditions with the aim to produce products, having good tensile strength as well as high ultimate elongation. To do so, the blended materials at a ratio of 50/50 (wt/wt) were cured using adapted IR-standard formulations with varied amounts of ZnO. The formulations can be seen in Table 9.

Film thicknesses of the IR/CR latex films (see Table 16) are dependent on the processing conditions. Films without pre-vulcanization have thicknesses between 169 and 178 µm, while those with pre-vulcanization are clearly thicker, with values of 185 to 191 µm. The formulation itself (A–C) does not influence the film thickness:

Table 16. Film thickness of IR/CR latex films using different curing formulations.

Formulation	no pre-vulc., 20 min, 120 °C	no pre-vulc., 30 min, 120 °C	pre-vulc, 20 min, 120 °C	pre-vulc, 30 min, 120 °C
	Film thickness [µm]			
A	172 ± 6	169 ± 8	191 ± 4	188 ± 8
B	178 ± 4	173 ± 6	185 ± 3	190 ± 7
C	171 ± 5	171 ± 10	188 ± 8	190 ± 8

A: using 2.75 phr PM-IR-3; **B:** using 5 phr PM-IR-3; **C**: using 2.75 phr PM-IR-3 and 5 phr ZnO

Gathered results of mechanical testing are shown in the appendix (Table 30). An illustration of tensile strength and ultimate elongation of the IR/CR latex films with adapted formulations are illustrated in Figure 20:

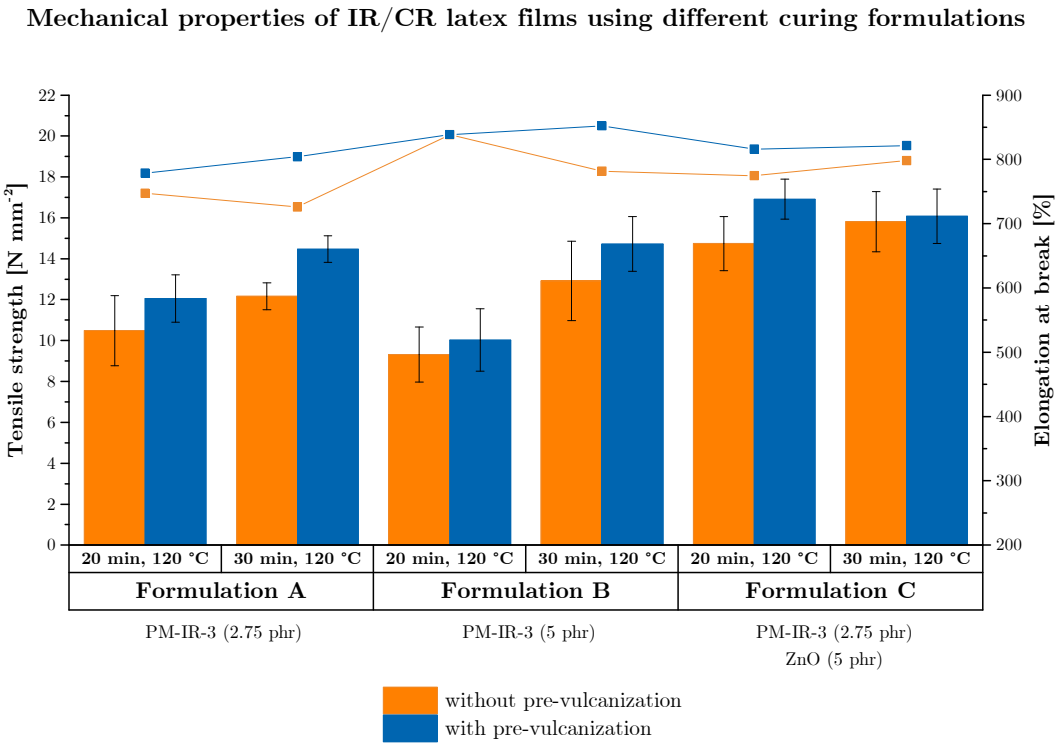

Figure 20. Mechanical properties of IR/CR latex films using different vulcanization formulations.

Formulations A and B show remarkably low tensile strength values for samples without pre-vulcanization, not exceeding the 12 N mm^{-2} mark. Clearly improved properties can be seen for pre-vulcanized samples, reaching values of above 14 N mm^{-2}. Also, longer curing times (30 min instead of 20 min) improves the properties of the product. Formulation C, in which additionally to 2.75 phr PM-IR-3 an amount of 5 phr ZnO (calculated in respect to the CR content) is used, shows clearly higher tensile strength compared to the other formulations, reaching 16.9 N mm^{-2}. The effect of pre-vulcanization is less significant though. The ultimate elongation for all samples is rather uniform and ranges from 700% to 850%, without significant differences between the formulations. Conclusively, for blends of IR and CR, the adaption of the vulcanization formulation is crucial. When using the standard formulation without adaption, the total amount content of ZnO for the cross-linking of CR is insufficient. By increasing the amount of ZnO in respect to the CR content, the mechanical properties can be optimized. Conclusively, the resulting values of tensile strength and elongation are lying in between those of the pure IR and CR latex materials.

5.2.5 NBR Latex Films

5.2.5.1 Formulation Variation and Film-Leaching

NBR latex (Kumho) was cross-linked using different combinations of ZnO, S and ZDBC (as shown by formulations A–C in Table 10). In doing so, the influence of increased amounts of ZnO, additional sulfur as well as ZDBC was investigated. Additionally, these mixtures were produced in two different ways: once with implementation of a leaching step (wet-gel and dry-gel leaching) and once without any film leaching. Leaching in general, is an essential step within the coagulant dipping process of latex films, primarily applied to remove residual chemicals and support the process of gelling.[34] For different types of rubber latexes, the combination of wet-gel and dry-gel leaching reportedly has improving effects on the mechanical properties.[74; 75]

Results of film thickness determination and tensile tests on the final products can be seen in Table 17 and Figure 21 respectively. All results, including moduli, are shown in Table 31 the appendix.

Table 17. Film thickness of NBR latex films with different formulations (without and with leaching).

Formulation	without leaching, 20 min, 120 °C	with leaching, 20 min, 120 °C
	Film thickness [µm]	
A	96 ± 2	96 ± 1
B	100 ± 4	97 ± 3
C	97 ± 4	100 ± 6

A: using 3.5 phr ZnO; **B:** using 3.5 phr ZnO, 2 phr S and 0.5 phr ZDBC; **C**: using 5 phr ZnO, 2 phr S and 0.5 phr ZDBC

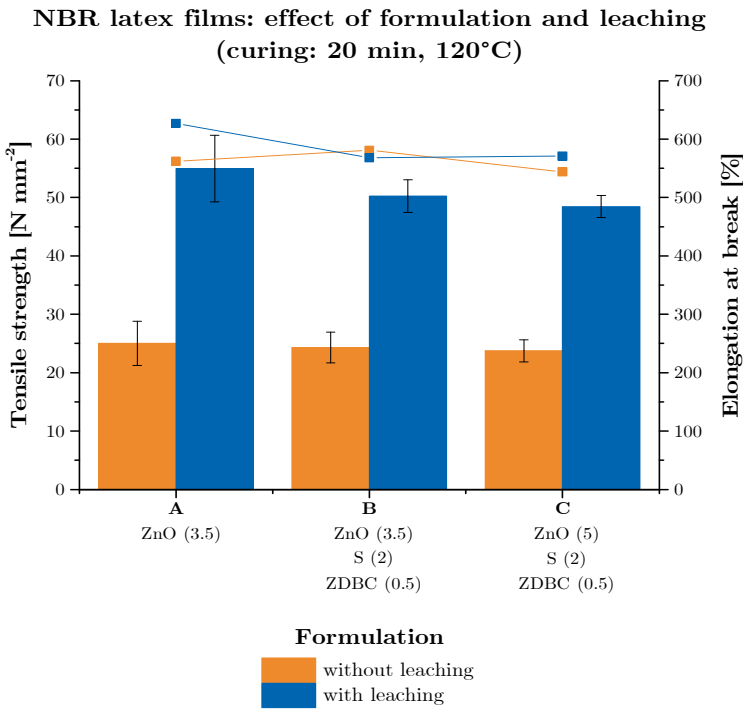

*(**bar charts** refer to left y-axis/tensile strength, **line charts** refer to right y-axis/elongation)*

Figure 21. Effect of leaching on mechanical properties of NBR latex films.

When comparing the different curing formulations without leaching, all of them result in highly comparable tensile strength values, ranging from 23.8 to 25.0 N mm^{-2} and ultimate elongations of 540 to 560%. That implies, that the addition of S and ZDBC (as in formulation B and C), does not positively influence the mechanical properties. Leaching obviously has a tremendous effect on the mechanical properties of the NBR films, improving the tensile strength from 25.0 N mm^{-2} up to 54.5 N mm^{-2} for formulation A, which uses only ZnO. Also, the ultimate elongation increases, yet to a lower extent. The very same effect can be seen for further samples (formulations B and C) yielding tensile strengths of 50.3 N mm^{-2} and 48.4 N mm^{-2} respectively. Overall, the tensile strength can be enhanced by about 110% using wet-gel and dry-gel leaching. This increase is higher as for comparable findings from *Ghazaly et al.*[76], reporting an average improvement of up to 60% simply by leaching of nitrile rubber films. However, the choice of NBR latex, as well as aging and various other factors are not identical, which does not allow a direct comparison.

5.2.5.2 Filled NBR latex films

Kumho NBR was filled with inexpensive, finely dispersed $CaCO_3$, up to a content of 20 phr and investigated in terms of mechanical properties. Applying the filling material had neither negative nor positive influence on the dipping performance or handling of the materials. The final products appear to have a slightly different haptic compared to the unfilled Kumho NBR films, being seemingly more brittle and having a rougher surface. Films were produced without and with pre-vulcanization and cured at varied

Results from film thickness measurements are shown in Table 18. The films have regular film thicknesses between 93 and 100 µm for materials without pre-vulcanization and slightly higher values in the range from 102 to 111 µm for pre-vulcanized ones. Increasing the filler loading from 5 phr up to 20 phr $CaCO_3$ has no effect on the thickness of the produced films:

Table 18. Film thickness of filled NBR latex films at different curing conditions.

Filler loading [phr]	no pre-vulc., 20 min, 120 °C	no pre-vulc., 30 min, 120 °C	pre-vulc, 20 min, 120 °C	pre-vulc, 30 min, 120 °C
	Film thickness [µm]			
5	96 ± 2	96 ± 1	102 ± 4	108 ± 6
10	100 ± 4	97 ± 3	107 ± 3	102 ± 4
15	98 ± 5	93 ± 6	111 ± 3	105 ± 3
20	98 ± 4	100 ± 6	109 ± 3	105 ± 2

Mechanical properties were determined using test specimen with a total length of 100 mm. Series of formulations with increasing filler load, starting with the unfilled Kumho NBR films at different curing conditions were compared. All measurement results are gathered in Table 32. In Figure 22, the graphical evaluations of two series (without and with pre-vulcanization; cured at 120 °C) are illustrated:

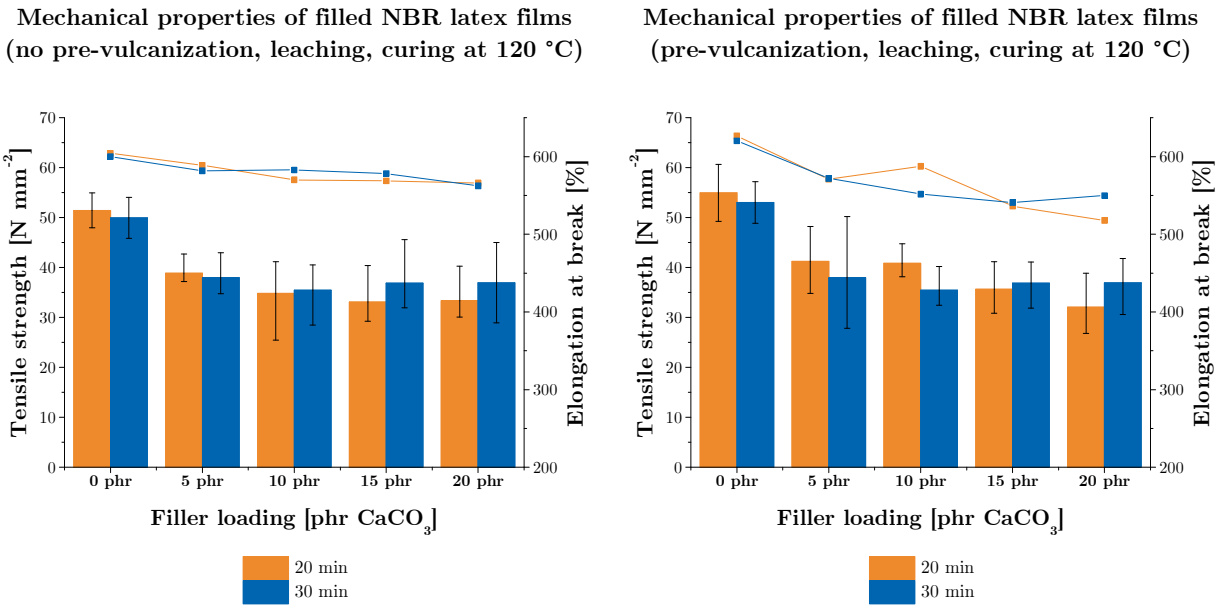

*(**bar charts** refer to left y-axis/tensile strength, **line charts** refer to right y-axis/elongation)*

Figure 22. Tensile strength and ultimate elongation of NBR latex films filled with $CaCO_3$ without (left) and with pre-vulcanization (right), cured at 120 °C.

As a general trend, tensile strength and ultimate elongation decrease by filling the rubber with calcium carbonate. In comparison with the unfilled materials, films loaded with 5 phr $CaCO_3$ experience a drop in tensile strength of approximately 20%. However, further increasing of the filler load results in rather stable values of both, tensile strength and ultimate elongation. In the range of 5 to 20 phr $CaCO_3$, films without pre-vulcanization reach tensile strengths of 33.4 to 38.9 N mm^{-2} and very uniform ultimate elongations of 560 to 600%. Pre-vulcanized mixtures produce a higher deviation regarding different curing times (20 and 30 min) and mean values vary from 32.0 N mm^{-2} for highly filled materials (20 phr) up to 41.2 N mm^{-2} for 5 phr filler loading. As calcium carbonate is a typical non-reinforcing filling material, the outcome of the experiments is just as anticipated. Worsening effects on the mechanical properties with an increasing portion of $CaCO_3$ have been reported in several research publications.[77; 78] Apart from this, the yielded results, especially in terms of tensile strength, are still significantly higher than for other materials, e.g. CR or IR films. As a reference point, as stated by the ASTM[79], nitrile rubber latex gloves (medical examination gloves) require a minimum tensile strength of 14 N mm^{-2}. This specification value can be easily surpassed by all tested materials in that experiment. Therefore, filling of NBR latex films with the used materials is a suitable approach for cost reduction of the general production procedure while still complying with the specifications.

5.2.3.3 NBR/NBR latex blends

Latex blend films were prepared from mixtures of two different NBR latexes (Synthomer and Kumho), by compounding the respective quantities and subsequent dipping and curing of the materials with ZnO (3.5 phr). The reason being, that in previous experiments by Semperit Techn. Produkte GmbH, films from NBR/NBR latex blends showed promising mechanical properties. Generally, dipping of the compounded NBR materials is convenient and all films exhibit a smooth surface and barely any defects.

All mechanical properties of the produced films are shown in Table 33. Film thicknesses of the materials are summarized in Table 19:

Table 19. Film thickness of NBR/NBR blend films at different curing conditions.

Blend (wt/wt)	no pre-vulc., 120 °C	no pre-vulc., 130 °C	pre-vulc, 120 °C	pre-vulc, 130 °C
	d [µm]			
S (100)	93 ± 6	97 ± 7	97 ± 3	97 ± 3
S/K (70/30)	97 ± 4	101 ± 2	93 ± 3	91 ± 5
S/K (50/50)	102 ± 5	106 ± 3	107 ± 2	99 ± 4
S/K (30/70)	102 ± 5	102 ± 7	104 ± 5	101 ± 3
K (100)	97 ± 5	100 ± 3	101 ± 5	103 ± 5

S = NBR Synthomer 6338, **K** = NBR Kumho KNL

All NBR/NBR blend films all show very uniform film thicknesses for each composition, independent of the curing conditions. Mean values range from about 93 to 105 µm, just as expected for the applied dipping dwell times. Comparing the mean thickness of films from different latex blend compositions, no significant deviation can be observed. Tensile tests to investigate the tensile strength and ultimate elongation were performed on tensile testing specimen with 100 mm total length. The results for a series of NBR/NBR blend films without and with pre-vulcanization, each cured at 130 °C are shown in Figure 23:

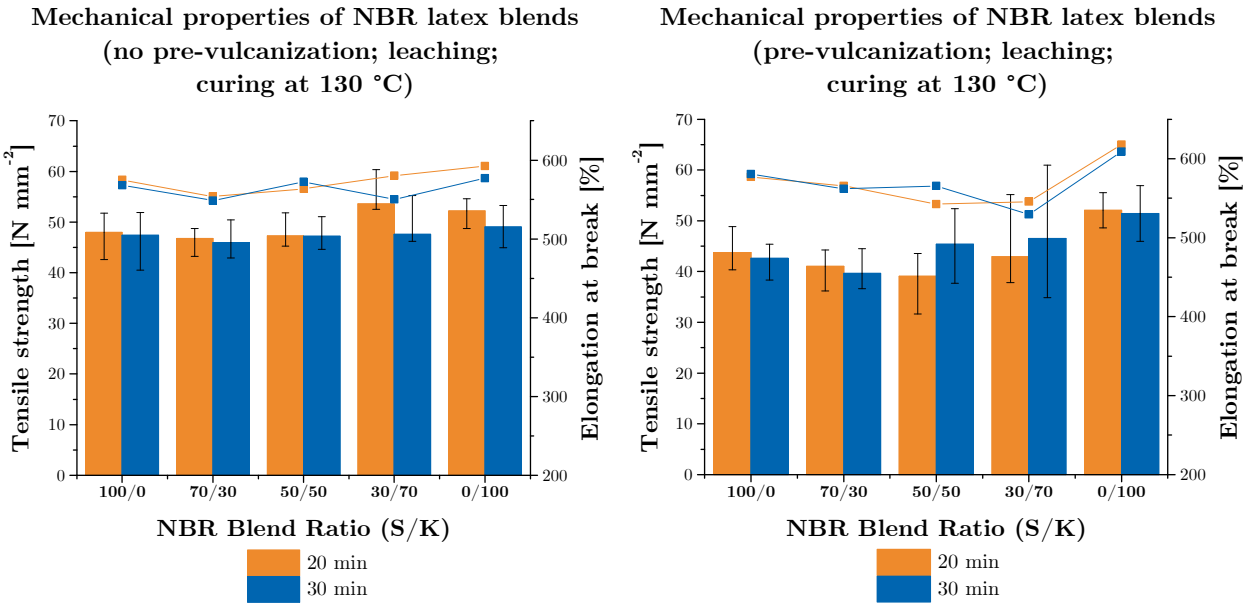

*(**bar charts** refer to left y-axis/tensile strength, **line charts** refer to right y-axis/elongation)*

Figure 23. Tensile strength and ultimate elongation of NBR/NBR latex blend films without (left) and with pre-vulcanization (right), cured at 130 °C.

Films without pre-vulcanization of the compositions S (100), S/K (70/30) and S/K (50/50) display rather constant mean tensile strength values between 45.9 and 48.0 N mm^{-2}, different curing times of 20 and 30 min do not affect the maximum values. Regarding the composition S/K (70/30), films cured for 20 min show a very good performance in tensile strength, exceeding a mean value of 55 N mm^{-2}. Finally, films from pure Kumho rubber, K (100), reach mean values of 52.2 N mm^{-2} (20 min curing time) and 49.0 N mm^{-2} (30 min curing time). Ultimate elongation for all compositions ranges from about 550% to 600% and does not show unexpected variations.

When comparing the results from latex films without and with pre-vulcanization, it becomes evident, that the tensile strength is significantly lowered. This holds true for all compositions except from K (100), which shows rather similar values of tensile strength and ultimate elongation. Especially S (100), S/K (70/30) and S/K (50/50) show inferior mean values ranging from only 36.8 N mm^{-2} to only 46.5 N mm^{-2}. It is also noticeable, that in some cases the curing time slightly effects the performance, however, a strong standard deviation for most samples can be seen. Ultimate elongations

of the pre-vulcanized samples do differ to some extent from the values for samples without pre-vulcanization. Though, the range of values from 525% to 620% is within the expectations. Conclusively, the properties of the single NBR rubber materials could be not significantly improved by blending them at different ratios. Further optimization could be performed, e.g. in terms of application of activating and accelerating agents.

5.3 Electron Microscopy and EDX

5.3.1 ESEM-Investigation of Latex Blends

ESEM-characterization of latex blends was done using a **FEI ESEM Quanta 600 FEG** Environmental Scanning Electron Microscope, to investigate the morphological properties. Secondary electron images as well as backscattered electron images were recorded up to magnifications of 24000x. However, as the resulting images of SE and BSE do not noticeably differ from each other, only recorded SE images are discussed in this section. Specimen used for the investigation were pure latexes and latex blends (see Table 13).

5.3.1.1 Morphology of Pure Latex Films

Figure 24 shows ESEM images of the tear fracture surface of a pure NR latex film at increasing magnifications:

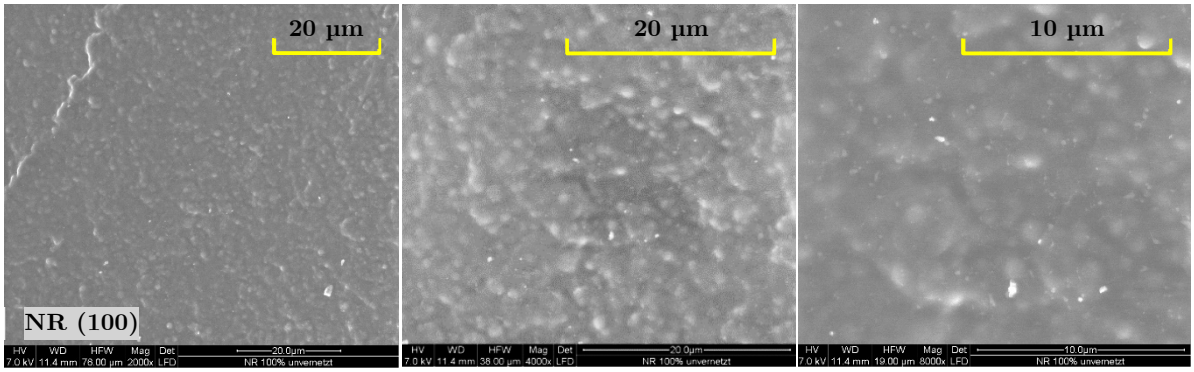

Figure 24. ESEM images (SE) of the tear fracture surface of a NR film (100) at magnifications of 2000x (left), 4000x (middle) and 8000x (right).

The microscopic images show a smooth tear fracture surface with very few tear paths. At higher magnification (4000x and 8000x) randomly distributed, non-orientated spherical particles can be observed, forming the surface of the specimen. The estimated

particle sizes range from approximately 500 to 1000 nm. These values are in agreement with the determined primary particle size by DLS. Further, the material seems rather homogenous without obvious impurities arising from the latex dipping process or air bubbles.

Images of a pure chloroprene rubber latex film at magnifications of 4000x, 8000x and 24000x can be seen in Figure 25:

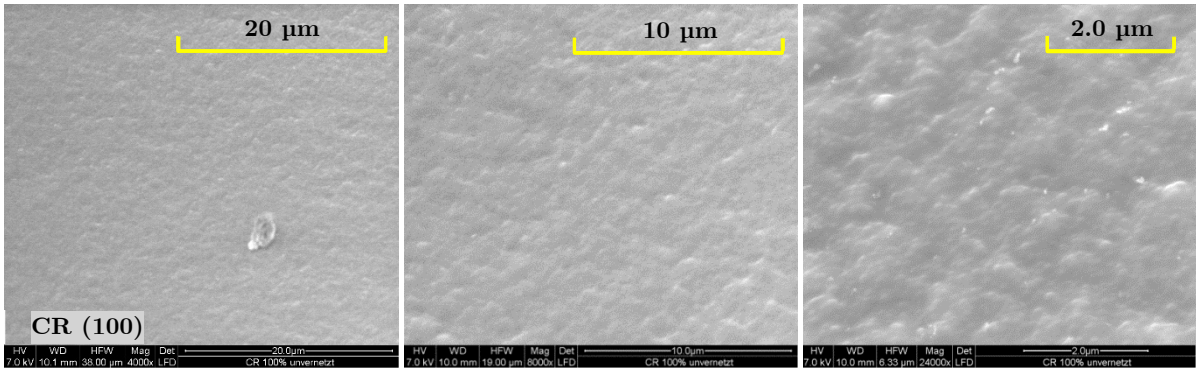

Figure 25. ESEM images (SE) of the tear fracture surface of a CR film (100) at magnifications of 4000x (left), 8000x (middle) and 24000x (right).

The pure CR sample shows a very smooth and plane surface in comparison to the NR specimen. Further, no obvious tear paths can be found on the fracture surface. At a higher magnification (24000x), the chloroprene rubber shows a homogenous distribution of partly distinct, but mainly deformed and joint particles. The size of the primary particles cannot be determined accurately. Regarding the high contact of the particles with each other, a high degree of film formation can be assumed.[80]

Finally, Figure 26 shows secondary electron images of the tear fracture surface of NBR (100) film at magnifications of 2000x, 4000x and 8000x:

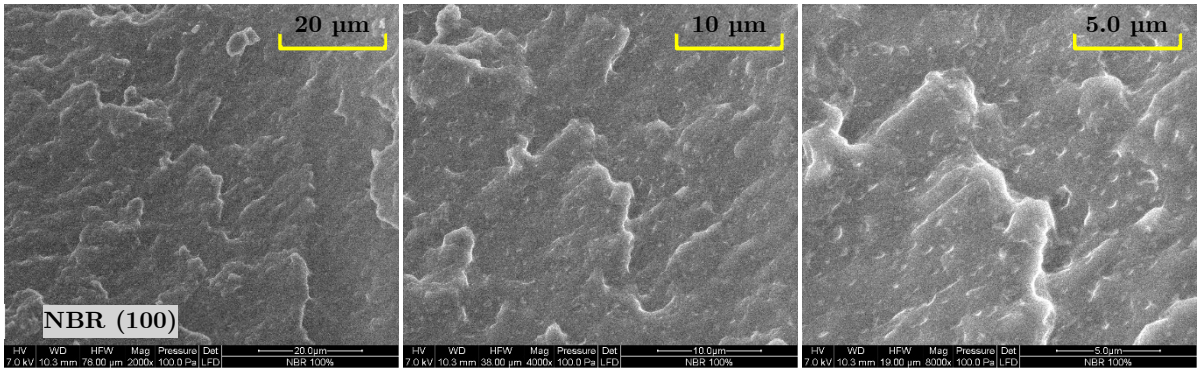

Figure 26. ESEM images (SE) of the tear fracture surface of an NBR film (100) at magnifications of 2000x (left), 4000x (middle) and 8000x (right).

The NBR latex film exhibits a quite different morphology, showing a high number of tear paths. No distinct spherical particles can be observed at any magnification. At a magnification of 8000x, shapeless structures of less than 500 nm in size become apparent, which could probably indicate inclusions.

5.3.1.2 Morphology of Blended Latex Films

Additionally to pure rubber latex materials, different blended materials were investgated using ESEM imaging. Figure 27 to Figure 29 show secondary electron images of NR/CR films at different blending ratios of 75/25, 50/50 and 25/75 (wt/wt):

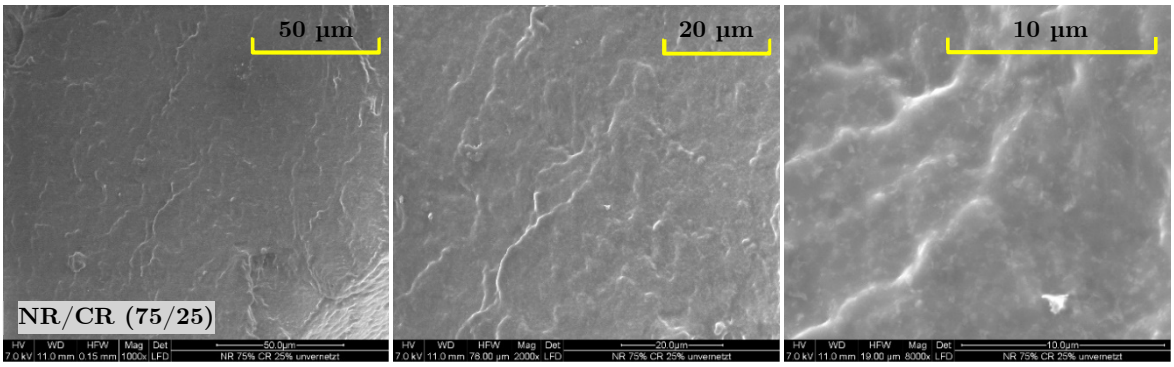

Figure 27. ESEM images (SE) of the tear fracture surface of a NR/CR-blend film (75/25) at magnifications of 1000x (left), 2000x (middle) and 8000x (right).

The tear fracture of the sample cotaining 75 % NR and 25 % CR exhibits a greater number of tear paths and a rougher fracture surface than the pure NR and CR latex films. In these images, areas of distinct NR- or CR-phases cannot be clearly assigned.

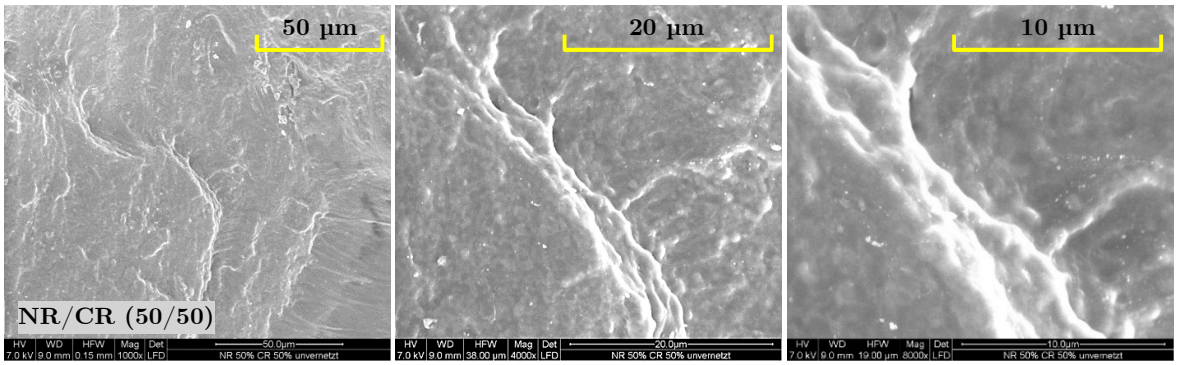

Figure 28. ESEM images (SE) of the tear fracture surface of a NR/CR-blend film (50/50) at magnifications of 1000x (left), 4000x (middle) and 8000x (right).

NR/CR-blend films (50/50) also show a very high number of tear paths (visible at 1000x magnification) compared to the other compositions. The surface appears much rougher than those of the previously discussed specimen and the degree of film formation is similar NR/CR blend films investigated. Practically no distinct spherical particles can be observed.

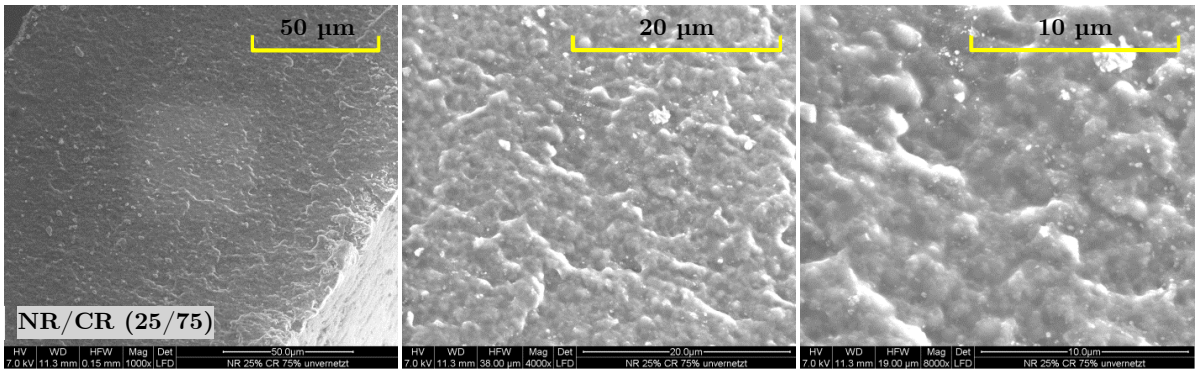

Figure 29. ESEM images (SE) of the tear fracture surface of a NR/CR-blend film (25/75) at magnifications of 1000x (left), 4000x (middle) and 8000x (right).

The last images, representing the 25/75 blend of NR and CR, show a surface of the tear fracture, which is quite similar to the one of pure NR latex. In images with magnifications of 4000x and 8000x few spherical, individual rubber particles, but mostly connected and deformed particles appear. On the left ESEM-image, the damaging impact of the electron beam can be seen in the form of a square-shaped, ligther area in the center of the sample. Due to this effect, the scan rates for all samples had to be rather quick, in order minimize the damage of the polymers.

ESEM imaging was not only used to investigate the morphology, but also to possibly extract information on phase effects, such as phase separation. Presumably, compartments or agglomerations which containing predominantly NR and CR can be distinguished by the different shading, meaning that darker regions represent a higher content of natural rubber, whilst brighter regions indicate predominantly chloroprene rubber. However, when using secondary electron ESEM imaging, statements regarding phase effects are not persuasive.

Besides blends of NR and CR, also IR/CR and NBR/CR blends were characterized. ESEM-images of those blends at different ratios are shown in Figure 30 and Figure 31:

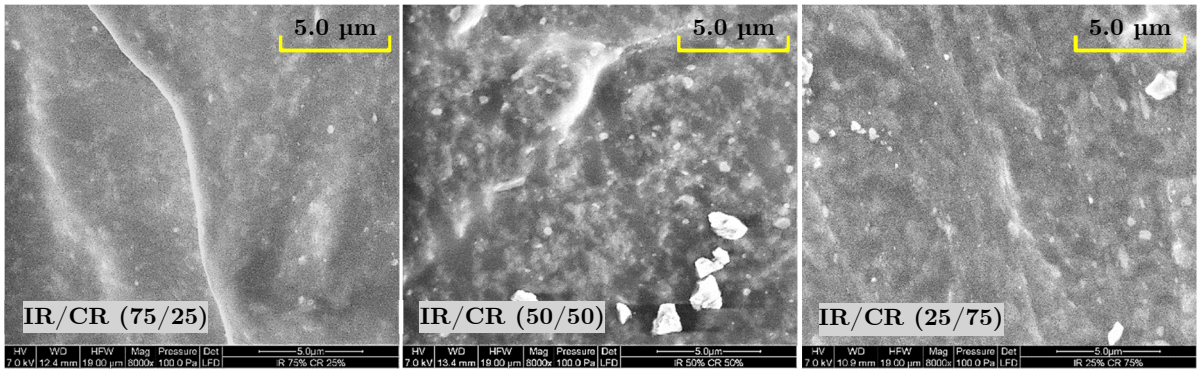

Figure 30. ESEM images (SE) of the tear fracture surface of IR/CR-blend films with the ratios of 75/25 (left), 50/50 (middle) and 25/75 (right) at a magnification of 8000x.

The microscopic images of the IR/CR latex blends show a smooth surface and a homogenous distribution of deformed and joint rubber particles. Bright, angular shaped particles, as in the image of the 50/50 sample, can be attributed to contamination by

ZnO or other metal containing particles. In all three compositions, some extent of shading between brighter and darker areas is visible, which could indicate regions of different Cl-concentrations. However, a clear distinction between the different ratios cannot be made.

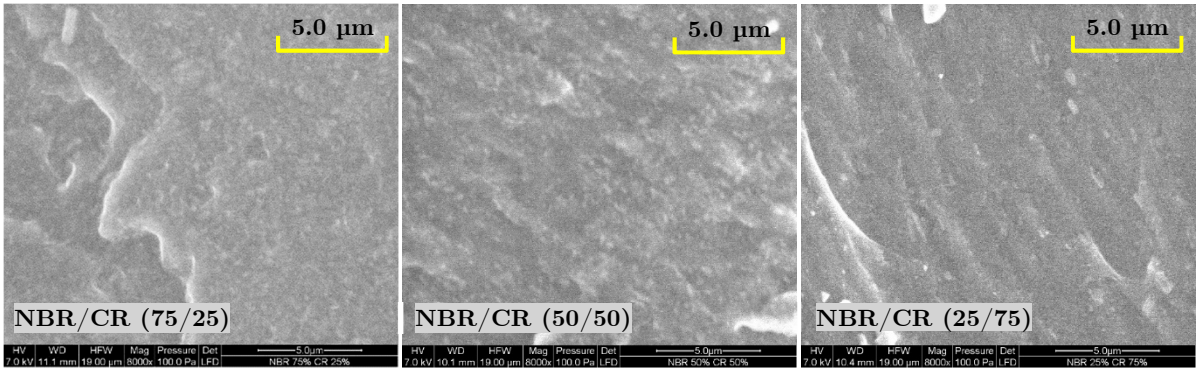

Figure 31. ESEM images (SE) of the tear fracture surface of NBR/CR-blend films with the ratios of 75/25 (left), 50/50 (middle) and 25/75 (right) at a magnification of 8000x.

NBR/CR latex blends at different ratios exhibit a very smooth and homogenous tear fracture surface and hardly any visible spherical particles. The images appear to be quite similar to the images of the NBR latex film specimen. All three compositions exhibit about the same surface morphologies and therefore no indications for a possible distinction between NBR- and CR-enriched areas.

Regarding the investigation of latex blends it must conclusively said that, even though the observation of phase separation with electron microscopy has been reported in literature, e.g. by *Moonprasith et al.*[81] or by *Nasir et al.*[82], it was not possible to show clear phase effects or to proof phase separation using ESEM or SEM imaging in the present work.

5.3.2 EDX-Mapping and Element Distribution

SEM-EDX mapping was performed utilizing a Zeiss Sigma 300 VP electron microscope, coupled with energy dispersive X-ray spectroscopy (EDX) on a series of NR/CR blends at ratios of 100/0, 75/25, 50/50, 25/75 and 0/100 (wt/wt). These materials were processed without additional vulcanization agents and only the most abundant elements were analyzed: carbon (C) and chlorine (Cl) as well as calcium (Ca), potassium (K) and oxygen (O). Main purpose of this characterization was to possibly observe or gather information about phase separation between the isoprene and chloroprene portions of the blended materials. For that reason, primarily the distribution of chlorine atoms, depending on the quantity of chloroprene rubber in the blend, was of interest. The resulting microscopic images are shown in Figure 32 to Figure 36. It must be noted, that the color brightness is automatically adjusted to the maximum intensity of each mapped element. Therefore, brightness in those images is not an indicator for the overall abundance of the elements in comparison with each other.

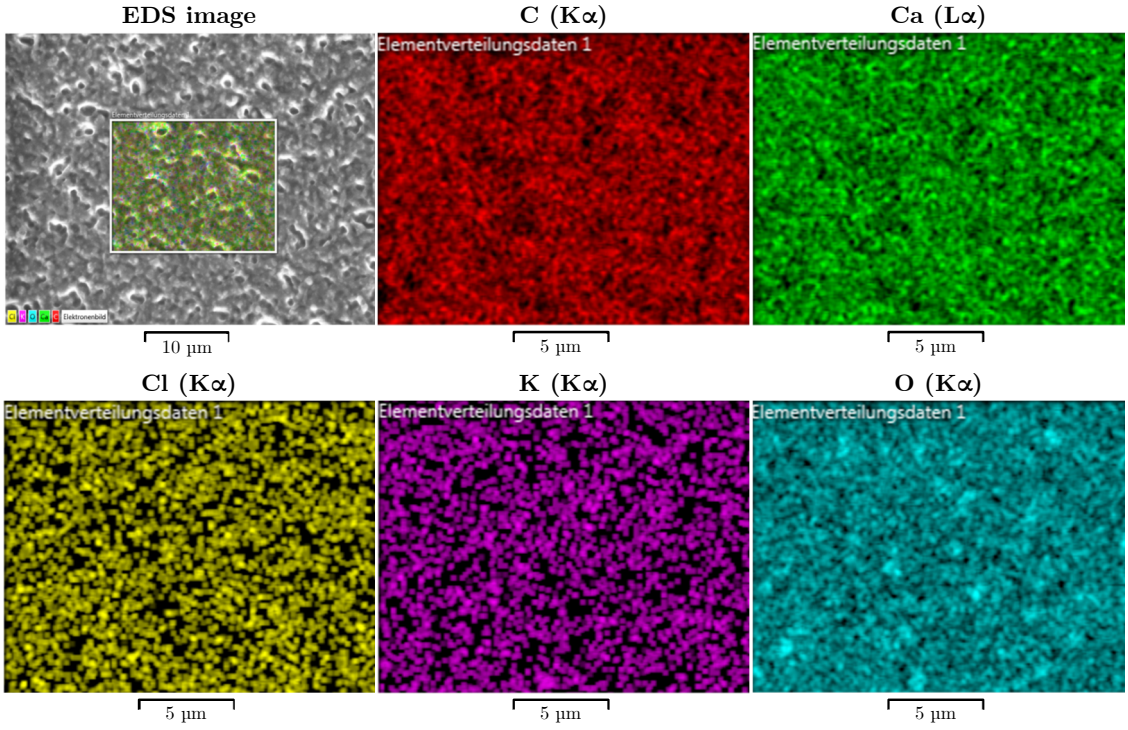

Figure 32. SEM image (top left) and EDX-mapping of C (red), Ca (green), Cl (yellow), K (purple) and O (blue) of the tear fracture surface of a NR film (100).

The SEM image of the pure vulcanized natural rubber latex film (top left) shows an equal morphology to the previously discussed ESEM-images and the same visible spherical particles. EDX-mapping was carried out for a selected area, indicated by the yellow rectangle. All elements are evenly distributed over the cross-section. Even though the sample does not contain significant amounts of Cl (0.2 wt%) or K (0.4 wt%), the mapping of these elements produces a strongly colored image. In fact, the strongest signal is automatically defined as the brightest possible color point. Smaller concentrations (weaker signals) are depicted darker accordingly. This way of generating the EDX-spectra holds true for all elements.

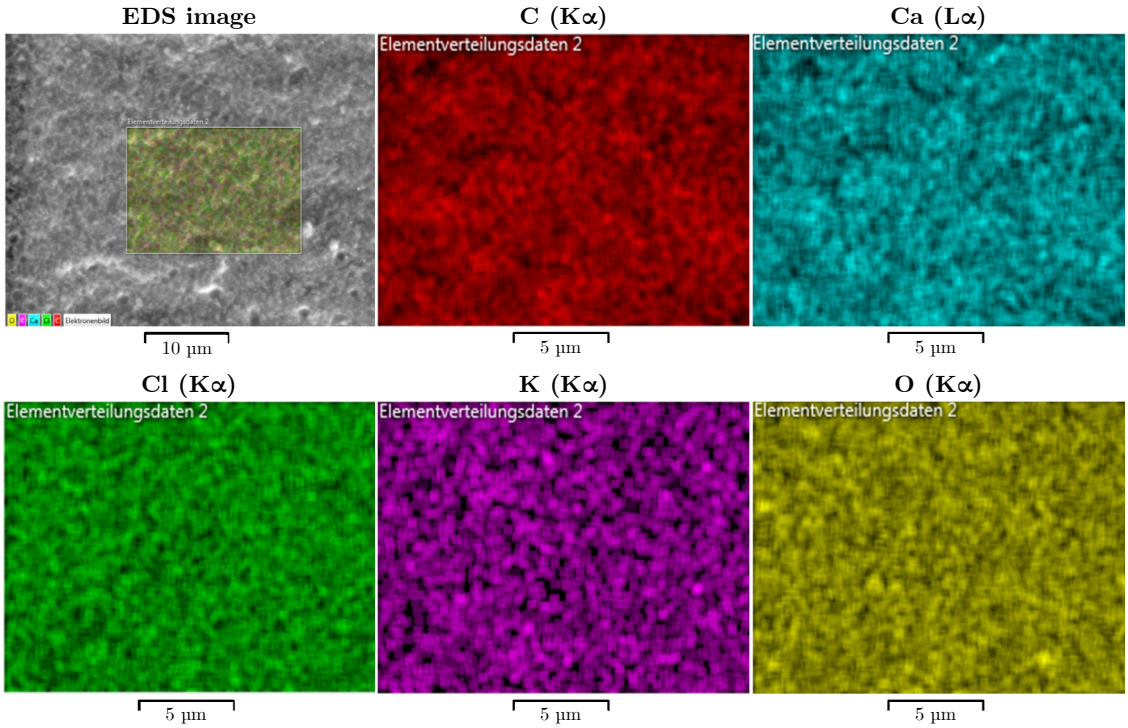

Figure 33. SEM image (top left) and EDX-mapping of C (red), Ca (blue), Cl (green), K (purple) and O (yellow) of the tear fracture surface of a NR/CR film (75/25).

The elemental distribution of C, Ca, Cl, K and O in the 75/25-blend does not differ noticeable from the NR (100) sample. Neither inhomogeneities, agglomerations nor phase effects are visible in the images. Besides that, the resolution of the images is comparable lower than for the other mapping experiments.

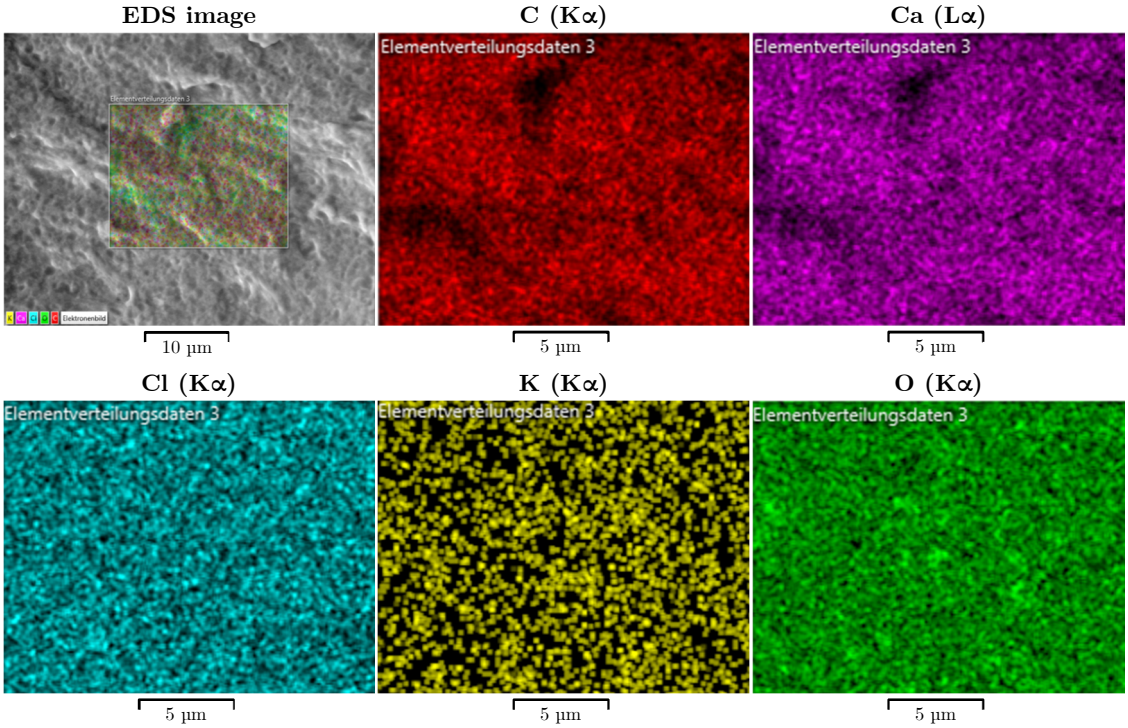

Figure 34. SEM image (top left) and EDX-mapping of C (red), Ca (purple), Cl (blue), K (yellow) and O (green) of the tear fracture surface of a NR/CR film (50/50).

Regarding the NR/CR (50/50) samples, the SEM image shows a seemingly rougher surface than the previous ones, probably arising from tear paths. Darker and perfectly coincident areas in the carbon and calcium spectra might originate from the surface morphology rather than real concentration gradients. Chlorine, potassium and oxygen do not show this shading, however. Cl-distribution of this sample suggests some extent of spherical agglomerations or particles on a scale of several hundred nanometers. The same observation holds true for potassium and oxygen, in which agglomerations to some extent are indicated.

The tear fracture surface of the 25/75-blend (shown in the following Figure 43) exhibits apparently some type of contamination, which is rich in oxygen and overlays the C and Ca signals, leading to darker areas accordingly. The Cl-mapping is not influenced by these particles on the surface and generally shows a very comparable distribution to the NR/CR (50/50) sample with few small, spherical agglomerations. An EDX-mapping for potassium could not be recorded, due to the low concentration (< 0.2 wt%).

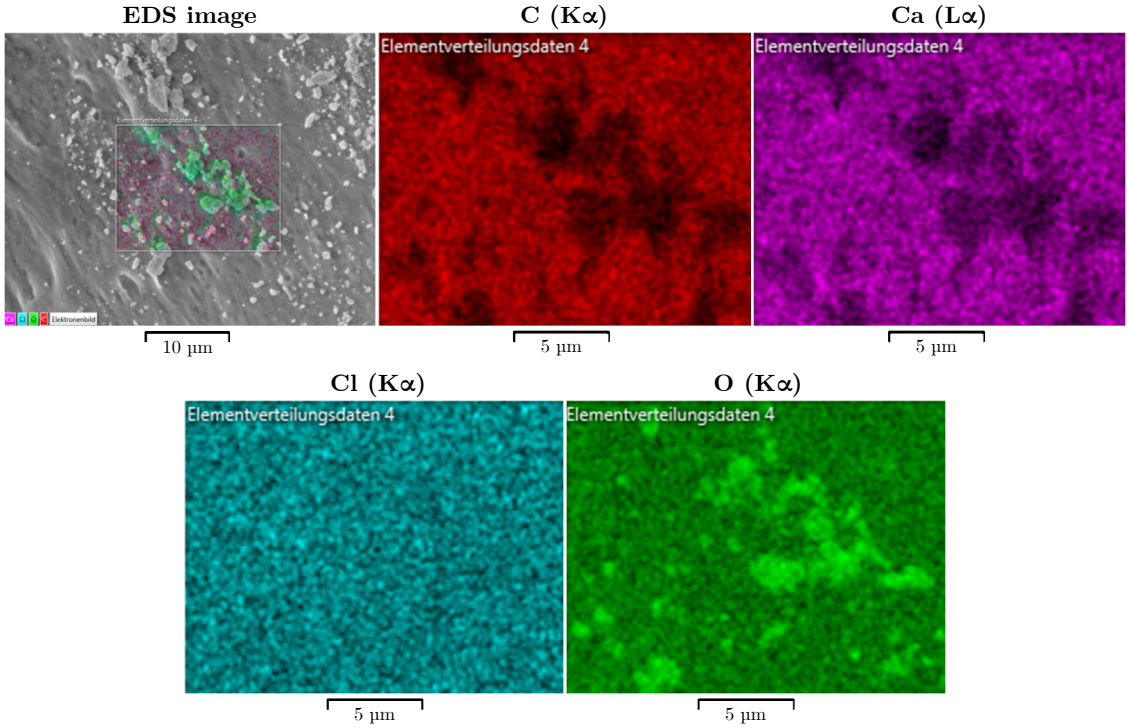

Figure 35. SEM image (top left) and EDX-mapping of C (red), Ca (purple), Cl (blue) and O (green) of the tear fracture surface of a NR/CR film (25/75).

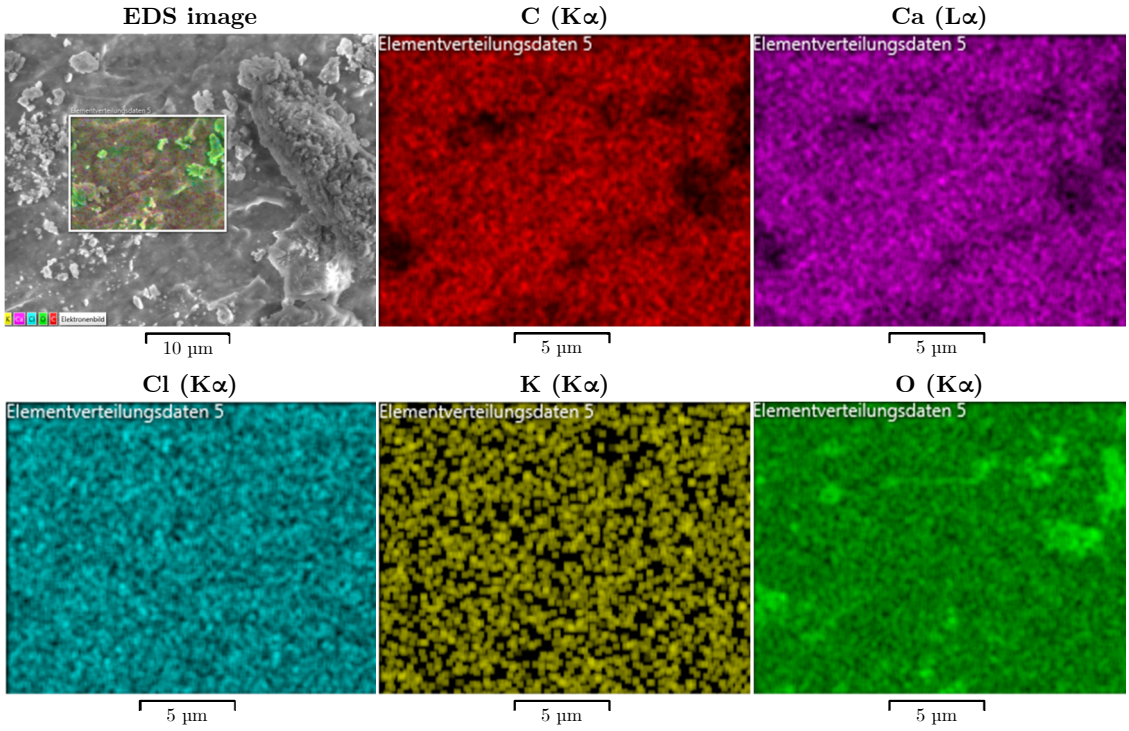

Figure 36. SEM image (top left) and EDX-mapping of C (red), Ca (purple), Cl (blue), K (yellow) and O (green) of the tear fracture surface of a CR film (100).

Finally, characterization of CR (100) shows again some surface contamination by oxygen enriched particles, just as in the NR/CR (25/75) sample. Anyway, the Cl-mapping is still unaffected and shows in again a multitude of seemingly spherical agglomerations of chlorine.

The microscopic images and EDX-mapping generally show a homogenous distribution of carbon and chlorine over the entire analyzed cross-section for all blending ratios. However, a separation into two distinct phases, of which one is enriched with chlorine atoms, is not visible. Further, calcium was found in all samples to a considerable amount, correlating with the distribution of the carbon atoms. The distribution of oxygen appears to be opposed to the distribution of carbon or calcium. As the color intensity of the shown images does not directly correspond to the quantity of the indicated element, the element distribution by weight percent was quantified from the obtained measurement data. Corresponding spectra can be seen in the appendix (Figure 40 to Figure 44) and the results are shown in Table 20:

Table 20. Elemental distribution (wt%) from EDX-mapping on NR/CR blends.

Atom	**NR (100)**	**NR/CR (75/25)**	**NR/CR (50/50)**	**NR/CR (25/75)**	**CR (100)**
			[wt%]		
Carbon	91.6 ± 0.1	87.4 ± 0.1	82.2 ± 0.2	72.8 ± 0.3	68.7 ± 0.3
Chlorine	0.2 ± 0	5.6 ± 0.1	7.8 ± 0.1	10.6 ± 0.1	12.5 ± 0.1
Calcium	2.0 ± 0.1	2.0 ± 0.1	3.8 ± 0.1	7.1 ± 0.1	8.2 ± 0.2
Oxygen	5.7 ± 0.1	4.6 ± 0.1	5.9 ± 0.1	9.3 ± 0.1	9.9 ± 0.1
Potassium	0.4 ± 0	0.4 ± 0	0.4 ± 0	0.2 ± 0.1	0.6 ± 0.1

By increasing the amount of chloroprene rubber latex in the NR/CR-blend, the content of carbon decreases steadily, while the chlorine amount increases. Although these results are in line with the expectations, the obtained values differ from the theoretical ratio of carbon to chlorine: experimentally determined amounts of chlorine are significantly

lower than the calculated reference values from the corresponding sum formula and ratio of the latex materials. Only less than 40% of the actual chlorine content could be detected by quantification of the EDX signals. This observation might be attributed to the fact, that for the applied acceleration voltage ($U_H = 7.5$ kV) the information depth for signals of each element varies. The theoretical information depth for carbon and chlorine was calculated using NIST DTSA II Monte Carlo Simulation. The results are shown in Figure 37 and Table 21:

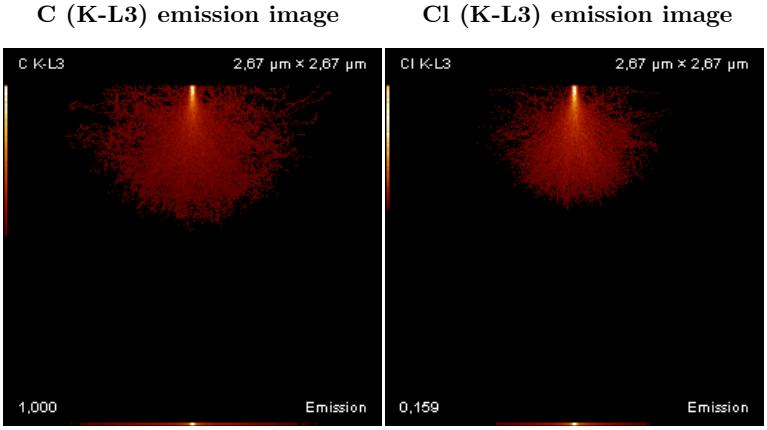

Figure 37. Electron interaction volume: depth distribution of electron-based X-ray excitation for C (left) and Cl (right) in a NR/CR blend specimen at $U_H = 7.5$ kV using NIST DTSA II Monte Carlo Simulation.

Table 21. Information depth for carbon and chlorine at $U_H = 7.5$ keV.

Atom	Ion. Energy [keV]	F(99.9%) Depth [µm]	F(99.9%) Volume [µm³]
Carbon (K)	0.284	1.031	1.517
Chlorine (K)	2.822	0.837	0.872

The simulated information depth F(99.9%) is apparently much higher for carbon than for chlorine, which might explain the deviation between the theoretical and experimental determined C/Cl-ratio.

Interestingly, the calcium content in all mixtures is rather high, especially for blends with a high CR content (2.0 to 8.2 wt%) and is seemingly rising with an increasing content of chloroprene rubber. The polarity of the chlorine residues of the CR could lead to agglomeration of Ca^{2+} in Cl-enriched compositions. Calcium is most likely to be incorporated into the latex film during the coagulation dipping step, originating from the coagulant dispersion ($CaNO_3$). Further, potassium appears to be present in all materials, but only to a negligible amount of up to 0.6% in the CR (100) sample. Though, the source of the potassium is not exactly definable, it is most likely a constituent of the raw rubber materials. Conclusively it must be noted, that SEM-EDX is not a suitable method for an exact quantitative analysis, but it can serve as a semi-quantitative approach for an estimation of the elemental distribution.

The images in Figure 38 show again the chlorine EDX-mapping of NR/CR latex blends at different ratios. Here, the color intensity is not normalized to the strongest signal but adjusted according to the quantified C/Cl-ratio. Meaning, that the color intensity corresponds to the actual concentration of chlorine in the sample:

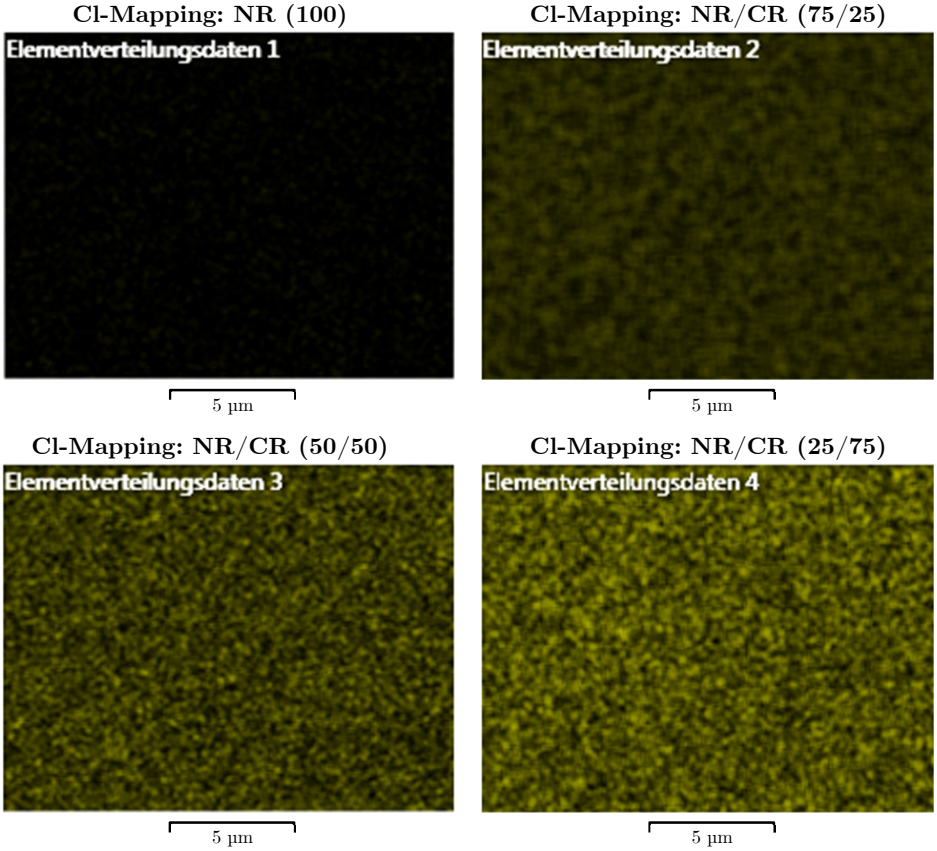

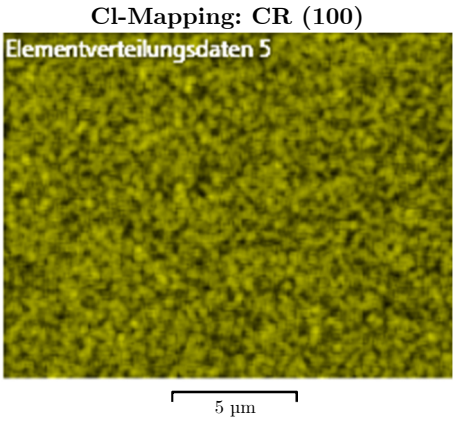

Figure 38. Chlorine mapping of NR/CR latex blends at different ratios with the color intensity adjusted according to the chlorine quantity.

A shift in Cl-concentration can be clearly followed: the first image of NR (100) proves, that factually no significant quantity of chlorine is present. By increasing the CR-content (from 25%, 50%, 75% to 100%) the color intensity and density of spherical agglomerations rises. Especially in the samples NR/CR (50/50) and (25/75) partially distinct spheres can be observed, having diameters of approximately 150 to 250 nm, which is quite in accordance with values obtained from DLS measurements. Nevertheless, also morphological effects must be considered when interpreting the elemental mapping. I.e. higher resolutions of the EDX-mapping images, which allows an elemental quantification per pixel of the image, would be required to make more accurate interpretations.

5.4 Differential Scanning Calorimetry

The thermal behavior and the effect of the blend composition on the glass transition temperatures were investigated using differential scanning calorimetry (DSC). For this purpose, pure NR-, CR-, IR- and NBR-films as well as blended materials of NR/CR, IR/CR with a blending ratio of 50/50 (wt/wt) and NBR/CR blends with blending ratios of 25/75, 50/50 and 75/25 (wt/wt) were prepared, without the addition of vulcanization agents nor accelerators. The obtained results are listed in Table 22:

Table 22. Glass transition temperatures from DSC measurements.

Rubber	T_g [°C]
NR	-63.7
IR Kraton 401	-62.8
CR Lipren T	-40.8
NBR Kumho KNL	-27.6
NR/CR (50/50)	-64.3 / -41.4
IR/CR (50/50)	-61.9 / -39.6
NBR Kumho KNL/CR (25/75)	-25.8 / -40.8
NBR Kumho KNL/CR (50/50)	-27.0 / -41.8
NBR Kumho KNL/CR (75/25)	-24.5 / -41.6

For the pure rubber materials, the determined glass transition temperatures match the expected values.[40] Evaluating the blended systems, two distinct glass transition temperatures can be found, which eminently correspond to the T_g-values of the respective single rubber component. The presence of two glass transition temperatures in each blend reveals, that those are thermodynamically not compatible and therefore immiscible. In case of partially miscible systems, the T_g values would be shifted more significantly in relation to the original values.[83] The findings are in agreement with those of previous investigations by *Raunicher J.*[69]

5.5 Particle Size Determination by DLS

The results obtained from the DLS measurements, namely the hydrodynamic diameter (D_H) as well as the polydispersity index (PDI) are shown in Table 23:

Table 23. Results obtained from Dynamic Light Scattering.

Rubber	D_H [nm]	PDI [1]
NR	1570	0.24
IR Kraton 401	525	0.22
CR Lipren T	188	0.15
NBR Kumho KNL	124	0.05
NBR Synthomer 6338	134	0.13

It can be observed that, with exception of the natural rubber latex, all tested latex dispersions are composed of submicron rubber beads. Natural rubber and isoprene rubber differ significantly regarding the average particle size of 1570 and 525 nm respectively, even though the chemical structure of the monomeric unit is basically identical. Both samples show an equally broad size distribution (PDI = 0.24 and 0.22). Highly comparable results were obtained for the different acrylonitrile butadiene rubber latexes: The Kumho NBR having an average particle size of 124 nm with a very narrow size distribution and the Synthomer NBR showing a particle size of 134 nm. Chloroprene rubber Lipren T exhibits a hydrodynamic diameter of 188 nm with a PDI of 0.12. All obtained results are in good agreement with reported values in literature.[3; 16; 30; 84]

5.6 Swelling and Crosslinking Density

Experiments with regards to the investigation of swelling characteristics and crosslinking density were performed on series of selected samples. The degree of volumetric swelling of a cured latex material in a suitable solvent can provide information on how densely the polymer chains are linked and therefore, about the efficiency of the vulcanization process. Additionally, by comparing the weight of the dry material before swelling and the weight after swelling and subsequent drying, the soluble fraction of the product can be determined. In all conducted experiments, toluene served as the swelling solvent. First swelling experiments were used to investigate the influence of curing time on the crosslinking density of IR latex films. Results are shown in Table 24:

Table 24. Swelling and cross-linking density of pre-vulcanized IR films, different curing conditions.

Curing at	$\mathbf{Q_m}$ **[1]**	$\mathbf{Q_V}$ **[1]**	**Sol. Fract. [%]**	$\mathbf{M_C}$ **[g mol^{-1}]**	$\boldsymbol{\nu_e}$ **[mmol g^{-1}]**
20 min, 120 °C	4.83	5.05	5.6	5060 ± 410	**0.198**
30 min, 120 °C	4.85	5.07	5.7	5100 ± 320	**0.197**
40 min, 120 °C	5.35	5.60	6.5	6340 ± 270	**0.159**
20 min, 120 °C (aged)	4.69	4.90	6.2	4780 ± 230	**0.210**

It can be seen, that variation of the curing time only has small effects on the average molecular mass between two crosslinks (M_C). Values are in the range of M_C = 4775 gmol^{-1} (or one crosslink per 55 units) for the aged (12 weeks) sample, cured for 20 min at 120 °C and 6339 g mol^{-1} (one crosslink per 72 units) for a curing time of 40 min. This would lead to the contradictive conclusion, that longer curing times causes slightly less dense crosslinking of the isoprene rubber latex. A possible explanation is the uncertainty of measurements, also indicated by the high standard deviations.

Another swelling experiment was performed on a series of NBR/NBR latex blends, to determine possible differences in the cross-linking in the different materials. Table 25 and Table 26 show the results for samples without and with pre-vulcanization:

Table 25. Swelling and cross-linking density of NBR/NBR blend films without pre-vulcanization

Blend	$\mathbf{Q_m}$ **[1]**	$\mathbf{Q_V}$ **[1]**	**Sol. Fract. [%]**	$\boldsymbol{M_C}$ **[g mol^{-1}]**	$\boldsymbol{\nu_e}$ **[mmol g^{-1}]**
S (100)	2.24	2.38	3.6	1170 ± 150	**0.858**
S/K (70/30)	2.23	2.37	2.8	1140 ± 190	**0.877**
S/K (50/50)	2.46	2.62	2.6	1610 ± 170	**0.620**
S/K (30/70)	2.75	2.95	7.6	2230 ± 240	**0.448**
K (100)	2.84	3.02	5.0	2320 ± 220	**0.432**

S = NBR Synthomer 6338, **K** = NBR Kumho KNL

By increasing the amount of KNL Kumho NBR later (K), the material experiences a higher degree of swelling in the solvent. Pure Synthomer 6338 NBR (S) represents the most densely crosslinked material with a M_C of 1165 g mol^{-1}. This average molecular weight in between the crosslinks steadily increases up to a value of 2317 g mol^{-1} for K (100). By dividing those values by the average molecular weight of the co-monomer units, roughly one crosslink per eleven units is found in the S (100) material whilst the K (100) film has about one crosslink per 24 units for the applied curing system. However, the cross-linking density is not a direct indicator for differences in mechanical properties (compare to results in Figure 23).

The very same trend can be found for the pre-vulcanized NBR/NBR latex blend materials: S (100) exhibits the densest crosslinking (M_C = 1316 or one crosslink per 13 units). The higher the portion of Kumho NBR in the blend, the lower the crosslinking density: S/K (30/70) and K (100) show values of M_C = 2877 g mol^{-1} and 2745 g mol^{-1} respectively:

Table 26. Swelling and cross-linking density of NBR/NBR blend films with pre-vulcanization.

Blend	$\mathbf{Q_m}$ **[1]**	$\mathbf{Q_V}$ **[1]**	**Sol. Fract. [%]**	$\mathbf{M_C}$ **[g mol^{-1}]**	$\boldsymbol{\nu_e}$ **[mmol g^{-1}]**
S (100)	2.32	2.47	3.83	1320 ± 210	**0.760**
S/K (70/30)	2.46	2.62	5.13	1570 ± 240	**0.637**
S/K (50/50)	2.84	3.06	2.75	2400 ± 310	**0.417**
S/K (30/70)	3.02	3.25	3.43	2880 ± 280	**0.348**
K (100)	2.99	3.21	4.10	2740 ± 190	**0.364**

S = NBR Synthomer 6338, **K** = NBR Kumho KNL

Pre-vulcanization clearly has no significant influence on the swelling characteristics of the NBR/NBR latex blends. In all cases, the soluble fraction of the material is rather low with values in between 3 and 8%.

It must be stated, that the swelling experiments with use of the Flory-Rehner theory do not represent a highly accurate method for determination of the crosslinking density. The choice of the solvent for the polymer to be tested may influence the outcome of the experiments. Additionally, polymers with identical chemical structures can exhibit different material characteristics, which is not considered in the evaluations. Thus, the method is quite susceptible to errors.

6 Conclusion and Outlook

The present work aimed at the optimization of formulations and processing parameters for dipped latex films (e.g. for disposable rubber gloves and examination gloves), made from synthetic rubber latex materials. The central and desired objective was the production of dipped latex goods, which exhibit improved physical properties as compared to commercially available state-of-the art materials. For this purpose, isoprene rubber latex (IR), chloroprene rubber latex (CR) and different acrylonitrile-butadiene rubber latexes (NBR), serving as substitutes for conventionally used natural rubber latex (NR), were used. The processing of cured films from the raw materials was performed using the coagulation dipping method.

Optimization of latex products can follow several different approaches, three of which were investigated in this work: the adaption of crosslinking formulations and processing parameters for single latex materials, the application of filling materials and finally the blending of different rubber latexes.

Vulcanization is a crucial processing step to tune the properties of a rubber product. Generally, this is done by the adaption of vulcanization chemicals, accelerating agents and various additives, which are added to the compounded latex. In this work, a range of different curing systems was tested for all kind of rubber latexes. To start with, isoprene rubber latex was crosslinked according to internal standard formulations using common curing condition. Progressively, those vulcanization formulations were altered by varying the quantity of vulcanization agents, as well as by changing the curing conditions (e.g. time and temperature), to find the ideal combination. In case of isoprene rubber latex (IR), the best results can be obtained using the initial standard formulation and film vulcanization at 130 °C for 30 min, yielding in tensile strengths of 24.8 N mm^{-2} and ultimate elongation of above 800%. For the treatment of chloroprene rubber latex (CR) more sophisticated curing systems were investigated: using a metal oxide-based vulcanization, a variety of primary and secondary accelerators (DPG, ETU, ZDBC, etc.) and combinations thereof was applied. Ultimately, combinations of ZnO and DPG/ETU

at varied quantities were found to be the most favourable curing system. CR films show tensile strengths of up to 17 N mm^{-2} and superior ultimate elongations of over 1300%. When using acrylonitrile-butadiene rubber latex, not only different curing additives were investigated, but also the influence of processing parameters, such as leaching. While various formulations were tested, vulcanization using only ZnO turned out to produce the best materials. Further, the mechanical properties can be significantly increased by implementing wet-gel and dry-gel leaching of the films, resulting in outstanding tensile strengths of above 55 N mm^{-2} and ultimate elongations of ca. 600%.

The second mentioned approach, filling of latex materials, was pursued by utilizing $CaCO_3$ as a non-reinforcing but inexpensive filling material for NBR latex. To do so, up to 20 phr filler loading was applied and films were produced according the previously determined ideal curing method. It was not unexpected, that the mechanical properties suffer due to the filler loading when compared to the properties of the unfilled material. However, the tensile strengths of the samples are remarkably constant at filler loadings between 5 phr and 20 phr, showing tensile strengths between 35 and 40 N mm^{-2} and elongations above 500%. With these values still easily surpassing the required specifications, $CaCO_3$ could sever as a potential mean of cost-reduction for the processing of nitrile rubber gloves.

Blending of latex materials was realized by IR/CR latex blends at the ratio of 50/50 (wt/wt) as well as NBR/NBR latex blends at varied ratios of 70/30, 50/50 and 30/70 (wt/wt). Varied curing formulations and conditions were screened to obtain the most favourable product. By blending of IR and CR, the comparably high tensile strength of IR and the superior ultimate elongation of CR should be unified in the resulting product. Adapted formulations, comprising the vulcanization agents for IR with additional ZnO for CR cross-linking, yield tensile strengths of about 18 N mm^{-2} with elongations of above 850%. Since these values do not represent a significant improvement of the initial properties of pure IR rubber, further optimization of the blend processing and vulcanization would be needed. Attempts of blending two NBR latex materials from different suppliers were carried out to take advantage of possible diverse product characteristics (e.g. dissimilar ratio of monomeric units, different particle size, etc.). Mechanical testing showed, that the blending results in just slightly improved tensile

strength for individual mixtures e.g. S/K (30/70) with curing at 130 °C in comparison to values of the single latex films. Further it can be seen, that pre-vulcanization has a clearly negative influence on the mechanical properties of NBR/NBR latex blend films.

Besides mechanical testing, the produced materials were investigated using electron microscopy (ESEM and SEM) to gain information on the morphology of single and blended materials. All materials exhibit smooth tear fracture surfaces and high degree of film formation could be observed. However, it was not possible to make phase separation or phase effects visible using the mentioned methods. SEM-EDX experiments were carried out on NR/CR blends, showing a clear shift in the carbon/chlorine ratio by varying the CR content of the mixture. Nevertheless, using SEM-EDX as a tool for qualitative characterisation of the elemental composition proved to be an inadequate method for the present polymer samples.

Miscibility of the blended latexes was determined by performing DSC. All measured blends (NR/CR, IR/CR, NBR/CR) represent totally immiscible systems, all showing two distinct glass transition temperatures, directly corresponding to the respective single latex materials. Employing dynamic light scattering (DLS), the average particle size and particle size distribution of the crude materials in highly diluted aqueous dispersion was measured. Altogether, the latex materials consist of submicron rubber particles in the expected size range with rather narrow PDI values.

On a final note it can be concluded, that the present work constitutes a basic screening of different approaches towards the optimization of dipped latex products. Even though most tested materials already meet the required specifications for their applications, constant improvement as well as cost reduction for existing materials is desired considering the fierce market competition. Research and development in either direction needs to be continued. Possibilities are the continuation of optimizing curing systems for CR and IR latexes by replacing conventional accelerators by novel and more efficient chemicals. Additionally, NBR latexes and NBR/NBR latex blends, which were showing promising properties, can possibly be further improved by adapting curing formulations and processing parameters. Application of filling materials, either for cost-reduction or reinforcement, is another approach to be followed in the further course.

7 REFERENCES

[1] Mark, James E.; Erman, Burak; Roland, Michael C. **(2013)**: The Science and Technology of Rubber. 4th ed.; Elsevier Academic Press.

[2] Messenger, T. H. **(1938)**: The Chemistry and Technology of Rubber Latex. In *Nature* 142 (3587), pp. 185–186. DOI: 10.1038/142185a0.

[3] Röthemeyer, Fritz; Sommer, Franz **(2013)**: Kautschuk-Technologie - Werkstoffe, Verarbeitung, Produkte. 3rd ed.; Hanser.

[4] Hofmann, Werner **(1989)**: Rubber Technology Handbook; Hanser.

[5] Hurley, Paul E. **(1981)**: History of Natural Rubber. In *J. Macromol. Sci. Part A Chem.* 15 (7), pp. 1279–1287. DOI: 10.1080/00222338108056785.

[6] Hayashi, Yasuyuki **(2009)**: Production of natural rubber from Para rubber tree. In *Plant biotechnol.* 26 (1), pp. 67–70. DOI: 10.5511/plantbiotechnology.26.67.

[7] Akabane, Tetsuya **(2015)**: Production Method and Market Trend of Rubber Gloves. In *Nihon Gomu Kyokaishi* 88 (9), pp. 369–373. DOI: 10.2324/gomu.88.369.

[8] FIIT Research; Foong, Michelle: Rubber Gloves (Global Market Research). Available online at *www.supermax.com.my/html/filedownload.aspx?file=DEUTSCHE%20BANK%20-20100510.PDF,* accessed on 01.12.18.

[9] Nirmal Ghosh, Oriparambil Sivaraman; Gayathri, S.; Sudhakara, P.; Misra, S. K.; Jayaramudu, J. **(2017)**: Natural Rubber Nanoblends: Preparation, Characterization and Applications. In Gordana Markovic, Visakh P. M. (Eds.): Rubber Nano Blends, vol. 46. Cham: Springer International Publishing (Springer Series on Polymer and Composite Materials), pp. 15–65.

[10] Meleth, Jose P. **(2012)**: An Introduction to Latex Gloves: Types, manufacture, properties and Quality Control. 1st ed.; LAP LAMBERT Academic Publishing.

[11] Carey, Renee N.; Fritschi, Lin; Driscoll, Timothy R.; Abramson, Michael J.; Glass, Deborah C.; Darcey, Ellie et al. **(2018)**: Latex glove use among healthcare workers

in Australia. In *Am. J. Infect. Control* 46 (9), pp. 1014–1018. DOI: 10.1016/j.ajic.2018.03.011.

[12] Yip, Esah; Cacioli, Paul **(2002)**: The manufacture of gloves from natural rubber latex. In *J. Allergy Clin. Immunol.* 110 (2), S3-S14. DOI: 10.1067/mai.2002.124499.

[13] Blackley, D. C. **(1997)**: Latex-dipping processes. In D. C. Blackley (Ed.): Polymer Latices: Springer Netherlands, pp. 155–228.

[14] Ahmad, Hazwani S.; Ismail, Hanafi; Rashid, Azura A. **(2016)**: Tensile Properties and Morphology of Epoxidized Natural Rubber/Recycled Acrylonitrile-Butadiene Rubber (ENR 50/NBRr) Blends. In *Procedia Chem.* 19, pp. 359–365. DOI: 10.1016/j.proche.2016.03.024.

[15] Markovic, Gordana; P. M., Visakh (Eds.) **(2017)**: Rubber Nano Blends. Cham; Springer International Publishing (Springer Series on Polymer and Composite Materials).

[16] Wales, M. **(1962)**: Particle Size Distribution in Rubber Latex. In *J. Phys. Chem.* 66 (10), pp. 1768–1772. DOI: 10.1021/j100816a003.

[17] Porstendörfer, Justin; Heyder, Joachim **(1972)**: Size distributions of latex particles. In *J. Aerosol Sci.* 3 (2), pp. 141–148. DOI: 10.1016/0021-8502(72)90150-4.

[18] Dierkes, Wilma **(2007)**: Raw Materials and Compounds in Rubber Industry. Manuscript. University of Twente (NL). Available online at *www.laroverket.com/wp-content/uploads/2015/03/Raw_materials_and_compounds.pdf,* accessed on 02.11.18.

[19] Pontén, Ann; Hamnerius, Nils; Bruze, Magnus; Hansson, Christer; Persson, Christina; Svedman, Cecilia et al. **(2013)**: Occupational allergic contact dermatitis caused by sterile non-latex protective gloves: clinical investigation and chemical analyses. In *Contact Derm.* 68 (2), pp. 103–110. DOI: 10.1111/cod.12010.

[20] Kahn, Steven L.; Podjasek, Joshua O.; Dimitropoulos, Vassilios A.; Brown, Clarence W. **(2016)**: Natural rubber latex allergy. In *Dis. Mon.* 62 (1), pp. 5–17. DOI: 10.1016/j.disamonth.2015.11.002.

[21] Kelly, K.; Kurup, V.; Reijula, K.; Fink, J. **(1994)**: The diagnosis of natural rubber latex allergy. In *J. Allergy Clin. Immunol.* 93 (5), pp. 813–816. DOI: 10.1016/0091-6749(94)90370-0.

[22] Ebo, Didier G.; Stevens, Wim J.; Bridts, Chris H.; Clerck, Luc S. de **(1997)**: Latex-specific IgE, skin testing, and lymphocyte transformation to latex in latex allergy. In *J. Allergy Clin. Immunol.* 100 (5), pp. 618–623. DOI: 10.1016/S0091-6749(97)70165-9.

[23] Phaswana, Shumani Makwarela; Naidoo, Saloshni **(2013)**: The prevalence of latex sensitisation and allergy and associated risk factors among healthcare workers using hypoallergenic latex gloves at King Edward VIII Hospital, KwaZulu-Natal South Africa: a cross-sectional study. In *BMJ Open* 3 (12), e002900. DOI: 10.1136/bmjopen-2013-002900.

[24] Wu, Miaozong; McIntosh, James; Liu, Jian **(2016)**: Current prevalence rate of latex allergy: Why it remains a problem? In *J. Occup. Health* 58 (2), pp. 138–144. DOI: 10.1539/joh.15-0275-RA.

[25] Shuttleworth, M. J.; Watson, A. A. **(1981)**: Synthetic Polyisoprene Rubbers. In A. Whelan, K. S. Lee (Eds.): Developments in Rubber Technology—2. Dordrecht: Springer Netherlands, pp. 233–267.

[26] Kraton Corp. (Ed.) **(2011)**: Polyisoprene products: A review of synthetic latices in surgical glove use. Available online at *www.kraton.com/products/cariflex/synthetic_ latices.pdf,* accessed on 23.10.18.

[27] Kraton Corp. (Ed.) **(2014)**: Preparation of synthetic polyisoprene latex and its use in coagulant dipping (Technical Note). Available online at *www.kraton.com/products/pdf/Cariflex21_ Coagulant%20Dipping.pdf,* accessed on 23.10.18.

[28] Thickett, Stuart C.; Gilbert, Robert G. **(2007)**: Emulsion polymerization: State of the art in kinetics and mechanisms. In *Polymer* 48 (24), pp. 6965–6991. DOI: 10.1016/j.polymer.2007.09.031.

[29] Evans, William J.; Giarikos, Dimitrios G.; Allen, Nathan T. **(2003)**: Polymerization of Isoprene by a Single Component Lanthanide Catalyst Precursor. In *Macromolecules* 36 (12), pp. 4256–4257. DOI: 10.1021/ma034385s.

[30] Franta, I. **(2014)**: Elastomers and Rubber Compounding Materials; Elsevier.

[31] Salleh, S. Z.; Ismail, H.; Ahmad, Z. **(2016)**: Properties of natural rubber latex-compatibilized natural rubber/recycled chloroprene rubber blends. In *J. Elastom. Plast.* 48 (7), pp. 640–655. DOI: 10.1177/0095244315613620.

[32] Mitchell, Brian S. **(2004)**: An introduction to materials engineering and science; Wiley-Interscience.

[33] Feng, Jianrong; Winnik, Mitchell A.; Shivers, Richard R.; Clubb, Brian **(1995)**: Polymer Blend Latex Films: Morphology and Transparency. In *Macromolecules* 28 (23), pp. 7671–7682. DOI: 10.1021/ma00127a013.

[34] Blackley, D. C. (Ed.) **(1997)**: Polymer Latices; Springer Netherlands.

[35] Cross, L. C.; Klyne, W. **(1976)**: Rules for the Nomenclature of Organic Chemistry. Section E: Stereochemistry. In *Pure Appl. Chem.* 45 (1), pp. 11–30. DOI: 10.1351/pac197645010011.

[36] Hui, Jia; Shi, Yan; Fu, Zhi Feng **(2013)**: Synthesis and Characterization of well Defined Polychloroprene by RAFT Polymerization. In *AMR* 787, pp. 241–244. DOI: 10.4028/www.scientific.net/AMR.787.241.

[37] Anderson, Christopher D.; Daniels, Eric S. (2003): Emulsion polymerisation and applications of latex; Rapra Technology (Rapra Review Reports, 160).

[38] Mutar, Mohammed A. **(2010)**: A Study in Vulcanization of Neoprene Rubber (WRT) by Polymethylol Resin (RESOL). In *JNUS* 13 (3), pp. 1–6. DOI: 10.22401/JNUS.13.3.01.

[39] Desai, H.; Hendrikse, K. G.; Woolard, Christopher D. **(2007)**: Vulcanization of polychloroprene rubber. I. A revised cationic mechanism for ZnO crosslinking. In *J. Appl. Polym. Sci.* 105 (2), pp. 865–876. DOI: 10.1002/app.23904.

[40] DT Dichtungstechnik GmbH (Ed.) **(2013)**: Kenndaten Elastomere (Technical Note). Available online at *www.dt-bremen.de/UserFiles/file/pdf/Wissen/Wi-S02-06.pdf,* accessed on 24.10.18.

[41] Berry, Keith; Liu, Max; Chakraborty, Khirud; Pullan, Nikki; West, Andrew; Sammon, Chris; Topham, Paul D. **(2015)**: Mechanism for Cross-Linking

Polychloroprene with Ethylene Thiourea and Zinx Oxide. In *Rubber Chem. Technol.* 88 (1), pp. 80–97. DOI: 10.5254/rct.14.85986.

[42] Eni Versalis (Ed.) **(2015)**: Nitrile Butadiene Rubber copolymers - Proprietary process technology (Technical Note). Available online at *www.versalis.eni.com/irj/go/km/docs/versalis/Contenuti%20Versalis/IT/Documenti/La%20nostra%20offerta/Licensing/Elastomeri/NBR.pdf,* accessed on 23.10.18.

[43] Ismail, Hanafi; Leong, H. C. **(2001)**: Curing characteristics and mechanical properties of natural rubber/chloroprene rubber and epoxidized natural rubber/chloroprene rubber blends. In *Poly. Test.* 20 (5), pp. 509–516. DOI: 10.1016/S0142-9418(00)00067-2.

[44] Kato, Hayato; Nakatsubo, Fumiaki; Abe, Kentaro; Yano, Hiroyuki **(2015)**: Crosslinking via sulfur vulcanization of natural rubber and cellulose nanofibers incorporating unsaturated fatty acids. In *RSC Adv.* 5 (38), pp. 29814–29819. DOI: 10.1039/c4ra14867c.

[45] Robeson, Lloyd M. **(2007)**: Polymer Blends: A Comprehensive Review; Hanser.

[46] Strobl, Gert R. **(op. 1996, 1997)**: The physics of polymers. Concepts for understanding their structures and behavior. 2nd ed.; Springer.

[47] Mangaraj, Duryodhan **(2002)**: Elastomer Blends. In *Rubber Chem. Technol.* 75 (3), pp. 365–427. DOI: 10.5254/1.3547677.

[48] Menges, Georg; Haberstroh, Edmund; Michaeli, Walter; Schmachtenberg, Ernst **(2014)**: Menges Werkstoffkunde Kunststoffe. 1. Aufl. s.l.; Carl Hanser Fachbuchverlag. Available online at *http://dx.doi.org/10.3139/9783446443532.*

[49] Bhowmick, A. K.; Mukhopadhyay, R.; De, S. K. **(1979)**: High Temperature Vulcanization of Elastomers. In *Rubber Chem. Technol.* 52 (4), pp. 725–734. DOI: 10.5254/1.3535236.

[50] Heideman, G.; Datta, R. N.; Noordermeer, J. W. M.; van Baarle, B. **(2005)**: Influence of zinc oxide during different stages of sulfur vulcanization. Elucidated by model compound studies. In *J. Appl. Polym. Sci.* 95 (6), pp. 1388–1404. DOI: 10.1002/app.21364.

[51] Kovacic, Peter **(1955)**: Bisalkylation Theory of Neoprene Vulcanization. In *Rubber Chem. Technol.* 28 (4), pp. 1021–1031. DOI: 10.5254/1.3542858.

[52] Stewart, Clare A. **(2000)**: Chloroprene. In : Kirk-Othmer Encyclopedia of Chemical Technology, vol. 53. Hoboken, NJ, USA: John Wiley & Sons, Inc, p. 4203.

[53] Vukov, Rastko **(1984)**: Zinc Oxide Crosslinking Chemistry of Halobutyl Elastomers—A Model Compound Approach. In *Rubber Chem. Technol.* 57 (2), pp. 284–290. DOI: 10.5254/1.3536008.

[54] Akrochem Corp. (Ed.) **(2015)**: Accelerators and Accelerator Systems (Technical Note). Available online at *www.akrochem.com/pdf/technical_papers/accelerators_part_two.pdf,* accessed on 23.10.18.

[55] Schwarz, Otto; Ebeling, Friedrich Wolfhard (Eds.) **(2005)**: Kunststoffkunde. Aufbau, Eigenschaften, Verarbeitung, Anwendungen der Thermoplaste, Duroplaste und Elastomere. 8., überarb. Aufl. Würzburg; Vogel (Vogel-Fachbuch).

[56] NOCIL Ltd. (Ed.) **(2010)**: Vulcanization & Accelerators (Technical Paper). Available online at *www.nocil.com/Downloadfile/DTechnicalNote-Vulcanization-Dec10.pdf,* accessed on 23.10.18.

[57] Cai, Han-Hai; Li, Si-Dong; Tian, Guo-Ren; Wang, Hua-Bi; Wang, Jian-Hong **(2003)**: Reinforcement of natural rubber latex film by ultrafine calcium carbonate. In *J. Appl. Polym. Sci.* 87 (6), pp. 982–985. DOI: 10.1002/app.11410.

[58] Chokanandsombat, Yotwadee; Sirisinha, Chakrit **(2013)**: MgO and ZnO as reinforcing fillers in cured polychloroprene rubber. In *J. Appl. Polym. Sci.* 128 (4), pp. 2533–2540. DOI: 10.1002/APP.38579.

[59] ADEKA **(2018)**: Types and Characteristics of Polymer Additives - Functionalizing Agents. Available online at *www.adeka.co.jp/en/chemical/products/plastic/knowledge_04.html,* accessed on 01.12.18.

[60] Fink, Johannes K. **(2013)**: Compatibilization. In : Reactive Polymers Fundamentals and Applications: Elsevier, pp. 373–409.

[61] Chirinos, H. D.; Guedes, S.M.L. **(1998)**: The Manufacture of Gloves using RVNRL: Parameters of the Coagulant Dipping Process. In *Braz. J. Chem. Eng.* 15 (4), pp. 334–342. DOI: 10.1590/S0104-66321998000400003.

[62] Than, Loong; Phang, Siew Wei; Ho, Kin Nam **(2018)**: Coagulant Dipping Time and Temperature Optimisation for Latex Glove Uneven Coating Investigation. In *MATEC Web Conf.* 152, p. 1013. DOI: 10.1051/matecconf/201815201013.

[63] Keddie, J. L.; Meredith, P.; Jones, R. A. L.; Donald, A. M. **(1995)**: Kinetics of Film Formation in Acrylic Latices Studied with Multiple-Angle-of-Incidence Ellipsometry and Environmental SEM. In *Macromolecules* 28 (8), pp. 2673–2682. DOI: 10.1021/ma00112a012.

[64] DIN-Normenausschuss Medizin **(2015)**: DIN EN 455-2:2015 - Medical gloves for single use - Part 2: Requirements and testing for physical properties; German version EN 455-2:2015.

[65] Mark, James E. **(2007)**: Physical properties of polymers handbook. 2. ed. New York, NY; Springer Science+Business Media LLC. Available online at *http://dx.doi.org/10.1007/978-0-387-69002-5.*

[66] Kozuch, Daniel; Zhang, Wenlin; Milner, Scott **(2016)**: Predicting the Flory-Huggins χ Parameter for Polymers with Stiffness Mismatch from Molecular Dynamics Simulations. In *Polymers (Basel)* 8 (6), p. 241. DOI: 10.3390/polym8060241.

[67] Bielinski, Dariusz M.; Kozłowski, Ryszard; Zajkov, Gennadij E. (Eds.) **(2015)**: High performance elastomer materials. An engineering approach. International Technological Conference ELASTOMERS 2013 "Science and Industry". Toronto; Apple Academic Press (AAP Research notes on chemistry).

[68] Flory, Paul J.; Rehner, John **(1943)**: Statistical Mechanics of Cross-Linked Polymer Networks II. Swelling. In *J. Chem. Phys.* 11 (11), pp. 521–526. DOI: 10.1063/1.1723792.

[69] Raunicher, Julia **(2018)**: Latex blends – influence of the blending ratio on the mechanical properties. Master's Thesis. Graz University of Technology (AUT).

[70] Arayapranee, Wanvimon; Rempel, Garry L. **(2008)**: Morphology and mechanical properties of natural rubber and styrene-grafted natural rubber latex compounds. In *J. Appl. Polym. Sci.* 109 (3), pp. 1395–1402. DOI: 10.1002/app.28217.

[71] Anand, K.; Varghese, Siby; Kurian, Thomas **(2015)**: Effect of Micro and Nano Zinc Oxide on the Properties of Pre-Vulcanized Natural Rubber Latex Films. In *Prog. Rubber Plast. Re.* 31 (3), pp. 145–156. DOI: 10.1177/147776061503100301.

[72] Das, A.; Naskar, N.; Datta, R. N.; Bose, P. P.; Debnath, S. C. **(2006)**: Naturally occurring amino acid: Novel curatives for chloroprene rubber. In *J. Appl. Polym. Sci.* 100 (5), pp. 3981–3986. DOI: 10.1002/app.23065.

[73] Berry, Keith I. **(2013)**: The Quest for a Safer Accelerator for Polychloroprene Rubber. Doctoral Thesis. Aston University (UK).

[74] Harahap, Hamidah; Surya, Elmer; Surya, Indra; Ismail, Hanafi; Azahari, Baharin **(2014)**: Effect of Leaching Treatment on Mechanical Properties of Natural Rubber Latex (NRL) Products Filled Modified Kaolin. In *AMM* 548-549, pp. 90–95. DOI: 10.4028/www.scientific.net/AMM.548-549.90.

[75] Amir-Hashim, M. Y.; Morris, M. D.; O'Brien, M. G.; Farid, A. S. **(1997)**: Effect of Leaching and Humidity on Prevulcanized NR Latex Films. In *Rubber Chem. Technol.* 70 (4), pp. 560–571. DOI: 10.5254/1.3538443.

[76] Hafsah bt. Mohd. Ghazaly; Lai, P. F.

[77] Ain, Z. N.; Azura, A. R. **(2011)**: Effect of different types of filler and filler loadings on the properties of carboxylated acrylonitrile-butadiene rubber latex films. In *J. Appl. Polym. Sci.* 119 (5), pp. 2815–2823. DOI: 10.1002/app.32984.

[78] Sadeghalvaad, Mehran; Dabiri, Erfan; Zahmatkesh, Sara; Afsharimoghadam, Pooneh **(2018)**: Preparation and properties evaluation of nitrile rubber nanocomposites reinforced with organo-clay, CaCO3, and SiO2 nanofillers. In *Polym. Bull. (Berl)* 32, p. 819. DOI: 10.1007/s00289-018-2583-8.

[79] ASTM International **(2015)**: ASTM D6319-10(2015), Standard Specification for Nitrile Examination Gloves for Meical Application. ASTM International, West Conshohocken, PA. Available online at *www.astm.org/Standards/D6319.htm, accessed on* 12/1/2018.

[80] Dragnevski, Kalin I.; Donald, Athene M. **(2008)**: An environmental scanning electron microscopy examination of the film formation mechanism of novel acrylic latex. In *Colloids Surf. A Physicochem. Eng. Asp.* 317 (1-3), pp. 551–556. DOI: 10.1016/j.colsurfa.2007.11.042.

[81] Moonprasith, N.; Suchiva, K.; Tongcher, O. **(2006)**: Blending in Latex Form of Natural Rubber and Nitrile Latices: A Preliminary Study of Morphology and Mechanical Properties. Available online at *www2.mtec.or.th/th/seminar/msativ/pdf/PP13.pdf,* accessed on 18.12.18.

[82] Nasir, R. M.; El-Tayeb, N. S.M. **(2012)**: Surface morphology, mechanical and tribological properties of blended deproteinized natural and polyisoprene rubbers. In *J. Thermoplast. Compos. Mater.* 25 (6), pp. 701–715. DOI: 10.1177/0892705711412812.

[83] Rao, Vijayalakshmi; Johns, Jobish **(2008)**: Thermal behavior of chitosan/natural rubber latex blends TG and DSC analysis. In *J. Therm. Anal. Calorim.* 92 (3), pp. 801–806. DOI: 10.1007/s10973-007-8854-5.

[84] Ross Hallett, F. **(1994)**: Particle size analysis by dynamic light scattering. In *Food Res. Int.* 27 (2), pp. 195–198. DOI: 10.1016/0963-9969(94)90162-7.

8 APPENDIX

8.1 List of Figures

8.2 List of Tables

8.3 Abbreviations

8.3.1 Analytical Methods

BSE	Back scattered electrons (in ESEM)
C2D	Cascade Current Detector
D_H	Hydrodynamic diameter (in DLS)
DLS	Dynamic light scattering
DSC	Differential scanning calorimetry
EDX	Energy dispersive X-ray spectroscopy
EHT	electron high tension (in ESEM)
ESEM	Environmental scanning electron microscopy
FEG	Field Emission Gun (in SEM)
LFD	Large field detector (in ESEM)
M50	50% Modulus (force at 50% elongation)
M100	100% Modulus (force at 100% elongation)
M300	300% Modulus (force at 300% elongation)
M500	500% Modulus (force at 500% elongation)
Mag.	Magnification (in ESEM)
PDI	Polydispersity index (in DLS)
SE	Secondary electrons (in ESEM)
SEM	Scanning electron microscopy
SSD	Solid-state backscattered electron detector (in ESEM)
WD	Working distance (in ESEM)

8.3.2 Chemicals

$Ca(NO_3)_2$	Calcium nitrate
$CaCO_3$	Calcium carbonate
$CaCl_2$	Calcium chloride
CBS	*N*-cyclohexyl-2-benzothiazole sulfenamide
CR	Chloroprene Rubber
DETU	Diethyl thiourea
diH_2O	Deionized water
DOTG	Di-*o*-tolylguanidine
DPG	1,3-Diphenyl guanidine
DPTU	Diphenyl thiourea
Et_2O	Diethyl ether
ETU	Ethylene thiourea
IR	Isoprene Rubber
KOH	Potassium Hydroxide
MBT	2-Mercaptobenzothiazole
MBTS	2-Mercaptobenzothiazole disulfide
N_2	Nitrogen
NBR	Acrylonitrile-Butadiene Rubber
NR	Natural Rubber
S	Sulphur (S_8)
TBBS	*N*-tert-butyl-2-benzothiazole sulfenamide
TMTM	Tetramethylthiuram monosulfide
TMTD	Tetramethylthiuram disulfide
XNBR	Carboxylated Acrylonitrile Butadiene Rubber

ZDBC	Zinc(II) dibutyl dithiocarbamate
ZDEC	Zinc(II) diethyl dithiocarbamate
ZDMC	Zinc(II) dimethyl dithiocarbamate
ZMBT	Zinc(II) 2-mercaptobenzothiazole
ZnO	Zinc(II) Oxide

8.3.3 Other Abbreviations and Symbols

°C	degree Celsius
cps	counts per second
drc	dry rubber content
d.nm	particle diameter in nanometer
e.g.	exempli gratia (lat.: for example)
eq.	equivalents
et al.	et alii (lat.: and co-workers)
etc.	et cetera (lat.: and others)
g	gram
ΔG_{mix}	free energy of mixing
ΔH_{mix}	enthalpy of mixing
hrs	hour(s)
i.e.	id est (lat.: that is)
K	Kelvin
keV	kiloelectron volts
kN	kilonewton
kV	kilovolts
L	litre

LCST	lower critical solution temperature
M	molar (mol L^{-1})
$\overline{M_C}$	average molecular mass between two cross-links
min	minute(s)
mg	miligram
mL	milliliter
µL	microliter
mM	millimolar (mmol L^{-1})
µm	micrometer
mmol	millimole
mW	milliwatt
N	Newton
n.a.	not applied
v_e	cross-linking density
nm	nanometer
φ	volume fraction of component i
phr	parts per hundred rubber
Q_m	mass swelling
Q_V	volume swelling
rt	room temperature
σ	standard deviation
ΔS_{mix}	entropy of mixing
tsc	total solid content
UCST	upper critical solution temperature
(v/v)	volume/volume
(wt/wt)	weight/weight (based on dry rubber content)
wt%	percent of weight
χ	Flory-Huggins parameter

8.4 Additional Data and Spectra

8.4.1 Mechanical Properties

In this section, all obtained values for tensile strength, ultimate elongation as well as 50% modulus (M50), 100% modulus (M100), 300% modulus (M300) and 500% modulus (M500) of the tested materials are gathered.

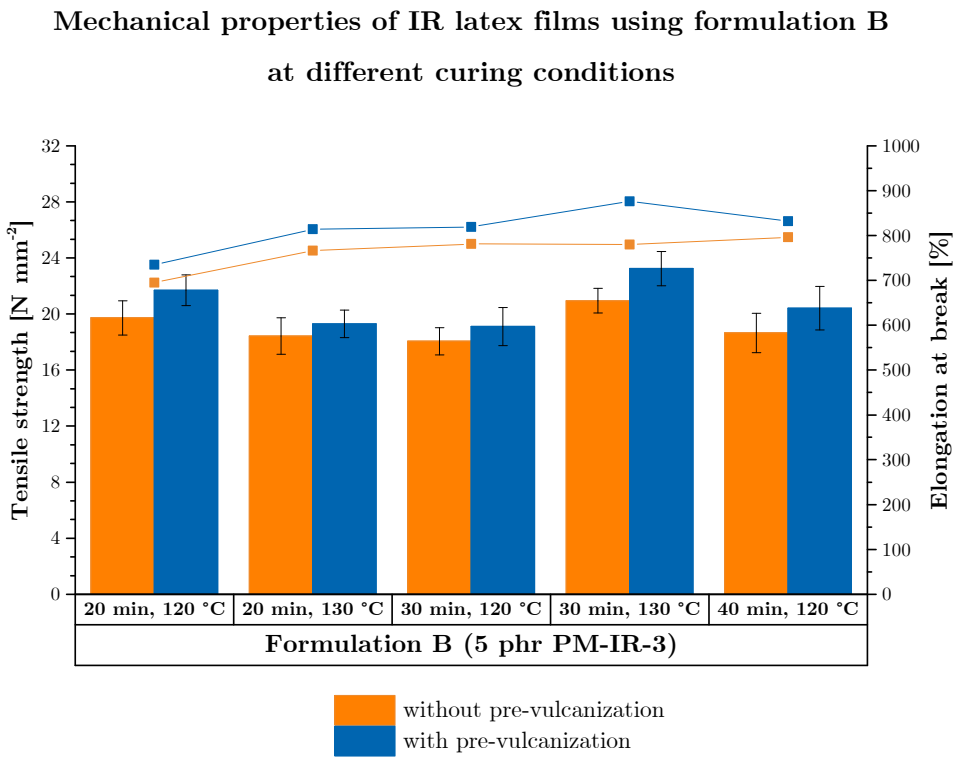

Figure 39. Mechanical properties of IR latex films using a formulation B at different curing conditions.

Table 27. Mechanical properties of IR films using different formulations.

Formulation	with pre-vulcanization; 20 min, 120 °C						with pre-vulcanization; 30 min, 120 °C					
	M50	**M100**	**M300**	**M500**	**TS**	**UE**	**M50**	**M100**	**M300**	**M500**	**TS**	**UE**
			[N mm^{-2}]			**[%]**			**[N mm^{-2}]**			**[%]**
A	0.46 ± 0.02	0.66 ± 0.03	1.44 ± 0.05	3.12 ± 0.24	24.8 ± 3.8	721 ± 59	0.45 ± 0.03	0.65 ± 0.05	1.42 ± 0.11	3.27 ± 0.77	17.1 ± 1.0	871 ± 75
B	0.31 ± 0.01	0.44 ± 0.01	0.81 ± 0.04	2.77 ± 0.04	21.7 ± 1.1	735 ± 66	0.37 ± 0.01	0.53 ± 0.01	1.08 ± 0.03	2.91 ± 0.17	19.1 ± 1.4	814 ± 62
Formulation	with pre-vulcanization; 40 min, 120 °C						with pre-vulcanization; 20 min, 130 °C					
	M50	**M100**	**M300**	**M500**	**TS**	**UE**	**M50**	**M100**	**M300**	**M500**	**TS**	**UE**
			[N mm^{-2}]			**[%]**			**[N mm^{-2}]**			**[%]**
A	0.55 ± 0.03	0.72 ± 0.03	1.35 ± 0.08	3.08 ± 0.24	19.9 ± 1.8	918 ± 78	0.35 ± 0.01	0.52 ± 0.03	1.11 ± 0.05	1.93 ± 0.03	19.8 ± 2.3	903 ± 85
B	n.a.	n.a.	n.a.	n.a.	20.4 ± 1.6	819 ± 53	0.39 ± 0.01	0.60 ± 0.05	1.30 ± 0.06	2.13 ± 0.15	19.3 ± 0.9	876 ± 71
Formulation	with pre-vulcanization; 30 min, 130 °C											
	M50	**M100**	**M300**	**M500**	**TS**	**UE**						
			[N mm^{-2}]			**[%]**						
A	0.39 ± 0.02	0.55 ± 0.04	1.02 ± 0.04	1.85 ± 0.09	24.7 ± 0.6	847 ± 61						
B	n.a.	n.a.	n.a.	n.a.	23.2 ± 1.2	832 ± 70						

M50 = 50% Modulus, M100 = 100% Modulus, M300 = 300% Modulus, M500 = 500% Modulus, TS = Tensile strength, UE = Ultimate elongation

Table 28. Mechanical properties of CR latex films using formulations with ZnO, S and DPG/ZDBC

Formulation	without pre-vulcanization; 20 min, 120 °C						with pre-vulcanization; 20 min, 120 °C					
	M50	**M100**	**M300**	**M500**	**TS**	**UE**	**M50**	**M100**	**M300**	**M500**	**TS**	**UE**
			[N mm^{-2}]			**[%]**			**[N mm^{-2}]**			**[%]**
A	0.51 ± 0.07	0.62 ± 0.06	0.99 ± 0.06	2.04 ± 0.10	14.0 ± 1.3	1160 ± 80	0.54 ± 0.05	0.68 ± 0.05	0.97 ± 0.08	2.13 ± 0.12	11.9 ± 1.0	1110 ± 80
B	0.48 ± 0.04	0.59 ± 0.04	1.01 ± 0.04	2.00 ± 0.05	11.6 ± 1.5	1090 ± 90	0.50 ± 0.05	0.63 ± 0.05	0.92 ± 0.06	2.04 ± 0.07	12.2 ± 1.2	1100 ± 80
C	0.51 ± 0.06	0.65 ± 0.07	1.13 ± 0.07	2.11 ± 0.06	11.8 ± 1.1	1070 ± 80	0.44 ± 0.03	0.59 ± 0.05	0.90 ± 0.05	1.98 ± 0.06	11.8 ± 0.9	1060 ± 90
D	0.56 ± 0.09	0.67 ± 0.09	1.05 ± 0.10	2.15 ± 0.11	13.6 ± 1.2	1100 ± 80	0.48 ± 0.04	0.72 ± 0.06	1.05 ± 0.06	2.32 ± 0.08	13.0 ± 0.7	1070 ± 70
E	0.52 ± 0.04	0.60 ± 0.06	1.01 ± 0.06	2.09 ± 0.07	13.1 ± 0.9	1090 ± 60	0.49 ± 0.10	0.69 ± 0.10	1.01 ± 0.11	2.20 ± 0.12	12.2 ± 0.4	1080 ± 50
F	0.50 ± 0.02	0.59 ± 0.03	0.98 ± 0.04	1.99 ± 0.05	11.9 ± 0.6	1060 ± 50	0.47 ± 0.04	0.61 ± 0.04	0.88 ± 0.05	2.02 ± 0.06	10.9 ± 0.8	985 ± 70

M50 = 50% Modulus, M100 = 100% Modulus, M300 = 300% Modulus, M500 = 500% Modulus, TS = Tensile strength, UE = Ultimate elongation

Table 29. Mechanical properties of CR latex films using formulations with ZnO, S and DPG/ETU

Formulation	without pre-vulcanization; 20 min, 120 °C						without pre-vulcanization; 20 min, 130 °C					
	M50	**M100**	**M300**	**M500**	**TS**	**UE**	**M50**	**M100**	**M300**	**M500**	**TS**	**UE**
			[N mm^{-2}]			**[%]**			**[N mm^{-2}]**			**[%]**
A	0.55 ± 0.15	0.64 ± 0.14	1.03 ± 0.22	2.15 ± 0.28	14.0 ± 0.6	1160 ± 50	0.73 ± 0.5	0.80 ± 0.5	1.17 ± 0.05	2.13 ± 0.04	15.3 ± 1.6	1230 ± 40
B	0.61 ± 0.08	0.66 ± 0.07	0.99 ± 0.08	2.07 ± 0.19	15.5 ± 1.5	1150 ± 50	0.71 ± 0.04	0.96 ± 0.11	1.24 ± 0.19	2.34 ± 0.15	17.1 ± 1.3	1110 ± 40
C	0.68 ± 0.13	0.72 ± 0.05	1.03 ± 0.20	1.91 ± 0.35	16.0 ± 0.7	1100 ± 60	0.83 ± 0.08	1.07 ± 0.16	1.32 ± 0.18	2.37 ± 0.18	17.9 ± 0.9	1090 ± 80
D	0.70 ± 0.05	0.93 ± 0.08	1.25 ± 0.08	2.03 ± 0.10	16.6 ± 0.4	1240 ± 40	0.60 ± 0.04	0.88 ± 0.05	1.21 ± 0.07	2.22 ± 0.18	16.6 ± 0.6	1250 ± 90
Formulation	with pre-vulcanization; 20 min, 120 °C						with pre-vulcanization; 20 min, 130 °C					
	M50	**M100**	**M300**	**M500**	**TS**	**UE**	**M50**	**M100**	**M300**	**M500**	**TS**	**UE**
			[N mm^{-2}]			**[%]**			**[N mm^{-2}]**			**[%]**
A	0.70 ± 0.04	0.82 ± 0.07	1.10 ± 0.06	2.03 ± 0.13	14.1 ± 1.4	1230 ± 60	0.89 ± 0.05	0.99 ± 0.04	1.38 ± 0.06	2.37 ± 0.06	16.7 ± 0.8	1230 ± 30
B	0.60 ± 0.09	0.82 ± 0.08	1.05 ± 0.11	2.03 ± 0.09	14.9 ± 1.3	1180 ± 70	0.66 ± 0.06	0.78 ± 0.06	1.18 ± 0.12	2.40 ± 0.10	16.4 ± 0.5	1190 ± 60
C	0.63 ± 0.05	0.71 ± 0.04	1.12 ± 0.06	2.13 ± 0.09	15.6 ± 0.7	1120 ± 40	0.93 ± 0.21	1.04 ± 0.20	1.16 ± 0.21	2.36 ± 0.24	17.4 ± 1.2	1140 ± 50
D	0.69 ± 0.06	0.84 ± 0.07	1.38 ± 0.07	2.55 ± 0.12	16.0 ± 2.0	1210 ± 40	0.82 ± 0.08	0.92 ± 0.09	1.22 ± 0.11	2.42 ± 0.22	15.5 ± 0.8	1170 ± 90

M50 = 50% Modulus, M100 = 100% Modulus, M300 = 300% Modulus, M500 = 500% Modulus, TS = Tensile strength, UE = Ultimate elongation

Table 30. Mechanical properties of IR/CR latex films using different curing formulations.

Formulation	without pre-vulcanization; 20 min, 120 °C						without pre-vulcanization; 20 min, 130 °C					
	M50	**M100**	**M300**	**M500**	**TS**	**UE**	**M50**	**M100**	**M300**	**M500**	**TS**	**UE**
			[N mm^{-2}]			**[%]**			**[N mm^{-2}]**			**[%]**
A	0.42 ± 0.02	0.57 ± 0.02	1.04 ± 0.02	2.14 ± 0.14	10.5 ± 1.7	747 ± 36	0.39 ± 0.03	0.52 ± 0.03	1.18 ± 0.04	2.07 ± 0.04	12.2 ± 0.7	726 ± 33
B	0.34 ± 0.02	0.49 ± 0.03	0.97 ± 0.03	1.89 ± 0.03	9.32 ± 1.3	838 ± 82	0.39 ± 0.03	0.48 ± 0.03	1.00 ± 0.05	2.01 ± 0.05	12.9 ± 1.9	781 ± 54
C	0.48 ± 0.05	0.55 ± 0.05	1.12 ± 0.05	2.30 ± 0.07	14.7 ± 1.3	774 ± 55	0.44 ± 0.02	0.56 ± 0.03	1.19 ± 0.03	2.42 ± 0.10	15.8 ± 1.5	798 ± 96
Formulation	with pre-vulcanization; 20 min, 120 °C						with pre-vulcanization; 20 min, 130 °C					
	M50	**M100**	**M300**	**M500**	**TS**	**UE**	**M50**	**M100**	**M300**	**M500**	**TS**	**UE**
			[N mm^{-2}]			**[%]**			**[N mm^{-2}]**			**[%]**
A	0.44 ± 0.02	0.60 ± 0.02	1.01 ± 0.02	2.03 ± 0.14	12.0 ± 1.2	778 ± 21	0.40 ± 0.05	0.49 ± 0.05	1.12 ± 0.06	2.16 ± 0.06	14.5 ± 0.6	804 ± 25
B	0.34 ± 0.02	0.49 ± 0.03	0.97 ± 0.03	1.89 ± 0.03	10.0 ± 1.5	838 ± 40	0.40 ± 0.03	0.52 ± 0.03	1.04 ± 0.04	2.00 ± 0.04	14.7 ± 1.3	838 ± 64
C	0.40 ± 0.06	0.47 ± 0.05	1.05 ± 0.06	2.03 ± 0.06	16.9 ± 1.0	810 ± 35	0.45 ± 0.02	0.55 ± 0.03	1.17 ± 0.03	2.25 ± 0.04	16.1 ± 1.3	821 ± 61

M50 = 50% Modulus, M100 = 100% Modulus, M300 = 300% Modulus, M500 = 500% Modulus, TS = Tensile strength, UE = Ultimate elongation

Table 31. Mechanical properties of NBR latex films with and without leaching.

Formulation	without leaching; 20 min, 120 °C						with leaching; 20 min, 120 °C					
	M50	**M100**	**M300**	**M500**	**TS**	**UE**	**M50**	**M100**	**M300**	**M500**	**TS**	**UE**
			[N mm^{-2}]			**[%]**			**[N mm^{-2}]**			**[%]**
A	1.75 ± 0.05	2.34 ± 0.07	4.92 ± 0.15	17.3 ± 1.10	25.0 ± 3.8	562 ± 38	1.85 ± 0.06	2.46 ± 0.06	4.92 ± 0.15	15.9 ± 1.15	54.9 ± 5.7	627 ± 45
B	1.90 ± 0.11	2.62 ± 0.20	5.30 ± 0.32	17.8 ± 1.93	24.3 ± 2.6	581 ± 30	1.96 ± 0.08	2.70 ± 0.08	6.01 ± 0.05	22.8 ± 1.28	50.3 ± 2.8	568 ± 46
C	2.00 ± 0.10	2.76 ± 0.14	6.35 ± 0.32	25.6 ± 1.74	23.8 ± 1.9	544 ± 42	1.64 ± 0.10	2.23 ± 0.12	4.89 ± 0.77	18.0 ± 1.24	48.4 ± 1.9	571 ± 51

M50 = 50% Modulus, M100 = 100% Modulus, M300 = 300% Modulus, M500 = 500% Modulus, TS = Tensile strength, UE = Ultimate elongation

Table 32. Mechanical properties of filled NBR latex films at different curing conditions.

Filler loading [phr]	without pre-vulcanization; 20 min, 120 °C						without pre-vulcanization; 30 min, 120 °C					
	M50	**M100**	**M300**	**M500**	**TS**	**UE**	**M50**	**M100**	**M300**	**M500**	**TS**	**UE**
			[N mm^{-2}]			**[%]**			**[N mm^{-2}]**			**[%]**
5	1.73 ± 0.07	2.38 ± 0.16	6.64 ± 0.31	24.0 ± 1.4	38.9 ± 2.8	588 ± 31	1.74 ± 0.12	2.37 ± 0.12	6.91 ± 0.14	26.3 ± 3.1	37.9 ± 3.8	581 ± 52
10	2.07 ± 0.12	2.83 ± 0.14	7.57 ± 0.39	20.8 ± 2.1	34.8 ± 6.8	569 ± 40	2.07 ± 0.12	2.83 ± 0.14	7.57 ± 0.39	22.0 ± 1.8	35.5 ± 5.4	582 ± 55
15	2.15 ± 0.13	2.93 ± 0.10	7.85 ± 0.16	21.3 ± 1.4	33.1 ± 5.0	568 ± 43	2.18 ± 0.60	2.84 ± 0.58	7.13 ± 1.51	21.9 ± 1.7	36.9 ± 6.5	578 ± 48
20	2.84 ± 0.79	3.66 ± 0.86	8.82 ± 0.87	20.8 ± 1.2	33.3 ± 4.7	566 ± 32	2.44 ± 0.15	3.41 ± 0.09	8.96 ± 0.39	22.3 ± 2.1	36.9 ± 8.0	562 ± 65
Filler loading [phr]	with pre-vulcanization; 20 min, 120 °C						with pre-vulcanization; 30 min, 120 °C					
	M50	**M100**	**M300**	**M500**	**TS**	**UE**	**M50**	**M100**	**M300**	**M500**	**TS**	**UE**
			[N mm^{-2}]			**[%]**			**[N mm^{-2}]**			**[%]**
5	2.38 ± 0.16	3.19 ± 0.23	8.53 ± 0.50	25.1 ± 1.0	41.2 ± 8.0	570 ± 40	2.44 ± 0.58	3.22 ± 0.59	8.27 ± 1.10	21.1 ± 1.9	38.0 ± 4.2	571 ± 33
10	2.44 ± 0.23	3.35 ± 0.62	5.66 ± 1.11	24.4 ± 1.9	40.9 ± 3.2	587 ± 43	1.84 ± 0.09	2.71 ± 0.19	8.26 ± 0.34	19.36 ± 1.4	35.2 ± 9.1	551 ± 45
15	3.06 ± 0.12	4.08 ± 0.08	6.51 ± 0.30	23.1 ± 1.7	35.7 ± 5.1	536 ± 29	3.47 ± 0.22	4.51 ± .027	10.6 ± 0.27	25.3 ± 2.5	36.7 ± 4.4	540 ± 62
20	2.91 ± 0.06	3.90 ± 0.11	10.5 ± 1.0	25.3 ± 2.2	32.0 ± 5.8	518 ± 35	3.01 ± 0.14	4.04 ± 0.19	10.4 ± 0.3	24.0 ± 2.8	37.0 ± 5.8	552 ± 29

M50 = 50% Modulus, M100 = 100% Modulus, M300 = 300% Modulus, M500 = 500% Modulus, TS = Tensile strength, UE = Ultimate elongation

Table 33. Mechanical properties of blended NBR latex films at different curing conditions.

Blend	without pre-vulcanization; 20 min, 130 °C						without pre-vulcanization; 30 min, 130 °C					
	M50	**M100**	**M300**	**M500**	**TS**	**UE**	**M50**	**M100**	**M300**	**M500**	**TS**	**UE**
			[N mm^{-2}]			**[%]**			**[N mm^{-2}]**			**[%]**
S (100)	2.83 ± 0.40	3.92 ± 0.45	10.6 ± 0.8	33.4 ± 3.1	48.0 ± 2.8	575 ± 40	2.65 ± 0.12	3.92 ± 0.25	11.4 ± 0.9	30.6 ± 2.0	47.4 ± 3.0	568 ± 35
S/K (70/30)	2.01 ± 0.41	2.95 ± 1.41	7.98 ± 1.44	27.6 ± 4.8	46.8 ± 1.9	553 ± 34	1.78 ± 0.64	2.50 ± 0.67	7.78 ± 1.22	24.2 ± 6.3	45.9 ± 1.9	548 ± 27
S/K (50/50)	2.16 ± 0.14	3.15 ± 0.14	5.69 ± 0.42	31.7 ± 1.5	47.3 ± 3.9	563 ± 22	2.02 ± 0.09	3.23 ± 0.14	5.77 ± 0.23	33.0 ± 2.6	47.2 ± 2.1	572 ± 30
S/K (30/70)	2.05 ± 0.16	2.89 ± 0.21	8.98 ± 1.11	29.7 ± 3.2	53.6 ± 5.2	580 ± 25	2.39 ± 0.09	3.49 ± 0.14	10.6 ± 00.3	34.4 ± 1.4	47.6 ± 2.4	550 ± 42
Blend	with pre-vulcanization; 20 min, 130 °C						with pre-vulcanization; 30 min, 130 °C					
	M50	**M100**	**M300**	**M500**	**TS**	**UE**	**M50**	**M100**	**M300**	**M500**	**TS**	**UE**
			[N mm^{-2}]			**[%]**			**[N mm^{-2}]**			**[%]**
S (100)	2.22 ± 0.12	3.31 ± 0.11	9.92 ± 0.32	31.8 ± 1.1	43.8 ± 4.2	582 ± 25	2.65 ± 0.12	3.20 ± 0.26	9.75 ± 0.83	31.3 ± 2.9	42.6 ± 3.0	581 ± 41
S/K (70/30)	2.14 ± 0.50	3.09 ± 0.95	7.98 ± 0.99	29.0 ± 5.5	41.1 ± 4.4	567 ± 32	1.94 ± 0.80	2.69 ± 0.83	6.61 ± 2.21	23.1 ± 7.4	39.6 ± 3.6	562 ± 30
S/K (50/50)	1.63 ± 0.81	2.31 ± 1.13	7.09 ± 1.40	21.1 ± 8.9	39.1 ± 5.3	542 ± 40	1.36 ± 0.22	1.98 ± 0.24	6.04 ± 1.41	19.0 ± 4.1	45.4 ± 7.1	566 ± 44
S/K (30/70)	1.33 ± 0.16	1.92 ± 0.17	6.08 ± 1.10	18.4 ± 4.0	42.9 ± 3.5	550 ± 38	1.49 ± 0.55	2.18 ± 0.82	6.73 ± 0.9	16.0 ± 3.8	46.5 ± 5.5	529 ± 19

M50 = 50% Modulus, M100 = 100% Modulus, M300 = 300% Modulus, M500 = 500% Modulus, TS = Tensile strength, UE = Ultimate elongation

8.4.2 SEM-EDX Spectra and Elemental Quantification

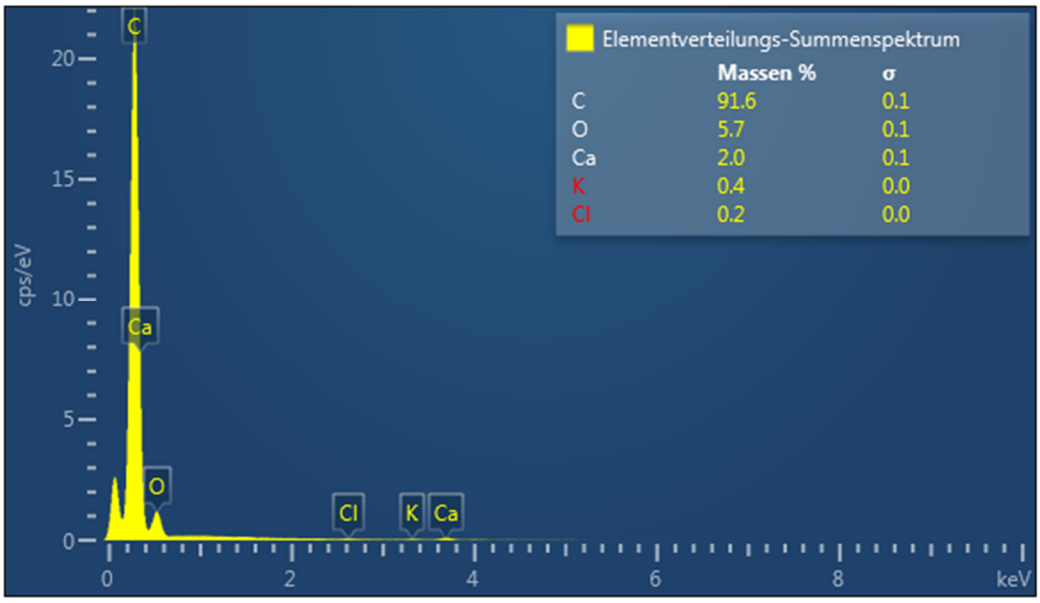

Figure 40. SEM-EDX spectrum and element distribution by weight percent of a NR film (100).

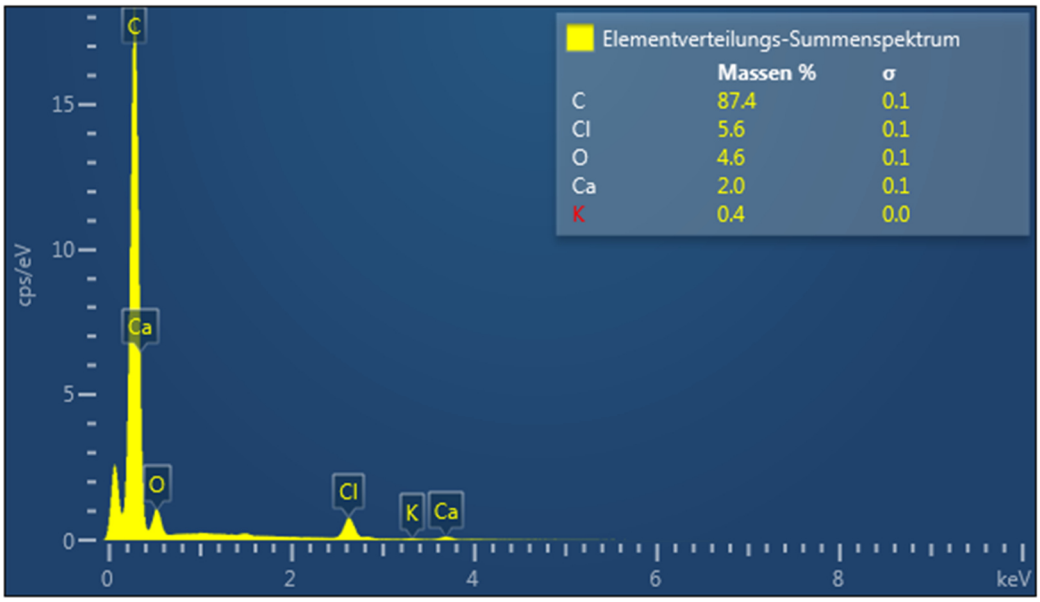

Figure 41. SEM-EDX spectrum and element distribution by weight percent of a NR/CR film (75/25).

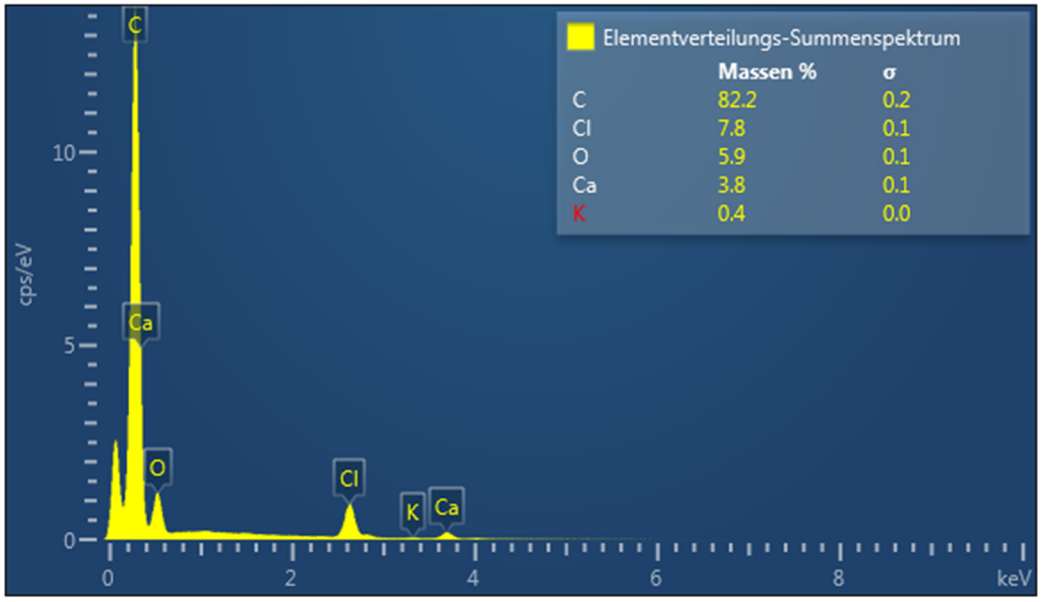

Figure 42. SEM-EDX spectrum and element distribution by weight percent of a NR/CR film (50/50).

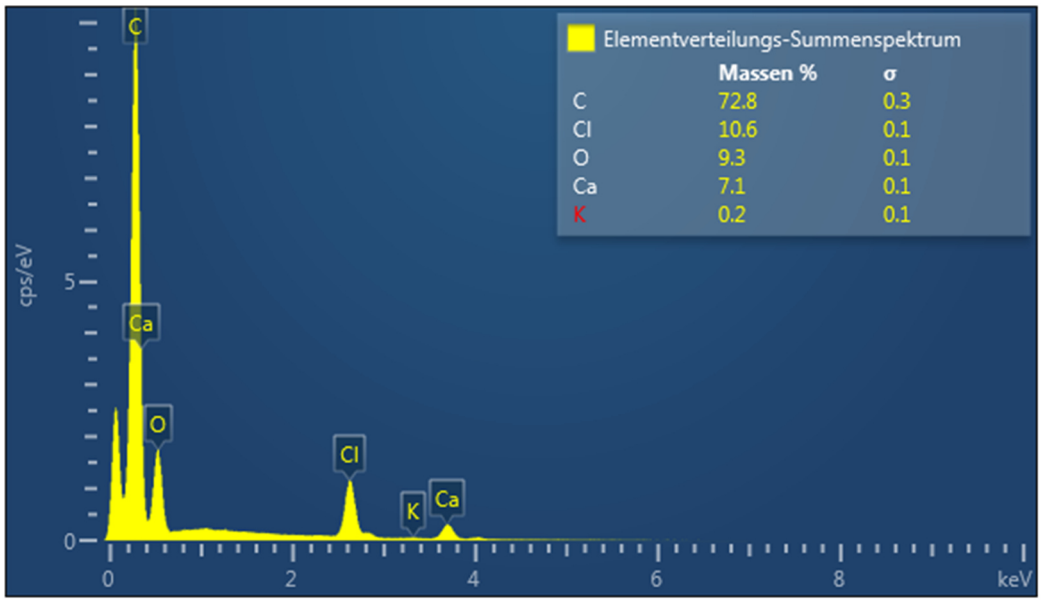

Figure 43. SEM-EDX spectrum and element distribution by weight percent of a NR/CR film (25/75).

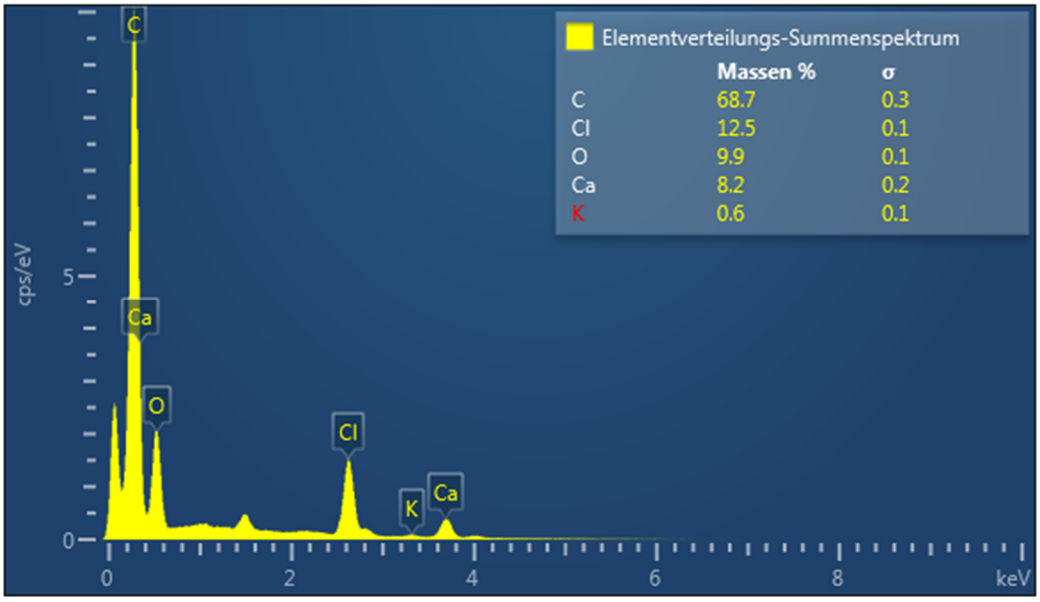

Figure 44. SEM-EDX spectrum and element distribution by weight percent of a CR (100) film.

8.4.3 DSC Curves of Latex Materials

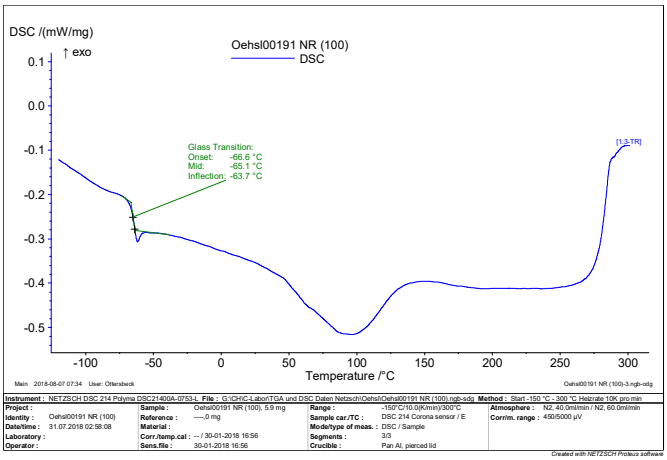

Figure 45. DSC curve of a NR film sample (100) without additives.

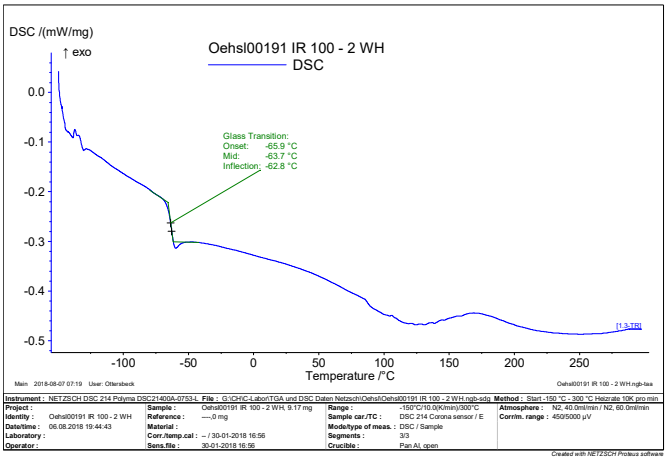

Figure 46. DSC curve of an IR film sample (100) without additives.

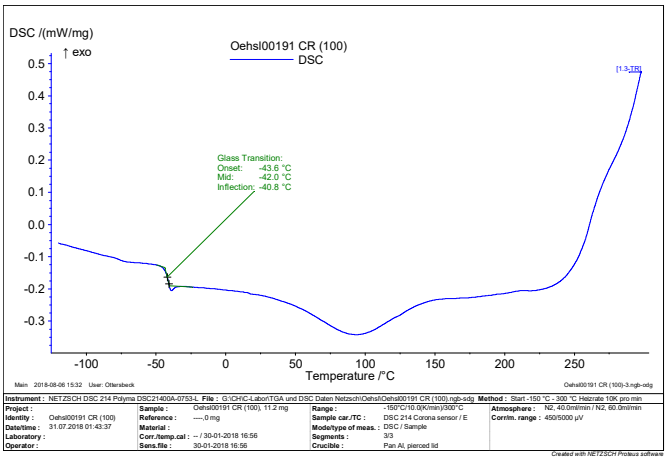

Figure 47. DSC curve of a CR film sample (100) without additives.

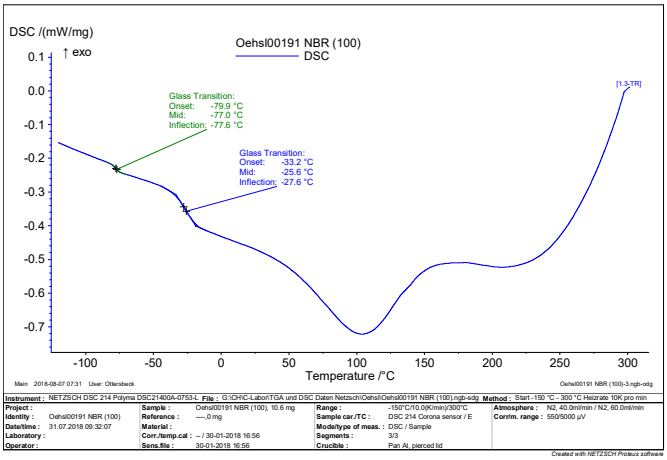

Figure 48. DSC curve of an NBR film sample (100) without additives.

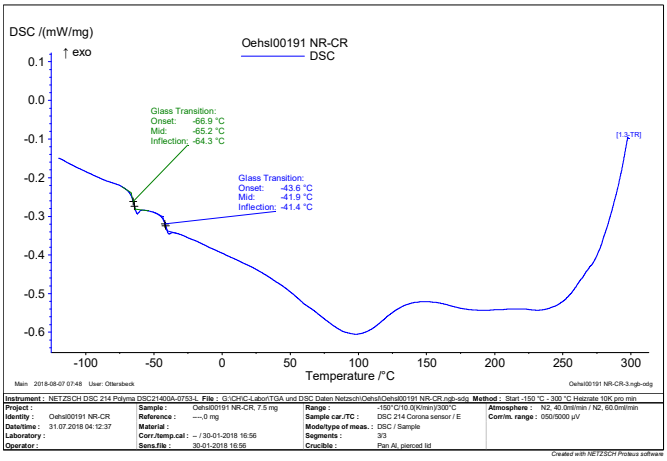

Figure 49. DSC curve of an NR/CR film sample (50/50) without additives.

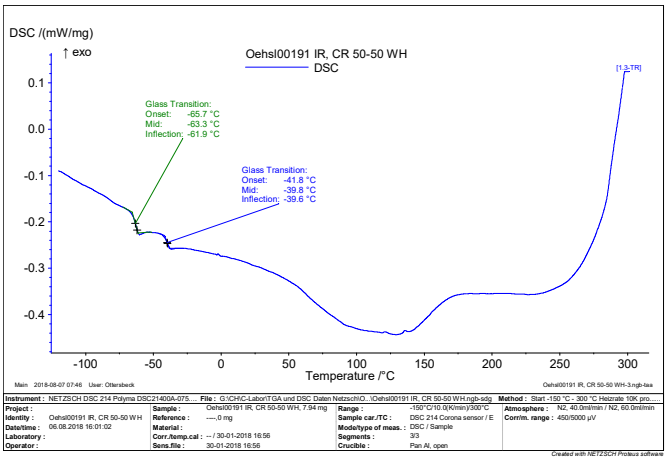

Figure 50. DSC curve of an IR/CR film sample (50/50) without additives.

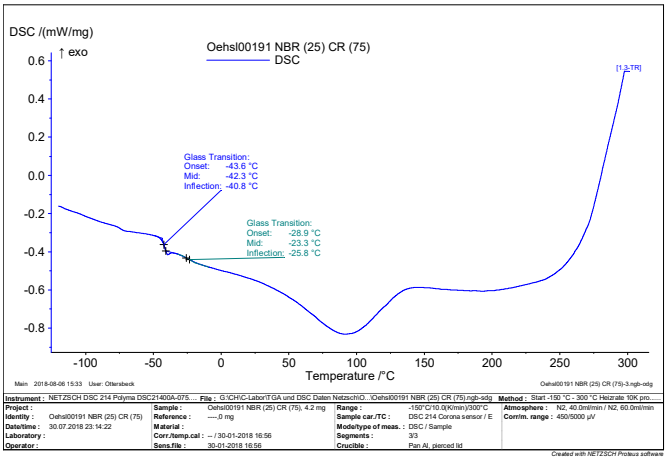

Figure 51. DSC curve of an NBR/CR film sample (25/75) without additives.

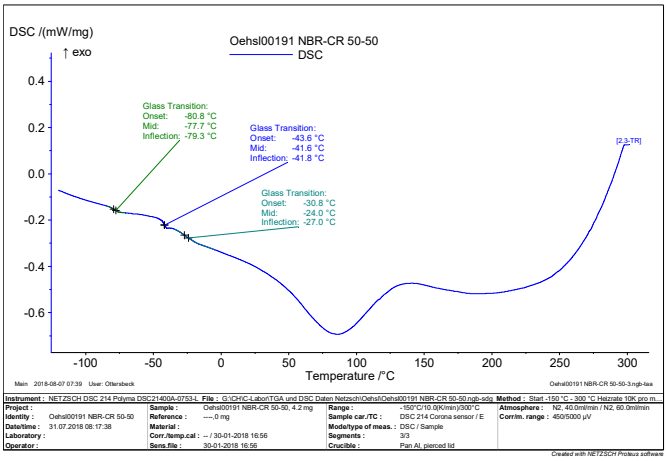

Figure 52. DSC curve of an NBR/CR film sample (50/50) without additives.

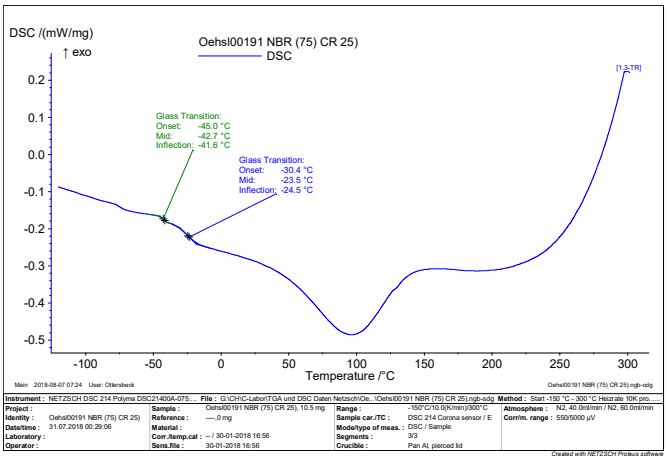

Figure 53. DSC curve of an NBR/CR film sample (75/25) without additives.